
Why Has Predicting Downstream Capabilities of Frontier AI Models with Scale Remained Elusive?

Anonymous Authors¹

Abstract

Predictable behavior from scaling advanced AI systems is an extremely desirable property. While a well-established literature exists on how pre-training performance scales, the literature on how particular downstream capabilities change with scale is significantly muddier. For instance, previous papers debated the origins of emergent abilities, and more recent work claimed that specific downstream capabilities become predictable only beyond a specific pretraining loss or if aggregated across dozens of benchmarks. In this work, we take a step back and ask: *what makes predicting specific downstream capabilities with scale difficult?* We identify a critical factor contributing to this difficulty on multiple-choice benchmarks. Using five model families and twelve widely-used benchmarks, we show that downstream performance is computed from negative log likelihoods via a sequence of transformations that progressively deteriorates the statistical relationship between performance and scale. We demonstrate that this deterioration is caused by metrics that require comparing the correct answer against a small number of specific incorrect answers, meaning that accurately predicting downstream capabilities requires predicting not just how probability mass concentrates on the correct behavior with scale, but also how probability mass changes on specific incorrect behaviors with scale. We empirically study how probability mass on the correct choice covaries with probability mass on incorrect choices with increasing compute, suggesting that scaling laws for *incorrect* choices might be achievable. Our work explains why pretraining scaling laws are regarded as more predictable and contribute towards establishing scaling-predictable evaluations of frontier AI models.

1. Introduction

Predictable scaling behavior of frontier AI systems such as GPT-4 (OpenAI, 2024; OpenAI et al., 2024), Claude (Anthropic, 2024) and Gemini (Team et al., 2023; Reid et al., 2024) is crucial for anticipating their capabilities and informing key decisions around their development and deployment (Anthropic, 2023; OpenAI, 2023; Dragan et al., 2024). While scaling laws describing relationships between parameters, data, compute, and pretraining loss are well-established (Hestness et al., 2017; Rosenfeld et al., 2019; Henighan et al., 2020; Kaplan et al., 2020; Gordon et al., 2021; Hernandez et al., 2021; Jones, 2021; Zhai et al., 2022; Hoffmann et al., 2022; Clark et al., 2022; Neumann & Gros, 2022; Hernandez et al., 2022; Maloney et al., 2022; Sardana & Frankle, 2023; Muennighoff et al., 2024; Besiroglu et al., 2024), the literature is less conclusive concerning predicting specific downstream capabilities with scale. For instance, prior work has observed that performance on standard natural language processing (NLP) benchmarks can exhibit *emergent abilities* (Brown et al., 2020; Ganguli et al., 2022; Srivastava et al., 2022; Wei et al., 2022) where performance changes unpredictably with scale, with further work suggesting that such unpredictable changes might at times be artifacts of researchers' analyses, i.e., choices of metrics and lack of resolution (Srivastava et al., 2022; Schaeffer et al., 2023; Hu et al., 2024). More recently, Du et al. (2024) claimed that downstream capabilities *can* be predicted, but *only* after the pretraining cross-entropy loss falls below a certain threshold, and Gadre et al. (2024) claimed that while performance on individual tasks can be difficult to predict, aggregating results across dozens of diverse benchmarks yields clearer scaling trends. In this work, we take a step back and ask: *why has predicting specific downstream capabilities with scale remained elusive?*

While many factors are certainly responsible, we identify a new factor that makes modeling the scaling behavior on widely used multiple-choice question-answering benchmarks challenging. We demonstrate that common multiple-choice scores from raw model outputs (negative log probabilities) via a sequence of transformations that progressively degrade the statistical relationship between those outputs and scaling parameters. The cause is that these metrics rely

¹Anonymous Institution, Anonymous City, Anonymous Region, Anonymous Country. Correspondence to: Anonymous Author <anon.email@domain.com>.

Preliminary work. Under review by the ICML NextGenAISafety 2024 Workshop. Do not distribute.

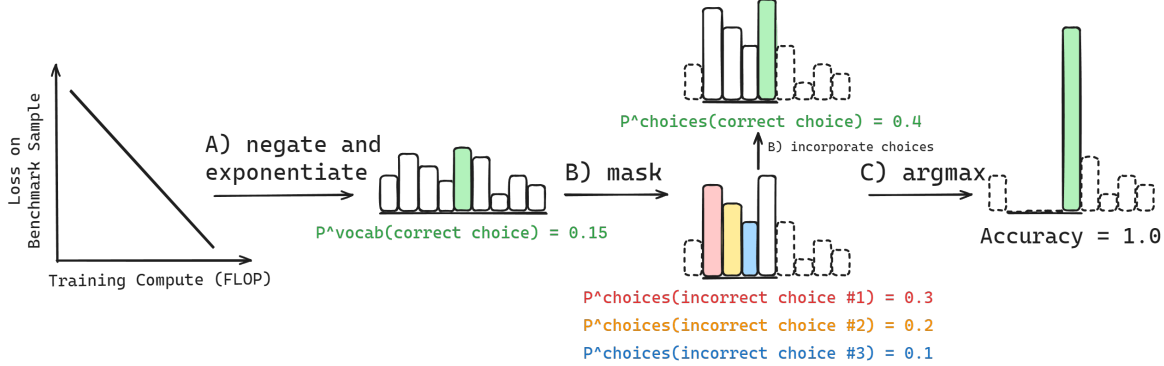


Figure 1. Multiple-choice benchmark accuracy is computed from negative log-likelihoods via a sequence of transformations that degrades predictability. Computing Accuracy begins with computing the negative log-likelihoods of each choice, then negating and exponentiating each to obtain the probability of each choice (A). Choices are then restricted to a set of available choices by *masking* invalid continuations, and renormalizing to obtain relative probability mass on each choice (B). Lastly, the model’s choice is defined as $\arg \max_i \{p^{\text{Choices}}(\text{Available Choice}_i)\}$, and Accuracy is 1 if and only if the model’s choice is the correct choice (C).

on a direct comparison between the ground truth output and a small set of specific incorrect outputs. As a result, *accurately predicting downstream performance requires modeling not only the concentration of probability mass on the correct output with increasing compute, but also modeling the fluctuations of probability mass on particular incorrect alternatives*, which (to-date) is a necessary but unaddressed step. We then empirically study how probability mass on incorrect choices fluctuates with increasing compute. Our findings help explain the apparent unpredictability of individual downstream metrics; more broadly, we argue that a precise understanding of the factors affecting downstream performance is essential for designing evaluations that can reliably track the progression of frontier AI capabilities.

2. Methodology: Data for Studying Scaling of Downstream Capabilities

To study how model families’ downstream capabilities on specific tasks change with scale, we generated per-sample scores from a large number of model families and multiple-choice NLP benchmarks. To ensure the computed scores were consistent with prior work, we used EleutherAI’s Language Model (LM) Evaluation Harness (Gao et al., 2023) rather than implementing our own evaluations. **Model Families** Because our goal was to explore the scaling behavior of evaluations with increasing compute, we chose to evaluate model families with dense combinations of parameter counts and token counts: Pythia (Biderman et al., 2023a), Cerebras-GPT (Dey et al., 2023), OLMo (Groeneveld et al., 2024), INCITE (AI, 2023) and LLM360 (Liu et al., 2023). For details, see App. D. **NLP Benchmarks** We evaluated the above model families on widely-used multiple-choice benchmarks: AI2 Reasoning Challenge (ARC) Easy and Hard (Clark et al., 2018), HellaSwag (Zellers et al., 2019),

MathQA (Amini et al., 2019), MCTACO (Zhou et al., 2019), MMLU (Hendrycks et al., 2020), OpenbookQA (Mihaylov et al., 2018), PIQA (Bisk et al., 2020), RACE (Lai et al., 2017), SciQ (Welbl et al., 2017), SIQA (Sap et al., 2019a), WinoGrande (Keisuke et al., 2019) and XWinoGrad En (Muennighoff et al., 2023). For MMLU, we analyzed each of the 57 subjects (e.g., Abstract Algebra) independently. For each benchmark, we used default evaluation settings from the LM Evaluation Harness (Gao et al., 2023). **Performance Metrics** We used common metrics for multiple choice benchmarks: Accuracy and probability mass on the correct choice relative to the available choices. **Compute Approximations** Following prior work, we approximated pretraining compute C (in terms of training FLOP) of a given model checkpoint as a function of the parameter count excluding the embedding layer N and the amount of training data seen in tokens D : $C = C(N, D) \approx 6N D$.

3. What Makes Predicting Downstream Performance Difficult?

Performance on multiple choice benchmarks is commonly presented as Accuracy or probability mass on the correct choice out of the available choices. These quantities are computed via a sequence of transformations that begins with the negative log-likelihood of the correct choice on this particular sample as some function $f(\cdot, \cdot)$ of compute:

$$\mathcal{L}_{\theta}^{\text{Vocab}}(\text{Correct Choice}) = f(\text{Compute}, \text{Benchmark Sample})$$

Two details are critical. Firstly, this negative log-likelihood is specific to this particular sample in the benchmark. *All the scores we discuss are per-sample*. Secondly, this negative log-likelihood is computed over the vocabulary of the model. One can then compute the probability mass of the correct

Why Has Predicting Downstream Capabilities of Frontier AI Models with Scale Remained Elusive?

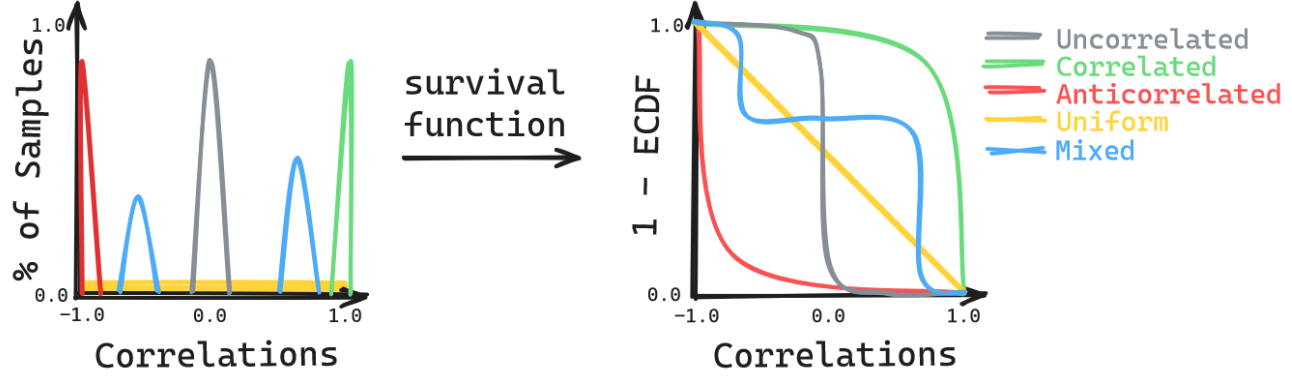


Figure 2. **Schematic distributions of compute-score correlations and their corresponding survival functions.** **Left:** For each benchmark, model family, performance metric and correlation metric, one can compute how correlated scores are with compute. This yields a distribution (over samples) of score-compute correlations. Note: the uniform (yellow) distribution is small but non-zero everywhere. **Right:** To easily extract what fraction of samples in a benchmark have score-compute correlations above any given threshold, we convert the probability distributions to *survival functions*, defined as 1 minus the empirical cumulative distribution function (ECDF).

Distributions of Score-Compute Correlations by Metric
Benchmark: ARC-Challenge

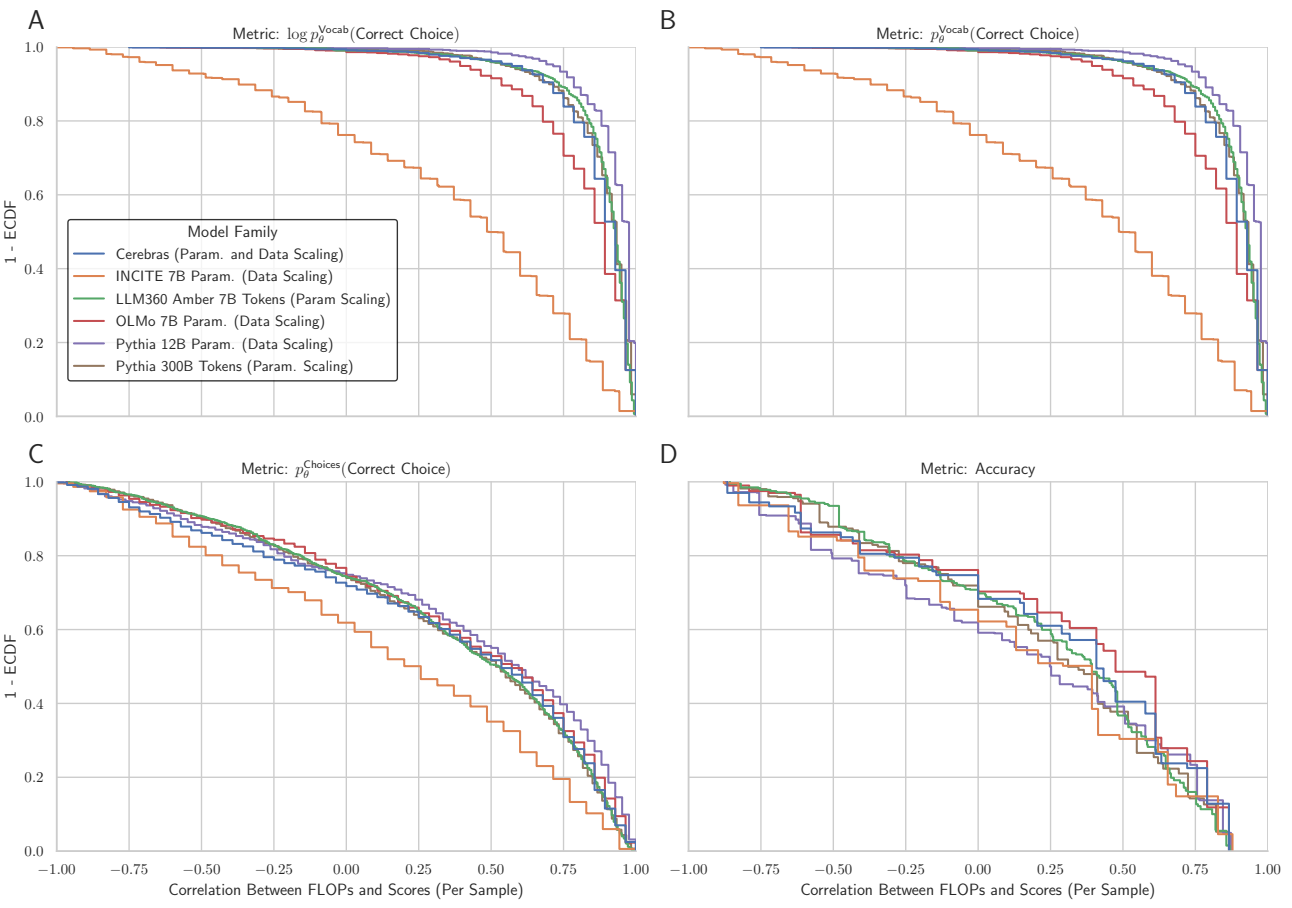


Figure 3. **Multiple-choice benchmark Accuracy is computed via a sequence of transformations that deteriorate correlations between performance scores and pretraining compute.** (A) Compute and scores $\log p_\theta^{\text{vocab}}$ (Correct Choice) begin highly correlated (shown: Spearman correlation). (B) Transforming $\log p_\theta^{\text{vocab}}$ (Correct Choice) into p_θ^{vocab} (Correct Choice) preserves the high score-compute correlations. (C) Transforming p_θ^{vocab} (Correct Choice) into $p_\theta^{\text{Choices}}$ (Correct Choice) decorrelates scores from compute. (D) Transforming $p_\theta^{\text{Choices}}$ (Correct Choice) into Accuracy further decorrelates scores from compute. Example from ARC Challenge (Clark et al., 2018). Results are consistent across NLP benchmarks and all three correlation metrics; for more, see App. I.

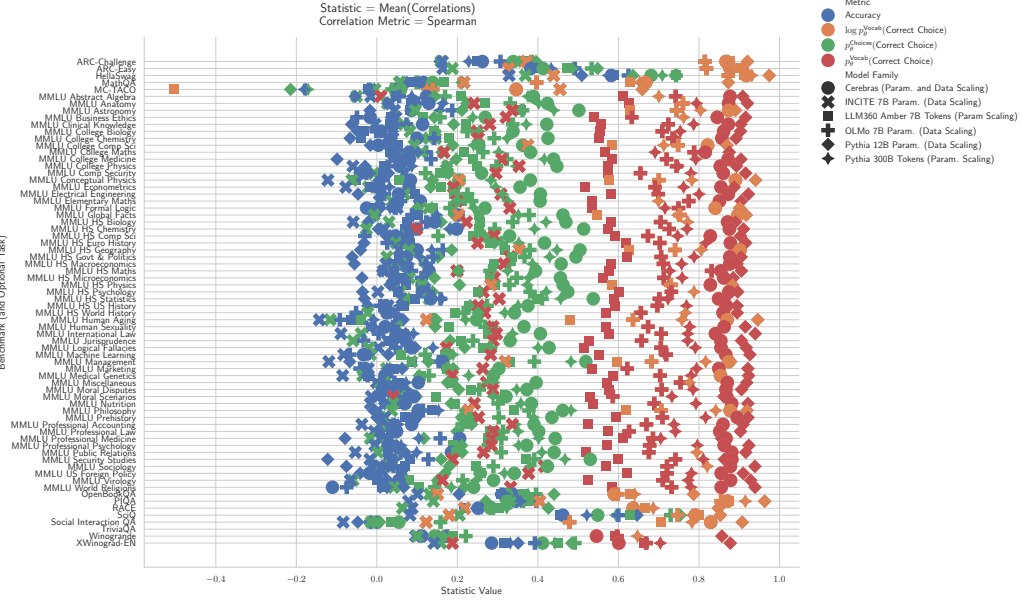


Figure 4. All four statistics of score-compute correlation distributions demonstrate that transforming $\log p_\theta^{\text{vocab}}(\text{Correct Choice}) \rightarrow p_\theta^{\text{vocab}}(\text{Correct Choice}) \rightarrow p_\theta^{\text{Choices}}(\text{Correct Choice}) \rightarrow \text{Accuracy}$ causes score-compute correlations to deteriorate. We find a consistent trend across benchmarks and model families for three correlation metrics (Spearman, Pearson and Kendall) and for four statistics of correlation distributions (mean, median, the area under the survival function, and negative Wasserstein distance from perfect correlation or perfect anti-correlation) that the sequence of transformations degrades score-compute correlations, as shown by the right-to-left red-to-orange-to-green-to-blue vertical stripes. See App. Figs. 7,8,9 for other statistics and other correlation metrics.

choice, again with respect to the vocabulary:

$$p_\theta^{\text{vocab}}(\text{Correct Choice}) = \exp(-\mathcal{L}_\theta^{\text{vocab}}(\text{Correct Choice}))$$

Next, probabilities are restricted to the set of available choices $\{\text{Available Choice}_i\}_{i=1}^{|\text{Available Choices}|}$ by masking invalid continuations and normalizing again:

$$p_\theta^{\text{Choices}}(\text{Correct Choice}) \stackrel{\text{def}}{=} \frac{p_\theta^{\text{vocab}}(\text{Correct Choice})}{\sum_i p_\theta^{\text{vocab}}(\text{Available Choice}_i)}$$

Finally, one uses the choices-normalized probability masses to compute accuracy:

$$\text{Acc}_\theta \stackrel{\text{def}}{=} \mathbb{1}\left(\text{Correct} = \arg \max_i \left\{ p_\theta^{\text{Choices}}(\text{Available}_i) \right\}\right)$$

where $\mathbb{1}(\cdot)$ is an indicator variable.

To quantify how this sequence of transformations affects predictability, we measured how correlated per-sample scores are with pretraining compute, and then studied how the distribution (over samples) of correlation values shifted as one transitions from loglikelihoods to $p_\theta^{\text{vocab}}(\text{Correct Choice})$ to $p_\theta^{\text{Choices}}(\text{Correct Choice})$ to Accuracy. Specifically, for each combination of (*model family*, *benchmark*, *performance metric*, *correlation metric*),

we computed a correlation value for each sample in the benchmark between pretraining compute and scores. This yielded a distribution (over samples) of correlation values for the combination (Fig. 2 left). Visualizing the distribution of correlations for the combination told us what fraction of samples in the benchmark yielded scores that are correlated, uncorrelated or anticorrelated with compute (Fig. 2 right). Pearson, Kendall (1938) and Spearman (1961) yielded consistent results. We present ARC Challenge (Clark et al., 2018) as an example, but note that all other benchmarks exhibited similar patterns (App. I). We visualized the distributions via their *complementary empirical cumulative distribution functions* (App. B; Fig. 2). For a given correlation value, e.g., 0.5, the survival function tells us what fraction of the benchmark’s samples have score-compute correlations greater than the given value (Fig. 3A). Beginning with log likelihoods, approximately 90% of samples exhibit a score-compute correlation > 0.75 , regardless of the model family (Fig. 3A). Transforming negative log-likelihoods into probability masses with respect to $p_\theta^{\text{vocab}}(\text{Correct Choice})$ does not affect the distribution of score-compute correlations for Spearman and Kendall correlations (Fig. 3B). However, transforming $p_\theta^{\text{vocab}}(\text{Correct Choice})$ into $p_\theta^{\text{Choices}}(\text{Correct Choice})$ causes a decrease in the distribution of score-compute correlations (Fig. 3C), with only 40% of samples having score-compute

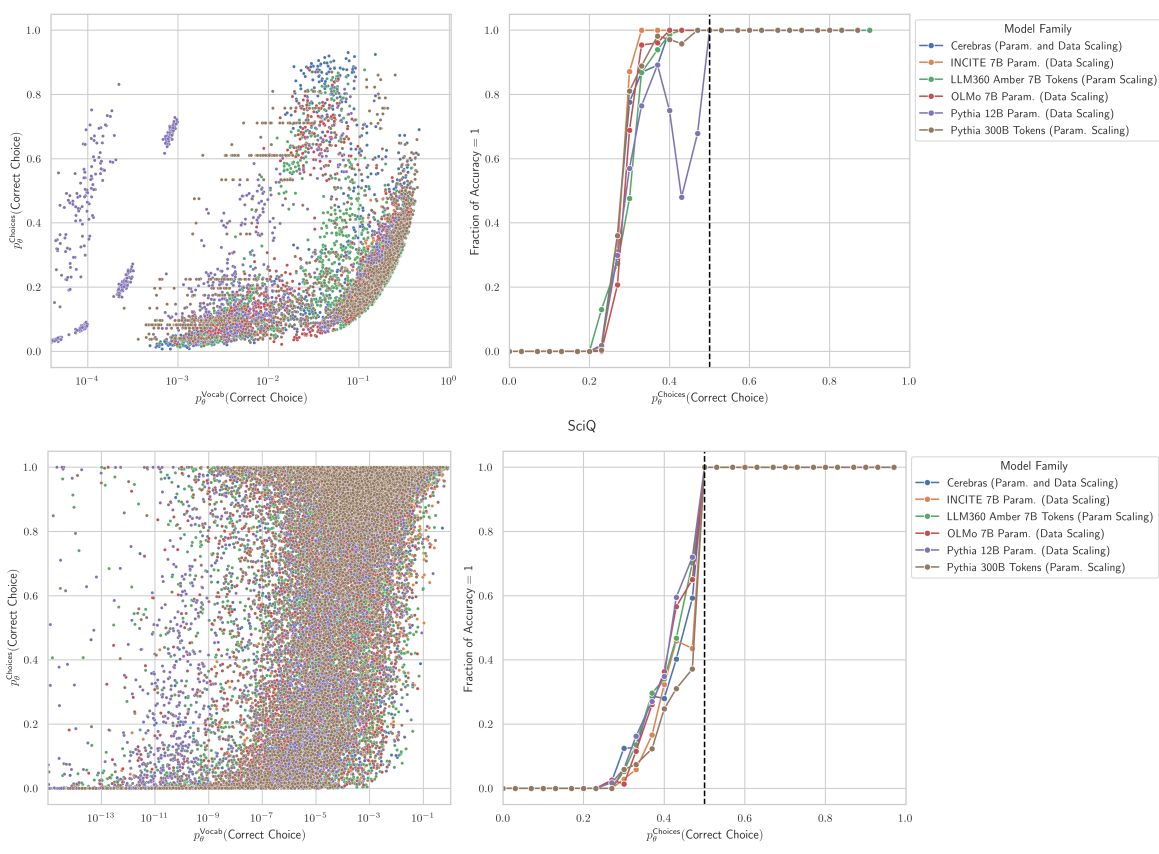


Figure 5. Predictability deteriorates because of probability mass fluctuating on specific incorrect choices with scale. **Left:** Transitioning from $p_\theta^{\text{Vocab}}(\text{Correct Choice})$ to $p_\theta^{\text{Choices}}(\text{Correct Choice})$ demonstrates that $p_\theta^{\text{Vocab}}(\text{Correct Choice})$ contains little information about $p_\theta^{\text{Choices}}(\text{Correct Choice})$ and vice versa; loosely speaking, any value of one can map to any value of the other. **Right:** While $p_\theta^{\text{Choices}}(\text{Correct Choice}) > 0.5$ must yield Accuracy = 1, for any $p_\theta^{\text{Choices}}(\text{Correct Choice}) < 0.5$, knowing $p_\theta^{\text{Choices}}(\text{Correct Choice})$ contains little information about Accuracy and vice versa. Two example benchmarks shown: MMLU Conceptual Physics (Hendrycks et al., 2020), SciQ (Welbl et al., 2017).

correlations > 0.75 . Transforming $p_\theta^{\text{Choices}}(\text{Correct Choice})$ into Accuracy (Fig. 3D) furthers that decrease; only 20% of samples hold correlations > 0.75 . To quantitatively test whether these transformations indeed decrease the correlation between scores and compute, we measured four statistics of these score-compute correlation distributions: the mean, the median, the area under the survival function and the negative of the minimum of two Wasserstein distances to ideal (anti) correlated distributions. Across all four summary statistics, for all benchmarks and for all model families, we discovered a consistent ordering among metrics of the score-compute correlation distributions (Fig. 4):

$$\begin{aligned} \text{Corr}(\text{Compute}, \log p_\theta^{\text{Vocab}}(\text{Correct Choice})) \\ \geq \text{Corr}(\text{Compute}, p_\theta^{\text{Vocab}}(\text{Correct Choice})) \\ > \text{Corr}(\text{Compute}, p_\theta^{\text{Choices}}(\text{Correct Choice})) \\ > \text{Corr}(\text{Compute}, \text{Accuracy}) \end{aligned}$$

4. Unknown Incorrect-Choice Probabilities Produce Unpredictability

What is the mechanism that causes this deterioration of correlations between scores and compute? Metrics with degraded correlations - depend not just on how the model's probability mass concentrates on the correct choice as compute increases, but also depend on how the model's probability mass fluctuates on incorrect available choices as compute increases. To demonstrate how drastically the probability mass placed on incorrect choices can alter performance, we visualized how $p_\theta^{\text{Vocab}}(\text{Correct Choice})$ relates to metrics that rely on probabilities assigned to each incorrect choice (Fig. 5). Once performance is evaluated using a metric which is a function of the incorrect choices, i.e. for $p_\theta^{\text{Choices}}(\text{Correct Choice})$ and for Accuracy, nearly any value of a score under one metric can map to any value of $p_\theta^{\text{Vocab}}(\text{Correct Choice})$ or $p_\theta^{\text{Choices}}(\text{Correct Choice})$ respectively (Fig. 5).

References

- Achiam, J., Adler, S., Agarwal, S., Ahmad, L., Akkaya, I., Aleman, F. L., Almeida, D., Altenschmidt, J., Altman, S., Anadkat, S., et al. Gpt-4 technical report. *arXiv preprint arXiv:2303.08774*, 2023.
- AI, T. Releasing 3b and 7b redpajama-incite family of models including base, instruction-tuned & chat models. <https://www.together.ai/blog/redpajama-models-v1>, 2023. Accessed: 2024-05-19.
- Amini, A., Gabriel, S., Lin, S., Koncel-Kedziorski, R., Choi, Y., and Hajishirzi, H. MathQA: Towards interpretable math word problem solving with operation-based formalisms. In Burstein, J., Doran, C., and Solorio, T. (eds.), *Proceedings of the 2019 Conference of the North American Chapter of the Association for Computational Linguistics: Human Language Technologies, Volume 1 (Long and Short Papers)*, pp. 2357–2367, Minneapolis, Minnesota, June 2019. Association for Computational Linguistics. doi: 10.18653/v1/N19-1245. URL <https://aclanthology.org/N19-1245>.
- Anthropic. Anthropic’s responsible scaling policy. <https://www.anthropic.com/news/anthropics-responsible-scaling-policy>, 2023. Accessed: 2024-05-19.
- Anthropic. Introducing the next generation of claude. <https://www.anthropic.com/news/claude-3-family>, 2024. Accessed: 2024-05-19.
- Beeching, E., Fourrier, C., Habib, N., Han, S., Lambert, N., Rajani, N., Sanseviero, O., Tunstall, L., and Wolf, T. Open llm leaderboard. https://huggingface.co/spaces/HuggingFaceH4/open_llm_leaderboard, 2023.
- Besiroglu, T., Erdil, E., Barnett, M., and You, J. Chinchilla scaling: A replication attempt, 2024.
- Biderman, S., Prashanth, U. S., Sutawika, L., Schoelkopf, H., Anthony, Q., Purohit, S., and Raff, E. Emergent and predictable memorization in large language models, 2023a.
- Biderman, S., Schoelkopf, H., Anthony, Q., Bradley, H., O’Brien, K., Hallahan, E., Khan, M. A., Purohit, S., Prashanth, U. S., Raff, E., Skowron, A., Sutawika, L., and van der Wal, O. Pythia: A suite for analyzing large language models across training and scaling, 2023b.
- Biderman, S., Schoelkopf, H., Sutawika, L., Gao, L., Tow, J., Abbasi, B., Aji, A. F., Ammanamanchi, P. S., Black, S., Clive, J., DiPofi, A., Etxaniz, J., Fattori, B., Forde, J. Z., Foster, C., Jaiswal, M., Lee, W. Y., Li, H., Lovering, C., Muennighoff, N., Pavlick, E., Phang, J., Skowron, A., Tan, S., Tang, X., Wang, K. A., Winata, G. I., Yvon, F., and Zou, A. Lessons from the trenches on reproducible evaluation of language models. *arXiv preprint*, 2024.
- Bisk, Y., Zellers, R., Bras, R. L., Gao, J., and Choi, Y. Piqa: Reasoning about physical commonsense in natural language. 2020.
- Bowman, S. R. Eight things to know about large language models, 2023.
- Brown, T., Mann, B., Ryder, N., Subbiah, M., Kaplan, J. D., Dhariwal, P., Neelakantan, A., Shyam, P., Sastry, G., Askell, A., et al. Language models are few-shot learners. *Advances in neural information processing systems*, 33: 1877–1901, 2020.
- Clark, A., De Las Casas, D., Guy, A., Mensch, A., Paganini, M., Hoffmann, J., Damoc, B., Hechtman, B., Cai, T., Borgeaud, S., et al. Unified scaling laws for routed language models. In *International Conference on Machine Learning*, pp. 4057–4086. PMLR, 2022.
- Clark, P., Cowhey, I., Etzioni, O., Khot, T., Sabharwal, A., Schoenick, C., and Tafjord, O. Think you have solved question answering? try arc, the ai2 reasoning challenge. *arXiv preprint arXiv:1803.05457*, 2018.
- contributors, W. Survival function, 2023. URL https://en.wikipedia.org/wiki/Survival_function. [Online; accessed 22-May-2024].
- DeepSeek-AI, : Bi, X., Chen, D., Chen, G., Chen, S., Dai, D., Deng, C., Ding, H., Dong, K., Du, Q., Fu, Z., Gao, H., Gao, K., Gao, W., Ge, R., Guan, K., Guo, D., Guo, J., Hao, G., Hao, Z., He, Y., Hu, W., Huang, P., Li, E., Li, G., Li, J., Li, Y., Li, Y. K., Liang, W., Lin, F., Liu, A. X., Liu, B., Liu, W., Liu, X., Liu, X., Liu, Y., Lu, H., Lu, S., Luo, F., Ma, S., Nie, X., Pei, T., Piao, Y., Qiu, J., Qu, H., Ren, T., Ren, Z., Ruan, C., Sha, Z., Shao, Z., Song, J., Su, X., Sun, J., Sun, Y., Tang, M., Wang, B., Wang, P., Wang, S., Wang, Y., Wang, Y., Wu, T., Wu, Y., Xie, X., Xie, Z., Xie, Z., Xiong, Y., Xu, H., Xu, R. X., Xu, Y., Yang, D., You, Y., Yu, S., Yu, X., Zhang, B., Zhang, H., Zhang, L., Zhang, L., Zhang, M., Zhang, M., Zhang, W., Zhang, Y., Zhao, C., Zhao, Y., Zhou, S., Zhou, S., Zhu, Q., and Zou, Y. Deepseek llm: Scaling open-source language models with longtermism, 2024.
- Dey, N., Gosal, G., Zhiming, Chen, Khachane, H., Marshall, W., Pathria, R., Tom, M., and Hestness, J. Cerebras-gpt: Open compute-optimal language models trained on the cerebras wafer-scale cluster, 2023.

- 330 Dragan, A., King, H., and Dafoe, A. Introducing
 331 the frontier safety framework. <https://deepmind.google/discover/blog/introducing-the-frontier-safety-framework/>,
 332 2024. Accessed: 2024-05-19.
- 333 Du, Z., Zeng, A., Dong, Y., and Tang, J. Understanding
 334 emergent abilities of language models from the loss perspective, 2024.
- 335 Gadre, S. Y., Smyrnis, G., Shankar, V., Gururangan, S.,
 336 Wortsman, M., Shao, R., Mercat, J., Fang, A., Li, J.,
 337 Keh, S., Xin, R., Nezhurina, M., Vasiljevic, I., Jitsev, J.,
 338 Dimakis, A. G., Ilharco, G., Song, S., Kollar, T., Carmon,
 339 Y., Dave, A., Heckel, R., Muennighoff, N., and Schmidt,
 340 L. Language models scale reliably with over-training and
 341 on downstream tasks, 2024.
- 342 Ganguli, D., Hernandez, D., Lovitt, L., Askell, A., Bai, Y.,
 343 Chen, A., Conerly, T., Dassarma, N., Drain, D., Elhage,
 344 N., et al. Predictability and surprise in large generative
 345 models. In *2022 ACM Conference on Fairness, Accountability, and Transparency*, pp. 1747–1764, 2022.
- 346 Gao, L., Schulman, J., and Hilton, J. Scaling laws for reward
 347 model overoptimization, 2022.
- 348 Gao, L., Tow, J., Abbasi, B., Biderman, S., Black, S., DiPofi,
 349 A., Foster, C., Golding, L., Hsu, J., Le Noac'h, A., Li,
 350 H., McDonell, K., Muennighoff, N., Ociepa, C., Phang,
 351 J., Reynolds, L., Schoelkopf, H., Skowron, A., Sutawika,
 352 L., Tang, E., Thite, A., Wang, B., Wang, K., and Zou,
 353 A. A framework for few-shot language model evaluation,
 354 12 2023. URL <https://zenodo.org/records/10256836>.
- 355 Gordon, M. A., Duh, K., and Kaplan, J. Data and parameter
 356 scaling laws for neural machine translation. In *Proceedings of the 2021 Conference on Empirical Methods in
 357 Natural Language Processing*, pp. 5915–5922, 2021.
- 358 Groeneveld, D., Beltagy, I., Walsh, P., Bhagia, A., Kinney,
 359 R., Tafjord, O., Jha, A. H., Ivison, H., Magnusson, I.,
 360 Wang, Y., Arora, S., Atkinson, D., Author, R., Chandu,
 361 K. R., Cohan, A., Dumas, J., Elazar, Y., Gu, Y., Hessel,
 362 J., Khot, T., Merrill, W., Morrison, J., Muennighoff, N.,
 363 Naik, A., Nam, C., Peters, M. E., Pyatkin, V., Ravichander,
 364 A., Schwenk, D., Shah, S., Smith, W., Strubell, E.,
 365 Subramani, N., Wortsman, M., Dasigi, P., Lambert, N.,
 366 Richardson, K., Zettlemoyer, L., Dodge, J., Lo, K., Sol-
 367 daini, L., Smith, N. A., and Hajishirzi, H. Olmo: Accelerating
 368 the science of language models, 2024.
- 369 Hendrycks, D., Burns, C., Basart, S., Zou, A., Mazeika,
 370 M., Song, D., and Steinhardt, J. Measuring massive
 371 multitask language understanding. *arXiv preprint arXiv:2009.03300*, 2020.
- 372 Hendrycks, D., Burns, C., Kadavath, S., Arora, A., Basart,
 373 S., Tang, E., Song, D., and Steinhardt, J. Measuring mathematical problem solving with the math dataset. 2021.
- 374 Henighan, T., Kaplan, J., Katz, M., Chen, M., Hesse, C.,
 375 Jackson, J., Jun, H., Brown, T. B., Dhariwal, P., Gray, S.,
 376 et al. Scaling laws for autoregressive generative modeling.
 377 *arXiv preprint arXiv:2010.14701*, 2020.
- 378 Hernandez, D., Kaplan, J., Henighan, T., and McCandlish,
 379 S. Scaling laws for transfer. *arXiv preprint arXiv:2102.01293*, 2021.
- 380 Hernandez, D., Brown, T., Conerly, T., DasSarma, N.,
 381 Drain, D., El-Showk, S., Elhage, N., Hatfield-Dodds,
 382 Z., Henighan, T., Hume, T., et al. Scaling laws and interpretability of learning from repeated data. *arXiv preprint arXiv:2205.10487*, 2022.
- 383 Hestness, J., Narang, S., Ardalani, N., Diamos, G., Jun, H.,
 384 Kianinejad, H., Patwary, M., Ali, M., Yang, Y., and Zhou,
 385 Y. Deep learning scaling is predictable, empirically. *arXiv preprint arXiv:1712.00409*, 2017.
- 386 Hoffmann, J., Borgeaud, S., Mensch, A., Buchatskaya, E.,
 387 Cai, T., Rutherford, E., Casas, D. d. L., Hendricks, L. A.,
 388 Welbl, J., Clark, A., et al. Training compute-optimal large language models. *arXiv preprint arXiv:2203.15556*, 2022.
- 389 Hu, S., Liu, X., Han, X., Zhang, X., He, C., Zhao, W.,
 390 Lin, Y., Ding, N., Ou, Z., Zeng, G., Liu, Z., and Sun,
 391 M. Predicting emergent abilities with infinite resolution evaluation, 2024.
- 392 Huang, Y., Zhang, J., Shan, Z., and He, J. Compression
 393 represents intelligence linearly, 2024.
- 394 Isik, B., Ponomareva, N., Hazimeh, H., Paparas, D., Vassilivitskii, S., and Koyejo, S. Scaling laws for downstream task performance of large language models, 2024.
- 395 Jones, A. L. Scaling scaling laws with board games. *arXiv preprint arXiv:2104.03113*, 2021.
- 396 Joshi, M., Choi, E., Weld, D., and Zettlemoyer, L. triv-
 397 iaqa: A Large Scale Distantly Supervised Challenge Dataset for Reading Comprehension. *arXiv e-prints*, art.
 398 arXiv:1705.03551, 2017.
- 399 Kaplan, J., McCandlish, S., Henighan, T., Brown, T. B.,
 400 Chess, B., Child, R., Gray, S., Radford, A., Wu, J., and
 401 Amodei, D. Scaling laws for neural language models.
 402 *arXiv preprint arXiv:2001.08361*, 2020.
- 403 Keisuke, S., Ronan, L., Chandra, B., and Yejin, C. Winogrande: An adversarial winograd schema challenge at scale. 2019.

- 385 Kendall, M. G. A new measure of rank correlation.
 386 *Biometrika*, 30(1/2):81–93, 1938.
- 387 Kleinbaum, D. G. and Klein, M. *Survival Analysis: A
 388 Self-Learning Text*. Springer, 3 edition, 2012. ISBN
 389 978-1441966452. doi: 10.1007/978-1-4419-6646-9.
- 390 Kwiatkowski, T., Palomaki, J., Redfield, O., Collins, M.,
 391 Parikh, A., Alberti, C., Epstein, D., Polosukhin, I., Kel-
 392 csey, M., Devlin, J., Lee, K., Toutanova, K. N., Jones,
 393 L., Chang, M.-W., Dai, A., Uszkoreit, J., Le, Q., and
 394 Petrov, S. Natural questions: a benchmark for question
 395 answering research. *Transactions of the Association of
 396 Computational Linguistics*, 2019.
- 397
- 398 Lai, G., Xie, Q., Liu, H., Yang, Y., and Hovy, E. RACE:
 399 Large-scale ReADING comprehension dataset from ex-
 400 aminations. In *Proceedings of the 2017 Conference on
 401 Empirical Methods in Natural Language Processing*, pp.
 402 785–794, Copenhagen, Denmark, September 2017. Asso-
 403 ciation for Computational Linguistics. doi: 10.18653/v1/
 404 D17-1082. URL <https://aclanthology.org/D17-1082>.
- 405
- 406 Liu, Z., Qiao, A., Neiswanger, W., Wang, H., Tan, B., Tao,
 407 T., Li, J., Wang, Y., Sun, S., Pangarkar, O., Fan, R., Gu,
 408 Y., Miller, V., Zhuang, Y., He, G., Li, H., Koto, F., Tang,
 409 L., Ranjan, N., Shen, Z., Ren, X., Iriondo, R., Mu, C.,
 410 Hu, Z., Schulze, M., Nakov, P., Baldwin, T., and Xing,
 411 E. P. Llm360: Towards fully transparent open-source
 412 llms, 2023.
- 413
- 414 Lyu, C., Wu, M., and Aji, A. F. Beyond probabilities:
 415 Unveiling the misalignment in evaluating large language
 416 models. *arXiv preprint arXiv:2402.13887*, 2024.
- 417
- 418 Maloney, A., Roberts, D. A., and Sully, J. A solvable model
 419 of neural scaling laws. *arXiv preprint arXiv:2210.16859*,
 420 2022.
- 421
- 422 McCandlish, S., Kaplan, J., Amodei, D., and Team, O. D.
 423 An empirical model of large-batch training, 2018.
- 424
- 425 McKenzie, I., Lyzhov, A., Parrish, A., Prabhu, A., Mueller,
 426 A., Kim, N., Bowman, S., and Perez, E. The inverse
 427 scaling prize, 2022. URL <https://github.com/inverse-scaling/prize>.
- 428
- 429 Mihaylov, T., Clark, P., Khot, T., and Sabharwal, A. Can a
 430 suit of armor conduct electricity? a new dataset for open
 431 book question answering. In *EMNLP*, 2018.
- 432
- 433 Muckatira, S., Deshpande, V., Lialin, V., and Rumshisky, A.
 434 Emergent abilities in reduced-scale generative language
 435 models, 2024.
- 436
- 437 Muennighoff, N., Wang, T., Sutawika, L., Roberts, A., Bi-
 438 derman, S., Scao, T. L., Bari, M. S., Shen, S., Yong,
 439 Z.-X., Schoelkopf, H., Tang, X., Radev, D., Aji, A. F., Al-
 440 mubarak, K., Albanie, S., Alyafeai, Z., Webson, A., Raff,
 441 E., and Raffel, C. Crosslingual generalization through
 442 multitask finetuning, 2023.
- 443
- 444 Muennighoff, N., Rush, A., Barak, B., Le Scao, T., Tazi,
 445 N., Piktus, A., Pyysalo, S., Wolf, T., and Raffel, C. A.
 446 Scaling data-constrained language models. *Advances in
 447 Neural Information Processing Systems*, 36, 2024.
- 448
- 449 Neumann, O. and Gros, C. Scaling laws for a multi-
 450 agent reinforcement learning model. *arXiv preprint
 451 arXiv:2210.00849*, 2022.
- 452
- 453 OpenAI. Openai’s approach to frontier risk.
<https://openai.com/global-affairs/our-approach-to-frontier-risk/>, 2023.
 Accessed: 2024-05-19.
- 454
- 455 OpenAI. Hello gpt-4o. <https://openai.com/index/hello-gpt-4o/>, 2024. Accessed: 2024-05-16.
- 456
- 457 OpenAI, Achiam, J., Adler, S., Agarwal, S., Ahmad, L.,
 458 Akkaya, I., Aleman, F. L., Almeida, D., Altenschmidt, J.,
 459 Altman, S., Anadkat, S., Avila, R., Babuschkin, I., Bal-
 460 aji, S., Balcom, V., Baltescu, P., Bao, H., Bavarian, M.,
 461 Belgum, J., Bello, I., Berdine, J., Bernadett-Shapiro, G.,
 462 Berner, C., Bogdonoff, L., Boiko, O., Boyd, M., Brakman,
 463 A.-L., Brockman, G., Brooks, T., Brundage, M., Button,
 464 K., Cai, T., Campbell, R., Cann, A., Carey, B., Carlson,
 465 C., Carmichael, R., Chan, B., Chang, C., Chantzis, F.,
 466 Chen, D., Chen, S., Chen, R., Chen, J., Chen, M., Chess,
 467 B., Cho, C., Chu, C., Chung, H. W., Cummings, D., Cur-
 468 rier, J., Dai, Y., Decareaux, C., Degry, T., Deutsch, N.,
 469 Deville, D., Dhar, A., Dohan, D., Dowling, S., Dunning,
 470 S., Ecoffet, A., Eleti, A., Eloundou, T., Farhi, D., Fedus,
 471 L., Felix, N., Fishman, S. P., Forte, J., Fulford, I., Gao, L.,
 472 Georges, E., Gibson, C., Goel, V., Gogineni, T., Goh, G.,
 473 Gontijo-Lopes, R., Gordon, J., Grafstein, M., Gray, S.,
 474 Greene, R., Gross, J., Gu, S. S., Guo, Y., Hallacy, C., Han,
 475 J., Harris, J., He, Y., Heaton, M., Heidecke, J., Hesse,
 476 C., Hickey, A., Hickey, W., Hoeschele, P., Houghton, B.,
 477 Hsu, K., Hu, S., Hu, X., Huizinga, J., Jain, S., Jain, S.,
 478 Jang, J., Jiang, A., Jiang, R., Jin, H., Jin, D., Jomoto, S.,
 479 Jonn, B., Jun, H., Kaftan, T., Łukasz Kaiser, Kamali, A.,
 480 Kanitscheider, I., Keskar, N. S., Khan, T., Kilpatrick, L.,
 481 Kim, J. W., Kim, C., Kim, Y., Kirchner, J. H., Kiros, J.,
 482 Knight, M., Kokotajlo, D., Łukasz Kondraciuk, Kondrich,
 483 A., Konstantinidis, A., Kosic, K., Krueger, G., Kuo, V.,
 484 Lampe, M., Lan, I., Lee, T., Leike, J., Leung, J., Levy, D.,
 485 Li, C. M., Lim, R., Lin, M., Lin, S., Litwin, M., Lopez, T.,
 486 Lowe, R., Lue, P., Makanju, A., Malfacini, K., Manning,
 487 S., Markov, T., Markovski, Y., Martin, B., Mayer, K.,
 488 Mayne, A., McGrew, B., McKinney, S. M., McLeavey, C.,
 489 McMillan, P., McNeil, J., Medina, D., Mehta, A., Menick,

- 440 J., Metz, L., Mishchenko, A., Mishkin, P., Monaco, V.,
 441 Morikawa, E., Mossing, D., Mu, T., Murati, M., Murk, O.,
 442 Mély, D., Nair, A., Nakano, R., Nayak, R., Neelakantan,
 443 A., Ngo, R., Noh, H., Ouyang, L., O'Keefe, C., Pachocki,
 444 J., Paino, A., Palermo, J., Pantuliano, A., Parascandolo,
 445 G., Parish, J., Parparita, E., Passos, A., Pavlov, M., Peng,
 446 A., Perelman, A., de Avila Belbute Peres, F., Petrov, M.,
 447 de Oliveira Pinto, H. P., Michael, Pokorny, Pokrass, M.,
 448 Pong, V. H., Powell, T., Power, A., Power, B., Proehl, E.,
 449 Puri, R., Radford, A., Rae, J., Ramesh, A., Raymond, C.,
 450 Real, F., Rimbach, K., Ross, C., Rotstod, B., Roussez,
 451 H., Ryder, N., Saltarelli, M., Sanders, T., Santurkar, S.,
 452 Sastry, G., Schmidt, H., Schnurr, D., Schulman, J., Sel-
 453 sam, D., Sheppard, K., Sherbakov, T., Shieh, J., Shoker,
 454 S., Shyam, P., Sidor, S., Sigler, E., Simens, M., Sitkin,
 455 J., Slama, K., Sohl, I., Sokolowsky, B., Song, Y., Stau-
 456 dacher, N., Such, F. P., Summers, N., Sutskever, I., Tang,
 457 J., Tezak, N., Thompson, M. B., Tillet, P., Tootoonchian,
 458 A., Tseng, E., Tuggle, P., Turley, N., Tworek, J., Uribe, J.
 459 F. C., Vallone, A., Vijayvergiya, A., Voss, C., Wainwright,
 460 C., Wang, J. J., Wang, A., Wang, B., Ward, J., Wei, J.,
 461 Weinmann, C., Welihinda, A., Welinder, P., Weng, J.,
 462 Weng, L., Wiethoff, M., Willner, D., Winter, C., Wolrich,
 463 S., Wong, H., Workman, L., Wu, S., Wu, J., Wu, M.,
 464 Xiao, K., Xu, T., Yoo, S., Yu, K., Yuan, Q., Zaremba,
 465 W., Zellers, R., Zhang, C., Zhang, M., Zhao, S., Zheng,
 466 T., Zhuang, J., Zhuk, W., and Zoph, B. Gpt-4 technical
 467 report, 2024.
- 468 Owen, D. How predictable is language model benchmark
 469 performance?, 2024.
- 470 Reid, M., Savinov, N., Teplyashin, D., Lepikhin, D., Lilli-
 471 crap, T., Alayrac, J.-b., Soricut, R., Lazaridou, A., Firat,
 472 O., Schrittwieser, J., et al. Gemini 1.5: Unlocking multi-
 473 modal understanding across millions of tokens of context.
 474 *arXiv preprint arXiv:2403.05530*, 2024.
- 475 Rosenfeld, J. S., Rosenfeld, A., Belinkov, Y., and Shavit,
 476 N. A constructive prediction of the generalization error
 477 across scales. In *International Conference on Learning
 478 Representations*, 2019.
- 479 Ruan, Y., Maddison, C. J., and Hashimoto, T. Observational
 480 scaling laws and the predictability of language model
 481 performance, 2024.
- 482 Sap, M., Rashkin, H., Chen, D., Le Bras, R., and Choi,
 483 Y. Social iqqa: Commonsense reasoning about social
 484 interactions. In *Proceedings of the 2019 Conference
 485 on Empirical Methods in Natural Language Processing
 486 and the 9th International Joint Conference on Natural
 487 Language Processing (EMNLP-IJCNLP)*, 2019a.
- 488 Sap, M., Rashkin, H., Chen, D., Le Bras, R., and Choi, Y.
 489 Socialiqqa: Commonsense reasoning about social interac-
 490 tions, 2019b.
- 491 Sardana, N. and Frankle, J. Beyond chinchilla-optimal:
 492 Accounting for inference in language model scaling laws,
 493 2023.
- 494 Schaeffer, R., Miranda, B., and Koyejo, S. Are emerg-
 495 ent abilities of large language models a mirage? In Oh,
 496 A., Naumann, T., Globerson, A., Saenko, K., Hardt,
 497 M., and Levine, S. (eds.), *Advances in Neural
 498 Information Processing Systems*, volume 36, pp. 55565–55581. Curran Associates, Inc.,
 499 2023. URL https://proceedings.neurips.cc/paper_files/paper/2023/file/adc98a266f45005c403b8311ca7e8bd7-Paper-Conference.pdf.
- 500 Spearman, C. The proof and measurement of association
 501 between two things. 1961.
- 502 Srivastava, A., Rastogi, A., Rao, A., Shoeb, A. A. M., Abid,
 503 A., Fisch, A., Brown, A. R., Santoro, A., Gupta, A.,
 504 Garriga-Alonso, A., et al. Beyond the imitation game:
 505 Quantifying and extrapolating the capabilities of language
 506 models. *arXiv preprint arXiv:2206.04615*, 2022.
- 507 Team, G., Anil, R., Borgeaud, S., Wu, Y., Alayrac, J.-B., Yu,
 508 J., Soricut, R., Schalkwyk, J., Dai, A. M., Hauth, A., et al.
 509 Gemini: a family of highly capable multimodal models.
 510 *arXiv preprint arXiv:2312.11805*, 2023.
- 511 Wei, J., Tay, Y., Bommasani, R., Raffel, C., Zoph, B.,
 512 Borgeaud, S., Yogatama, D., Bosma, M., Zhou, D., Met-
 513 zler, D., et al. Emergent abilities of large language models.
 514 *arXiv preprint arXiv:2206.07682*, 2022.
- 515 Welbl, J., Liu, N. F., and Gardner, M. Crowdsourcing
 516 multiple choice science questions. In Derczynski, L., Xu,
 517 W., Ritter, A., and Baldwin, T. (eds.), *Proceedings of the
 518 3rd Workshop on Noisy User-generated Text*, pp. 94–106,
 519 Copenhagen, Denmark, September 2017. Association for
 520 Computational Linguistics. doi: 10.18653/v1/W17-4413.
 521 URL <https://aclanthology.org/W17-4413>.
- 522 Zellers, R., Holtzman, A., Bisk, Y., Farhadi, A., and Choi,
 523 Y. Hellaswag: Can a machine really finish your sentence?
 524 *arXiv preprint arXiv:1905.07830*, 2019.
- 525 Zhai, X., Kolesnikov, A., Houlsby, N., and Beyer, L. Scaling
 526 vision transformers. In *Proceedings of the IEEE/CVF
 527 Conference on Computer Vision and Pattern Recognition*,
 528 pp. 12104–12113, 2022.
- 529 Zhou, B., Khashabi, D., Ning, Q., and Roth, D. “going
 530 on a vacation” takes longer than “going for a walk”: A
 531 study of temporal commonsense understanding. In Inui,
 532 K., Jiang, J., Ng, V., and Wan, X. (eds.), *Pro-
 533 ceedings of the 2019 Conference on Empirical Meth-
 534 ods in Natural Language Processing and the 9th In-*

495 *ternational Joint Conference on Natural Language Pro-*
496 *cessing (EMNLP-IJCNLP)*, pp. 3363–3369, Hong Kong,
497 China, November 2019. Association for Computational
498 Linguistics. doi: 10.18653/v1/D19-1332. URL <https://aclanthology.org/D19-1332>.
499
500
501
502
503
504
505
506
507
508
509
510
511
512
513
514
515
516
517
518
519
520
521
522
523
524
525
526
527
528
529
530
531
532
533
534
535
536
537
538
539
540
541
542
543
544
545
546
547
548
549

550 A. Related Work

551 **Language Model Evaluation** The capabilities of AI models are typically evaluated using constructed datasets to assess
 552 performance on a specific task, acting as a proxy for some real-world usage scenario. However, performing robust and
 553 reliable evaluations is a challenge, with many potential pitfalls and unsolved problems (Biderman et al., 2024). For example,
 554 we might prefer to ask models open-ended questions and evaluate their answers in natural language, but it then often
 555 becomes difficult to robustly score the resulting model outputs, especially for partial correctness. For this reason, it is
 556 common practice for evaluation benchmarks to simplify their scoring via approximations, such as extracting a sub-string
 557 from free-form outputs heuristically (Joshi et al., 2017; Kwiatkowski et al., 2019; Hendrycks et al., 2021) and checking that
 558 it matches a specific gold target string, or casting a task to a *multiple-choice* format, in which a closed set of correct and
 559 incorrect answers is known, and the model’s answer is determined by selecting the most likely option among these strings.
 560 For more details on the precise procedures typically used for multiple choice elsewhere in the literature, see Biderman et al.
 561 (2024). We believe that the multiple-choice format is valuable, due to its flexibility, popularity and relevance (Brown et al.,
 562 2020; Beeching et al., 2023; Biderman et al., 2024), but we discuss its limitations in Section ??.

563
 564
 565 **Scaling Laws** Many neural networks exhibit power-law scaling of the pretraining loss as a function of the amount of
 566 compute, data, or parameters used for training (Hestness et al., 2017; Brown et al., 2020; Hoffmann et al., 2022). These
 567 neural scaling laws demonstrate that the pretraining loss can be highly predictable as a function of these fundamental
 568 inputs, which has a number of practical applications: Scaling laws fit to smaller training runs can be used to predict the
 569 pretraining loss of a much larger training run, and can be used to determine effective hyperparameters (McCandlish et al.,
 570 2018; DeepSeek-AI et al., 2024), or the optimal allocation of dataset and model size for a given compute budget (Hoffmann
 571 et al., 2022; Muennighoff et al., 2024; Dey et al., 2023; Sardana & Frankle, 2023; Besiroglu et al., 2024). In some cases,
 572 such laws can be used to predict performance of a larger model in a particular domain, such as coding (Achiam et al., 2023).
 573 The existence of scaling laws turns deep learning into a predictable science at the macro level by providing a simple recipe
 574 for improving model quality and de-risking returns on increasing investment into scale (Ganguli et al., 2022; Bowman,
 575 2023).

576
 577
 578 **Emergent Abilities** Language models have been observed to exhibit apparent *emergent abilities*—behaviors on down-
 579 stream task performance that cannot be predicted from smaller scales (Wei et al., 2022; Srivastava et al., 2022). Emergence
 580 appears not to be simply a product of training compute or model size, but is also dependent on other factors such as dataset
 581 composition (Muckatira et al., 2024; Wei et al., 2022). Schaeffer et al. (2023) find that some emergent phenomena can be a
 582 “mirage” arising due to choices made by researchers such as the use of discontinuous metrics and insufficient resolution.
 583 However, Du et al. (2024) note that for many tasks, emergence remains despite the use of continuous metrics. Additionally,
 584 discontinuous metrics have been argued to often be the most reflective of real-world usefulness, so emergence in these hard
 585 metrics is important. Hu et al. (2024) found that for generative evaluations, infinite resolution can be achieved but requires
 586 significant compute and that generated answer be verifiable.

587
 588
 589 **Predicting Downstream Task Performance** Although predicting macroscopic pretraining loss is useful, a far more
 590 useful goal is to predict the scaling of model performance on particular downstream tasks or domains. If this was possible,
 591 then model developers could tune their datasets and training procedures in a more fine-grained way before launching
 592 computationally intensive training runs. Model performance on a particular downstream task is typically correlated with
 593 compute, albeit with a few exceptions (McKenzie et al., 2022; Huang et al., 2024). However, despite attempts to fit scaling
 594 laws to values other than loss, including benchmark scores (Gadre et al., 2024; Isik et al., 2024), model memorization
 595 (Biderman et al., 2023a), or reward (Gao et al., 2022), these downstream performance metrics are usually more noisy or
 596 require more compute to fit accurately. Owen (2024) and Gadre et al. (2024) both find that while *aggregate* benchmark
 597 performance with more compute can be predicted, the scaling behaviour of individual tasks can be noisy. Additionally,
 598 Owen (2024), Du et al. (2024) and Gadre et al. (2024) claim that predicting scaling behavior on a task without access to
 599 models exhibiting better-than-random performance (i.e., “before emergence occurs”) cannot be done reliably. Concurrently
 600 to our work, Ruan et al. (2024) propose Observational Scaling Laws by mapping model capabilities from compute to a
 601 shared low-dimensional space of capabilities across model families before predicting performance on novel tasks. Our goal
 602 in this work is to investigate the comparative unpredictability of individual downstream performance scores, and advise how
 603 to create more scaling-predictable evaluations that are closely coupled with real-world use-cases.

B. Definition of Survival Function

The survival function $S_X(x)$ – also known as the reliability function, the tail distribution, or the complementary cumulative distribution function – gives the probability that a random variable X exceeds a certain value x (Kleinbaum & Klein, 2012; contributors, 2023):

$$S_X(x) \stackrel{\text{def}}{=} \Pr[X > x] = \int_x^{\infty} f_X(x') dx' = 1 - F_X(x) \quad (1)$$

where $F_X(x) = \Pr[X \leq x]$ is the cumulative distribution function (CDF) and $f_X(x)$ is the probability density function (pdf) or probability mass function (pmf) of the random variable X . The CDF $F_X(x)$ gives the probability that the random variable X is at most x , while the survival function $S_X(x)$ gives the probability that X exceeds x .

When the true distribution of X is unknown, we can use the empirical CDF (ECDF) $\hat{F}_X(x)$ and the empirical survival function (ESF) $\hat{S}_X(x)$:

$$\hat{S}_X(x) \stackrel{\text{def}}{=} \frac{1}{n} \sum_{i=1}^n 1\{x_i > x\} = 1 - \hat{F}_X(x) \quad (2)$$

where n is the number of observations, x_i is the realized value of the random variable X for observation i , and $1\{x_i > x\}$ is the indicator function. The empirical survival function $\hat{S}_X(x)$ specifies the fraction of observations for which the sampled random variable X exceeds x .

C. Compute Resources for Experiments

Experiments were done across a wide family of model families and sizes. The GPUs we used for medium-sized models (7B parameters and above) used a single A100s with 80GB of vRAM. For smaller models (≤ 8 B) we used A100s with 80GB of vRAM, Quadro RTX 8000 with 48GB of vRAM, or RTX A4000 with 16GB of vRAM. For 70B parameter models, we used at least 2 A100 GPUs with 80GB of vRAM.

D. Additional Model Family Details

Here we provide further experimental details regarding our selection of model families.

- Pythia** (Biderman et al., 2023b): We consider two “families” for Pythia in our experiments. **Pythia (Parameter Scaling)** refers to the use of fully-trained checkpoints from 9 different model sizes (all model sizes documented in Biderman et al. (2023), as well as a 14M parameter model trained later by the authors). **Pythia-12B (Data Scaling)** refers to the use of 8 checkpoints across training for the Pythia-12B model, namely having seen 2M, 64M, 2B, 6B, 20B, 60B, 200B, and 300B tokens in training.
- Cerebras-GPT** (Dey et al., 2023): **Cerebras (Parameter and Data Scaling)** refers to our use of 1 checkpoint per model in the Cerebras-GPT family, each fully trained for differing quantities of data as documented by the model creators, for 7 checkpoints in total.
- OLMo** (Groeneveld et al., 2024): **OLMo (7B Data Scaling)** refers to the use of 7 checkpoints for OLMo-7B across training, namely, checkpoints having seen 4B, 44B, 133B, 442B, 885B, 1.5T, and 2.4T tokens.
- INCITE** (AI, 2023): **INCITE-7B (Data Scaling)** considers 6 checkpoints over training for the 7B parameter model, having seen 240B, 280B, 400B, 500B, 700B, and 1T tokens.
- LLM360** (Liu et al., 2023): **LLM360 Amber (Data Scaling)** considers 13 checkpoints of the Amber model, having seen 0B, 3.5B, 7B, 10.5B, 17.5B, 31.5B, 49B, 87.5B, 147B, 252B, 430B, 738B, and 1.26T tokens.

E. Broader Impact

This paper contributes to a better understanding of the predictability of large language models (LLMs), which can have both positive and negative societal impacts. On the positive side, by making LLM benchmarks more predictable, this research can help society anticipate and plan for potential challenges associated with their development and deployment. This increased predictability can facilitate proactive measures to mitigate risks and ensure the responsible use of AI technologies.

Why Has Predicting Downstream Capabilities of Frontier AI Models with Scale Remained Elusive?

660 However, the increased predictability of LLMs could theoretically be exploited by malicious actors to accelerate the
661 development of AI systems designed for malicious purposes. We also stress the importance of proactive risk assessment and
662 the implementation of safeguards to prevent the misuse of AI technologies.
663
664
665
666
667
668
669
670
671
672
673
674
675
676
677
678
679
680
681
682
683
684
685
686
687
688
689
690
691
692
693
694
695
696
697
698
699
700
701
702
703
704
705
706
707
708
709
710
711
712
713
714

715 **F. Scaling Behavior of Probability Mass on Incorrect Choices**

716
717 In order to accurately predict performance on multiple-choice question-answering benchmarks, one must predict not just how
718 probability mass concentrates on correct choices with scale, but how probability mass also fluctuates on incorrect choices
719 with scale. For metrics like Accuracy, these predictions *must* be made for each sample because knowing the average
720 (across many samples) mass placed on incorrect choices says little about how much mass is placed on any single incorrect
721 choice for a single sample. Achieving such a feat *might* be possible. We conduct a preliminary analysis how probability
722 mass on correct choices and probability mass on incorrect choices for samples scale with compute (Fig. 6). Although
723 preliminary, multiple benchmarks display strong positive relationships that suggest per-sample scaling laws predicting the
724 probability mass assigned to each of the *incorrect* choices might be possible. We leave this challenge to future work.

725

726

727

728

729

730

731

732

733

734

735

736

737

738

739

740

741

742

743

744

745

746

747

748

749

750

751

752

753

754

755

756

757

758

759

760

761

762

763

764

765

766

767

768

769

770
 771
 772
 773
 774
 775
 776
 777
 778
 779
 780
 781
 782
 783
 784
 785
 786
 787
 788
 789
 790
 791
 792
 793
 794
 795
 796
 797
 798
 799
 800
 801
 802
 803
 804
 805
 806
 807
 808
 809
 810
 811
 812
 813
 814
 815
 816
 817
 818
 819
 820
 821
 822
 823
 824

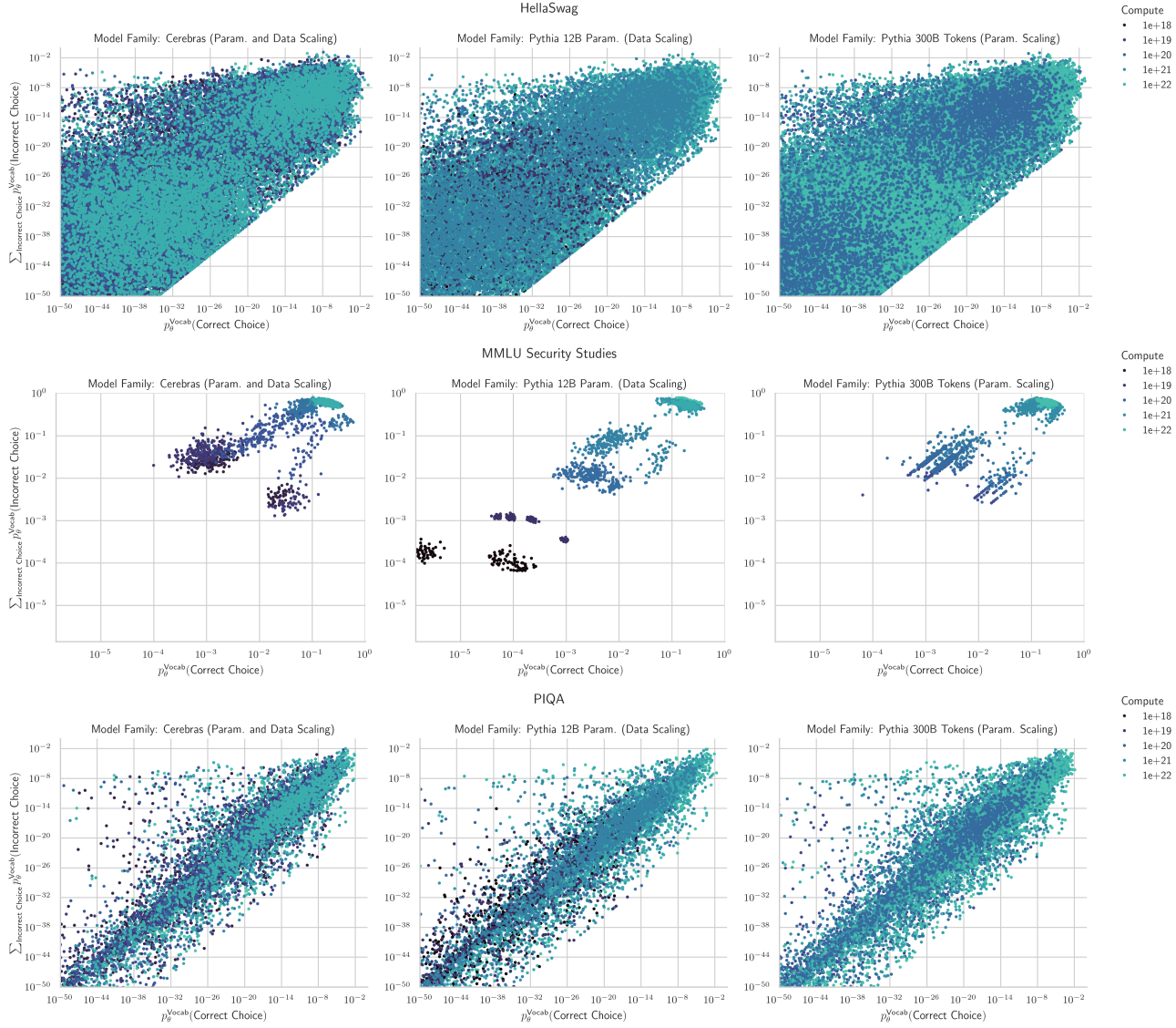


Figure 6. Probability masses on correct versus incorrect are correlated but can fluctuate substantially. We can observe clear linear correlations between the probability mass on correct choices and on incorrect choices. However, the spread is high: for any given value of $p_\theta^{\text{Vocab}}(\text{Correct Choice})$, the probability mass across incorrect choices can vary by several orders of magnitude.

825 G. Discussion, Related Work and Future Directions

826 This work presents a mechanism that explains the (lack of) predictability of downstream task performance with compute.
827 Our results have implications for the design of future evaluations for frontier AI models that are reliably predictable with
828 scaling. We hope that our work will be extended to further the science of scaling-predictable evaluation of AI systems,
829 especially for complex and important model capabilities. We note several future directions for extension of our work and we
830 hope that the community also adopts our framing to further improve scaling-predictable evaluations.
831

832 **Related Work** For a treatise of related work, please see App. A.
833

834 **Direction 1: Beyond Multiple Choice Benchmarks** Our study is restricted to benchmarks evaluated via loglikelihood-
835 based multiple-choice formats. While we believe this is inherently valuable due to the usefulness and prevalence of such
836 tasks, this limits the application of our findings. We hope that our discoveries and proposed mechanisms may be used to
837 inform the study of predictable and reliable evaluation writ large, and that future work should explore the extent to which
838 our findings can be generalized to more complex capabilities. Our findings corroborate those of Lyu et al. (2024), who
839 find that multiple-choice answer scores often diverge from generative evaluations. Consequently, a particularly important
840 direction for further study is to investigate generative evaluations, which may contain similar transformations distancing
841 performance from the observed loss.
842

843 **Direction 2: Predicting Benchmark Performance A Priori** Our work indicates a reason for multiple-choice benchmark
844 performance to not be easily predictable for metrics such as Accuracy and Brier Score, as observed in the literature (Du
845 et al., 2024). However, our analyses assume access to entire model families’ scores across several orders of magnitude of
846 pretraining FLOPs, and do not employ backtesting, as sensibly recommended by Owen (2024). A predictive model should
847 be able to identify emergence points well-before scores rise on standard metrics like Accuracy.
848

849
850
851
852
853
854
855
856
857
858
859
860
861
862
863
864
865
866
867
868
869
870
871
872
873
874
875
876
877
878
879

880

H. Score-Compute Correlation Distributions' Statistics

881

H.1. Pearson Correlations

882

883

884

885

886

887

888

889

890

891

892

893

894

895

896

897

898

899

900

901

902

903

904

905

906

907

908

909

910

911

912

913

914

915

916

917

918

919

920

921

922

923

924

925

926

927

928

929

930

931

932

933

934

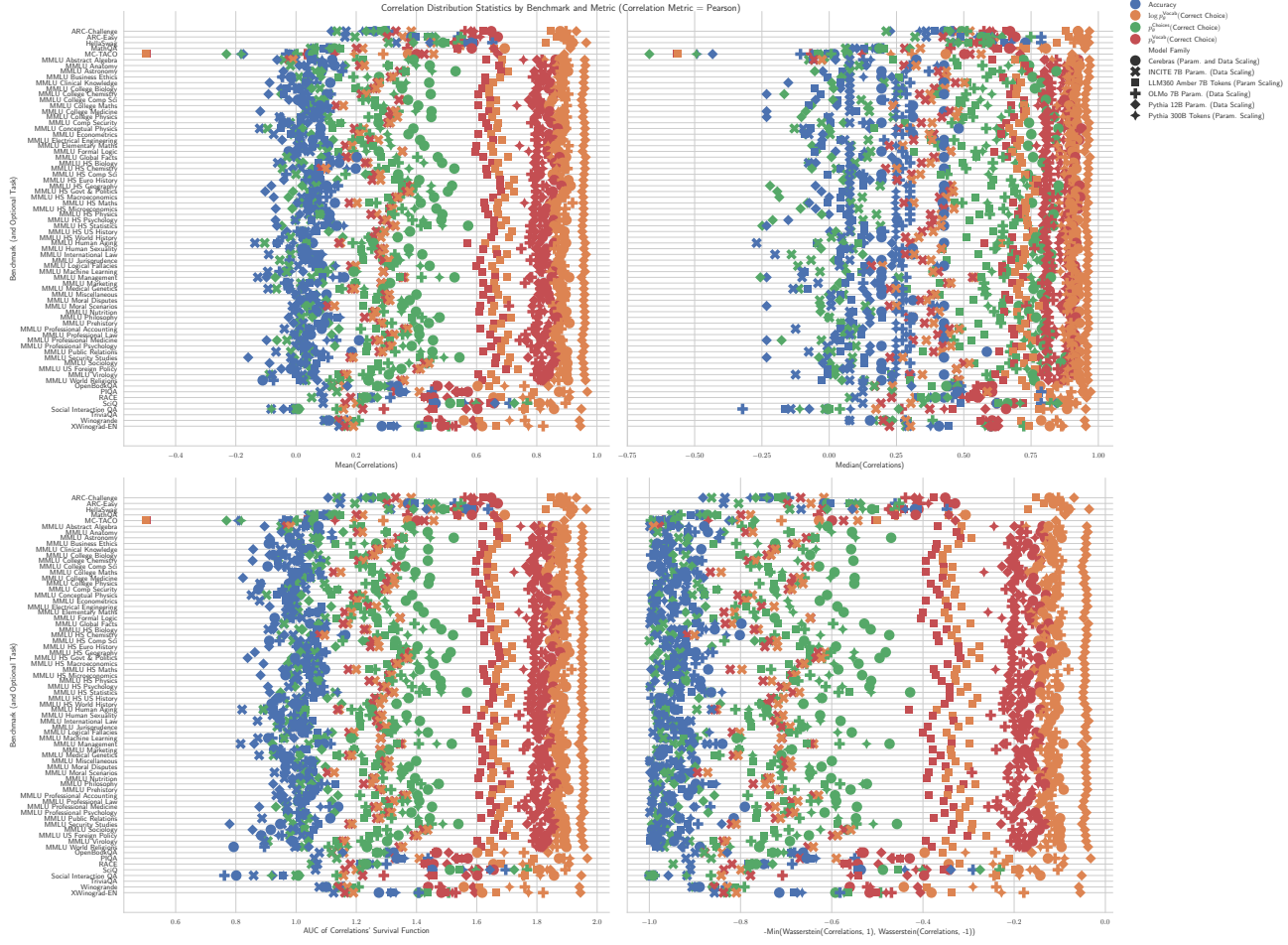
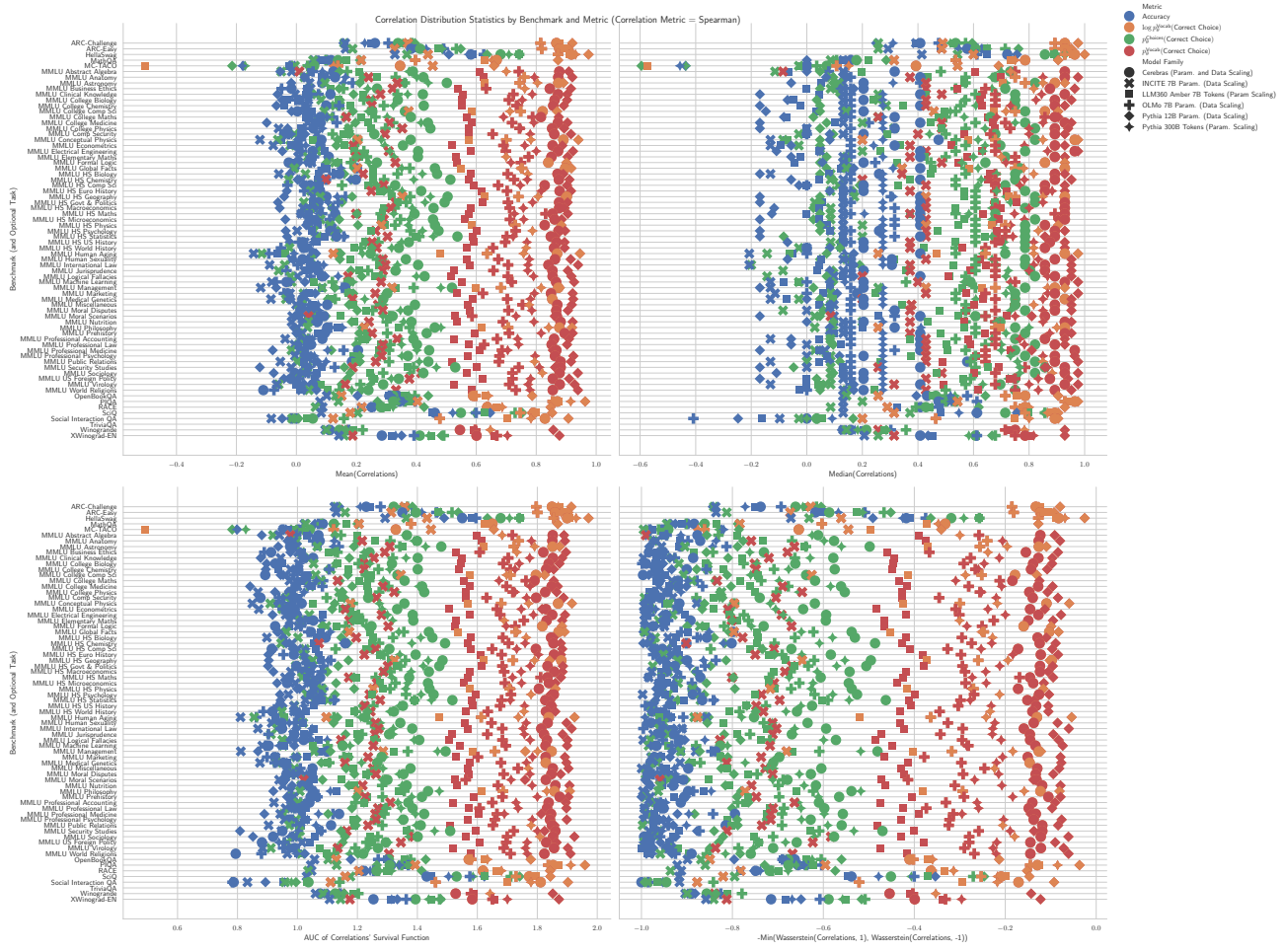


Figure 7. Statistics for empirical distributions of correlations between scores and compute for all benchmarks and model families. These correlation values were computed with Pearson correlation and are consistent with the main text's results computed with Spearman correlation (Fig. 4): The sequence of transformations from $\log p_\theta^{\text{vocab}}(\text{Correct Choice}) \rightarrow p_\theta^{\text{vocab}}(\text{Correct Choice}) \rightarrow p_\theta^{\text{Choices}}(\text{Correct Choice}) \rightarrow \text{Accuracy}$ degrades predictability.

935 H.2. Spearman Correlations
 936
 937


969 **Figure 8. Statistics for empirical distributions of correlations between scores and compute for all benchmarks and model families.**
 970 These correlation values were computed with Spearman correlation. The sequence of transformations from $\log p_\theta^{\text{vocab}}(\text{Correct Choice}) \rightarrow p_\theta^{\text{vocab}}(\text{Correct Choice}) \rightarrow p_\theta^{\text{choices}}(\text{Correct Choice}) \rightarrow \text{Accuracy}$ degrades predictability.
 971
 972
 973
 974
 975
 976
 977
 978
 979
 980
 981
 982
 983
 984
 985
 986
 987
 988
 989

H.3. Kendall Correlations

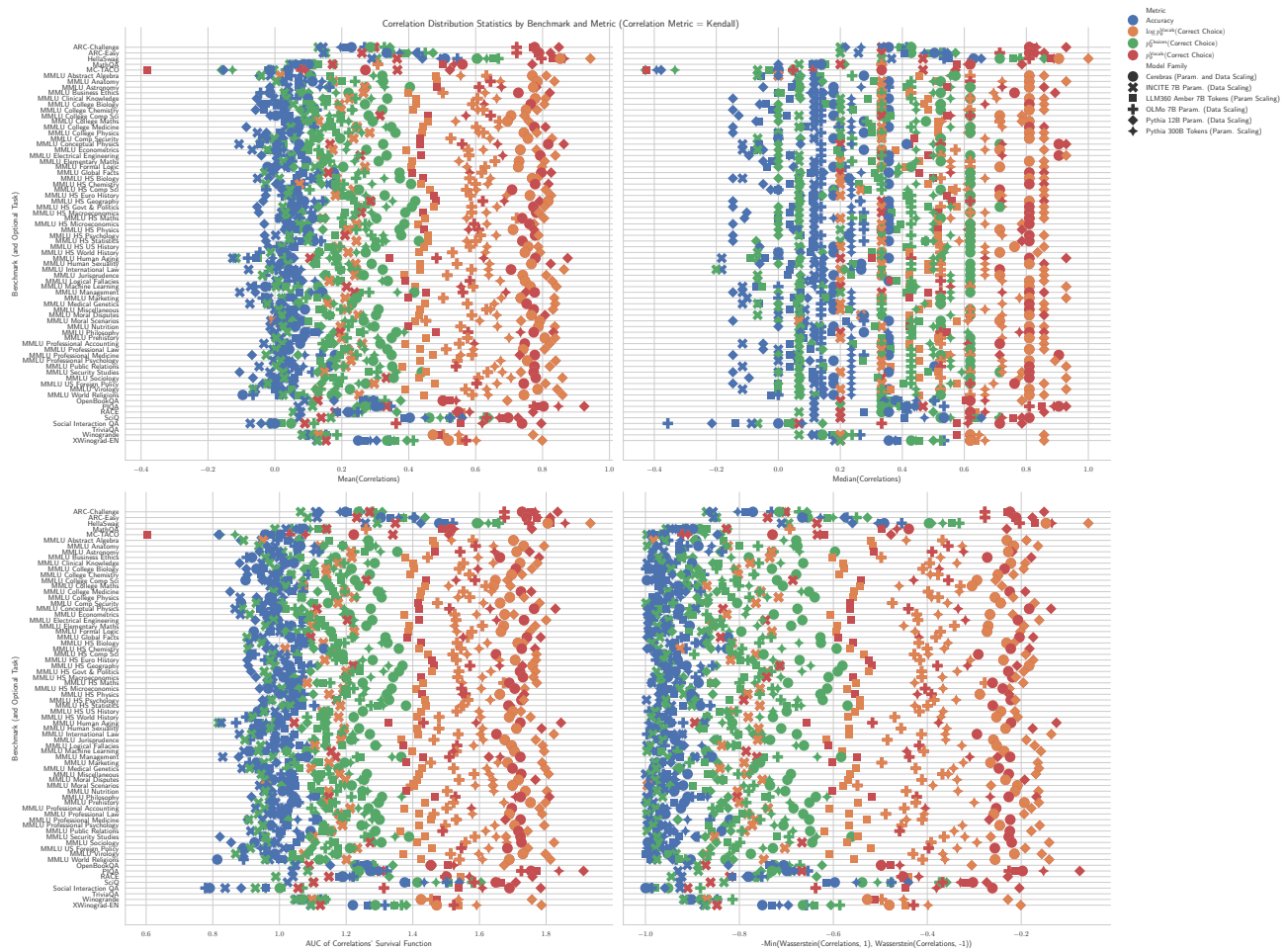


Figure 9. Statistics for empirical distributions of correlations between scores and compute for all benchmarks and model families. These correlation values were computed with Kendall correlation and are consistent with the main text's results computed with Spearman correlation (Fig. 4): The sequence of transformations from $\log p_\theta^{\text{vocab}}(\text{Correct Choice}) \rightarrow p_\theta^{\text{vocab}}(\text{Correct Choice}) \rightarrow p_\theta^{\text{Choices}}(\text{Correct Choice}) \rightarrow \text{Accuracy}$ degrades predictability.

I. Per-Benchmark Score-Compute Correlation Distributions

I.1. NLP Benchmark: ARC Challenge (Clark et al., 2018)

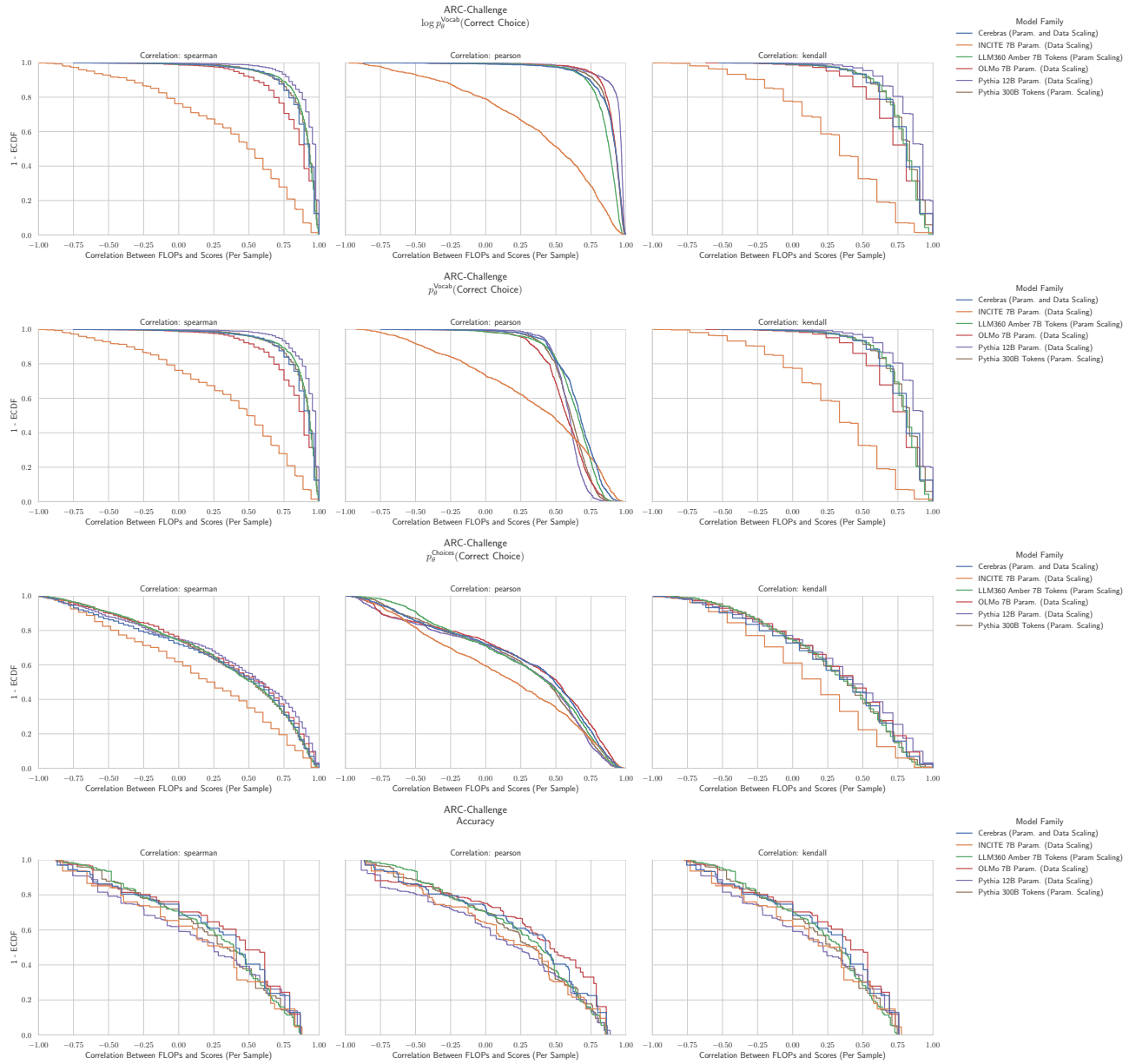
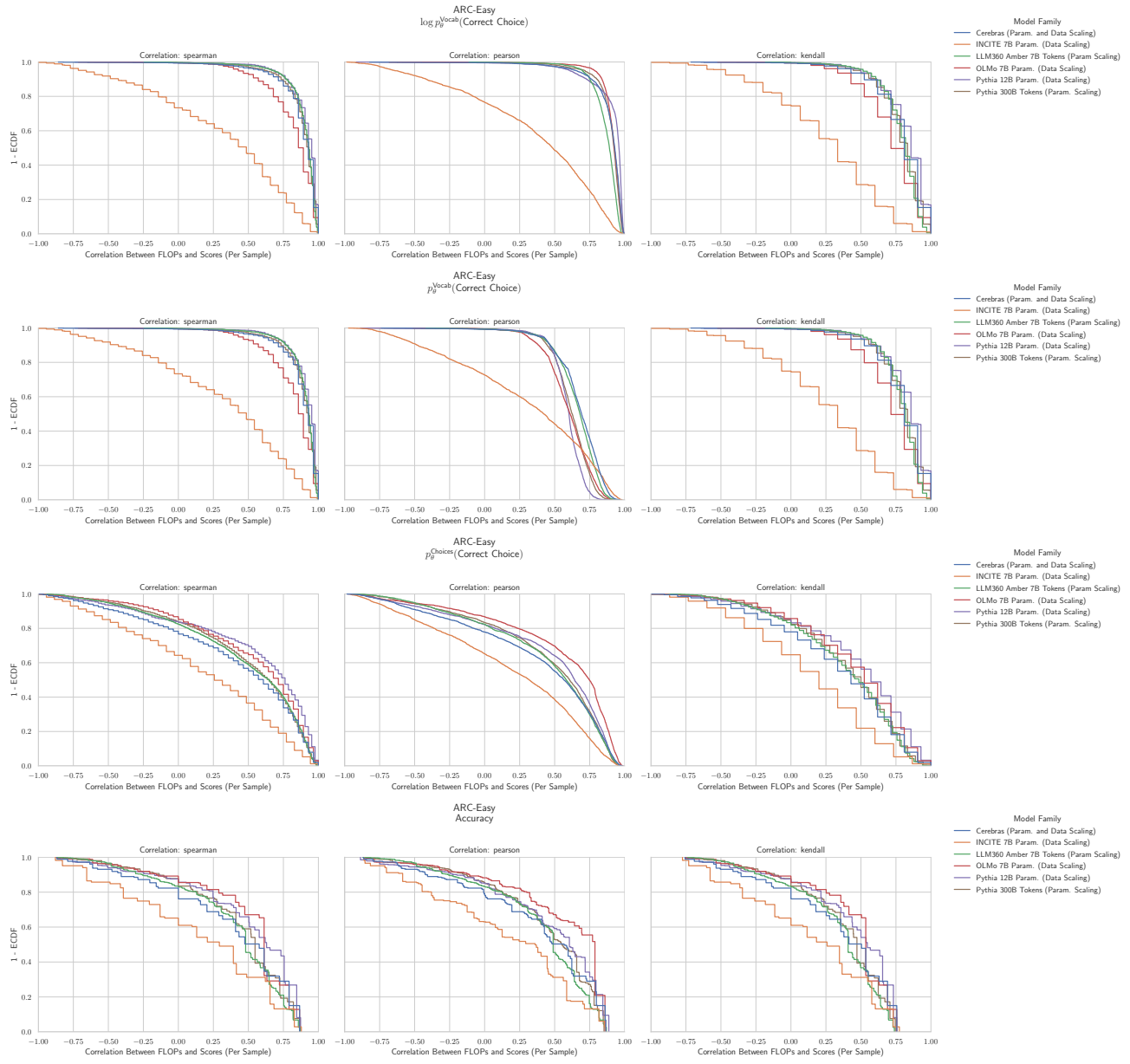
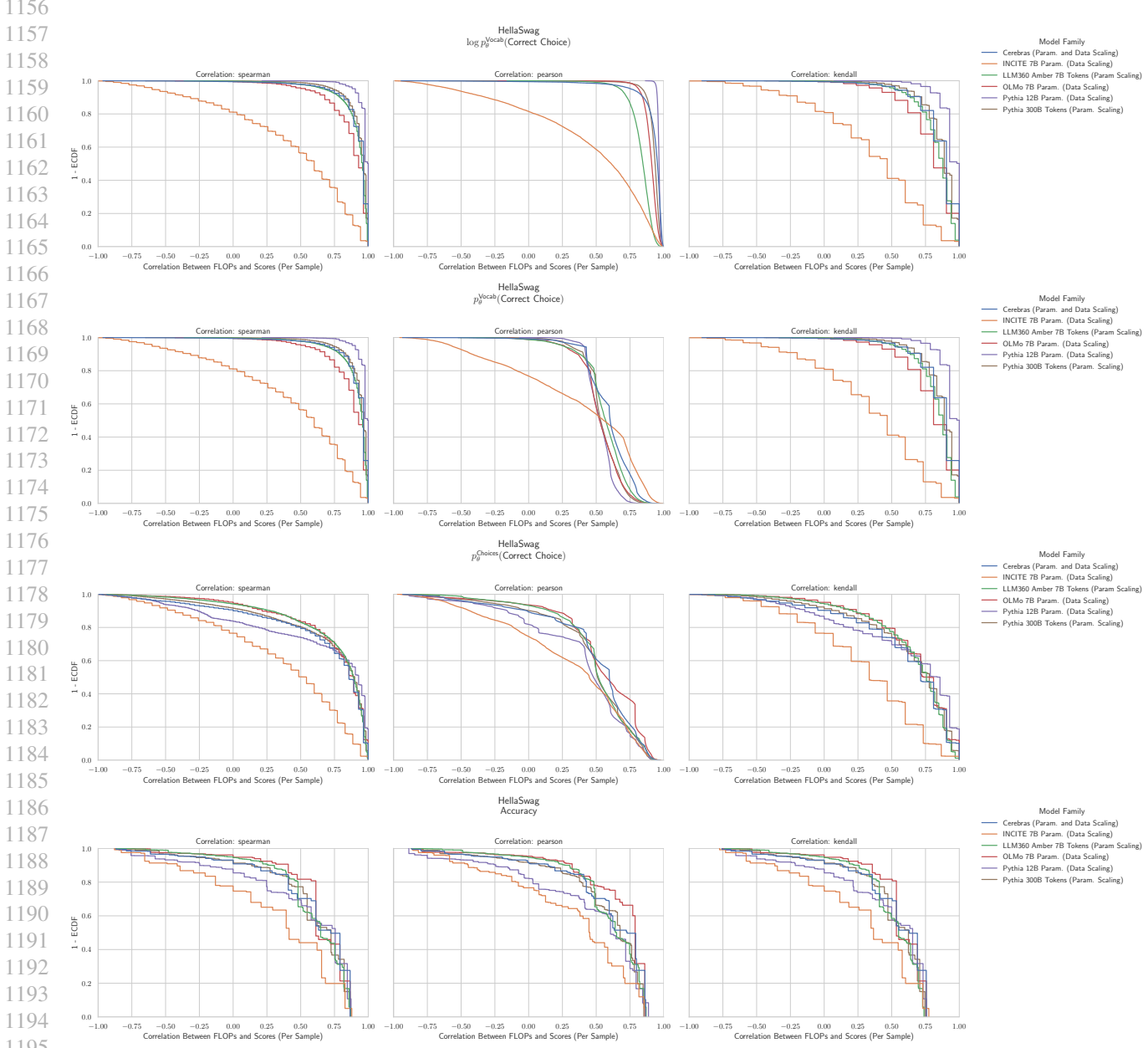


Figure 10. ARC Challenge: Downstream performance is computed via a sequence of transformations that deteriorate correlations between scores and pretraining compute.

1100 I.2. NLP Benchmark: ARC Easy (Clark et al., 2018)


 1142 **Figure 11. ARC Easy:** Downstream performance is computed via a sequence of transformations that deteriorate correlations
 1143 between scores and pretraining compute.
 1144

1155 I.3. NLP Benchmark: HellaSwag (Zellers et al., 2019)


 1197 **Figure 12. HellaSwag: Downstream performance is computed via a sequence of transformations that deteriorate correlations
1198 between scores and pretraining compute.**

 1199
1200
1201
1202
1203
1204
1205
1206
1207
1208
1209

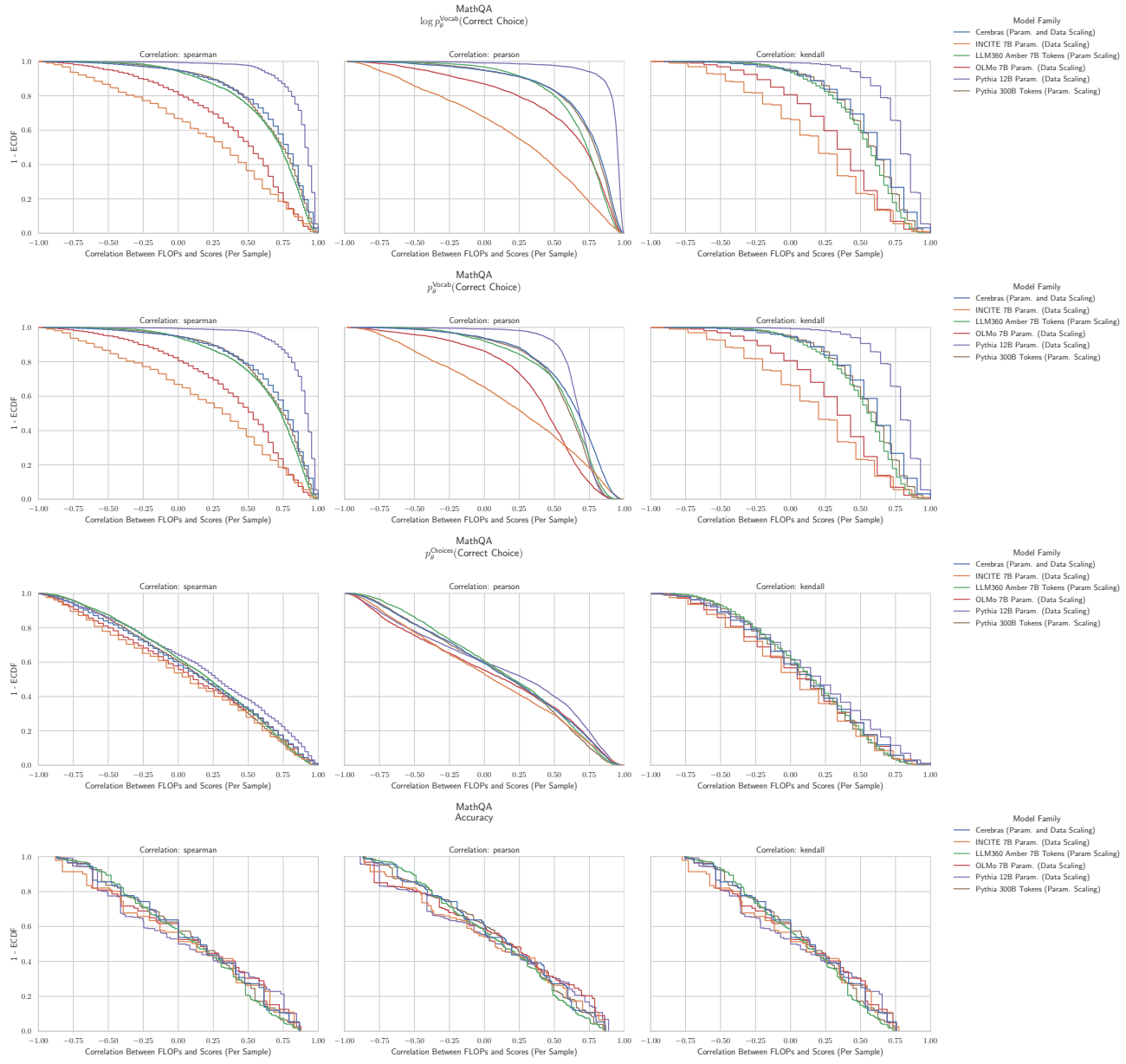
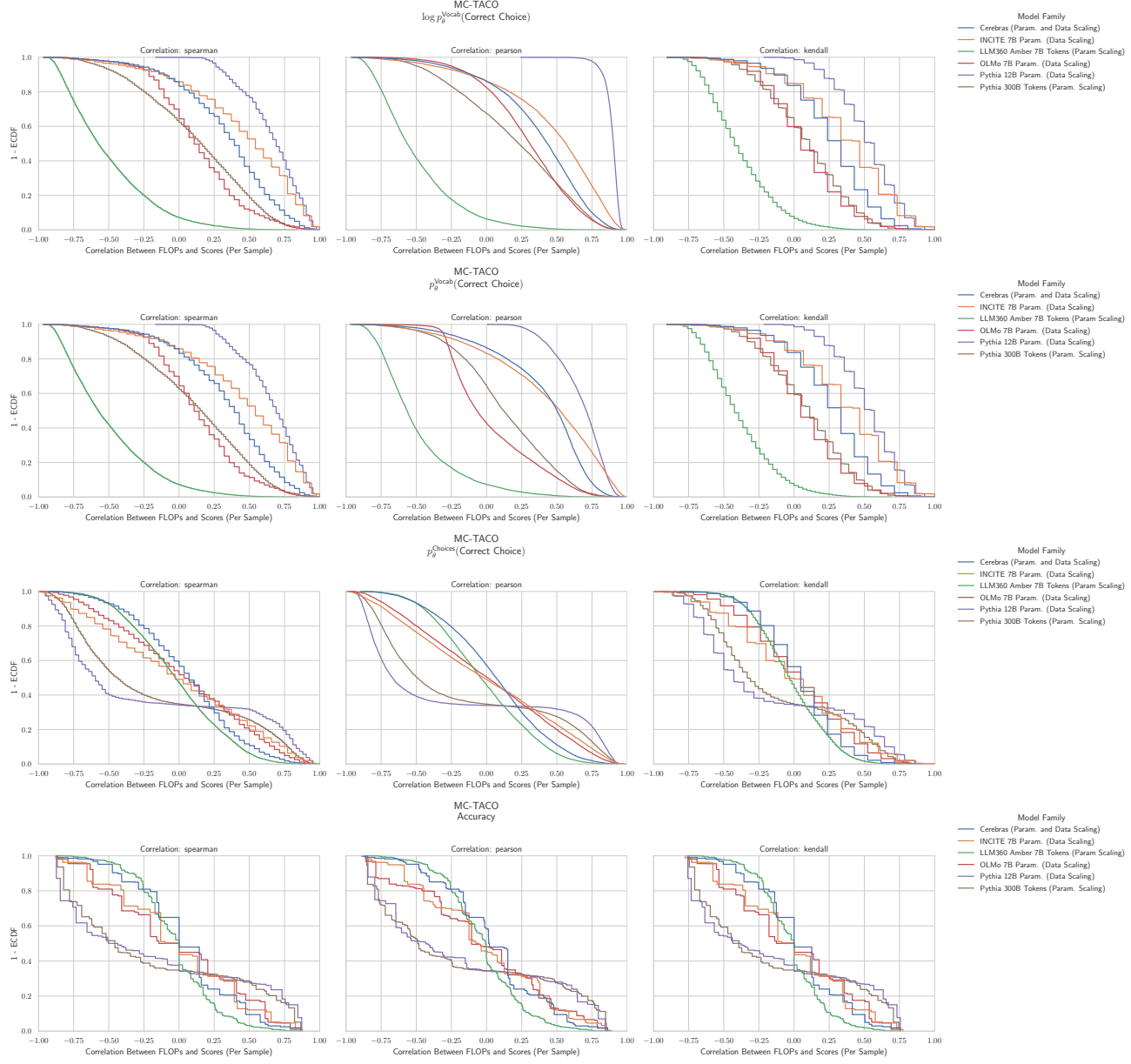
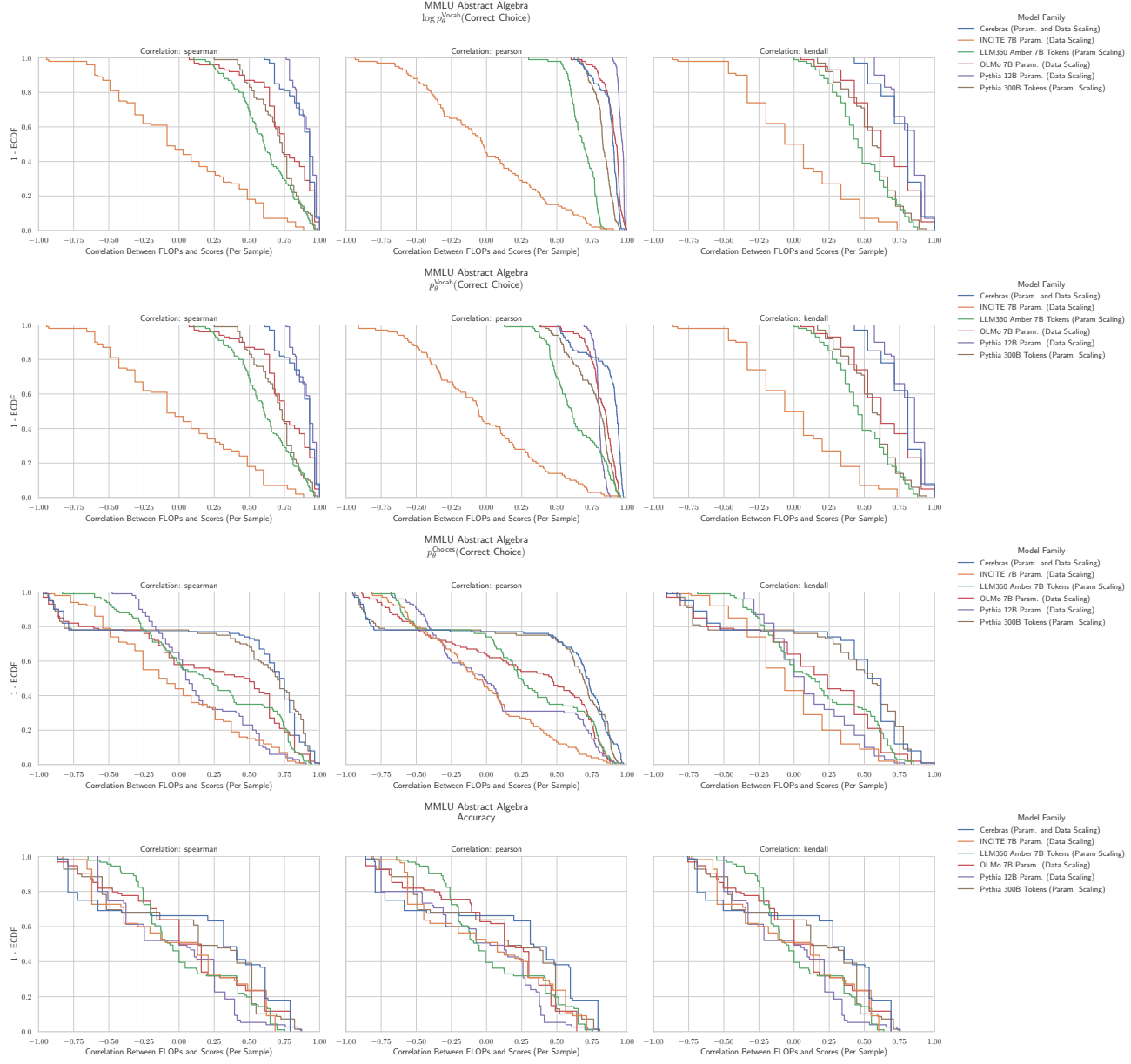
I.4. NLP Benchmark: MathQA (Amini et al., 2019)


Figure 13. HellaSwag: Downstream performance is computed via a sequence of transformations that deteriorate correlations between scores and pretraining compute.

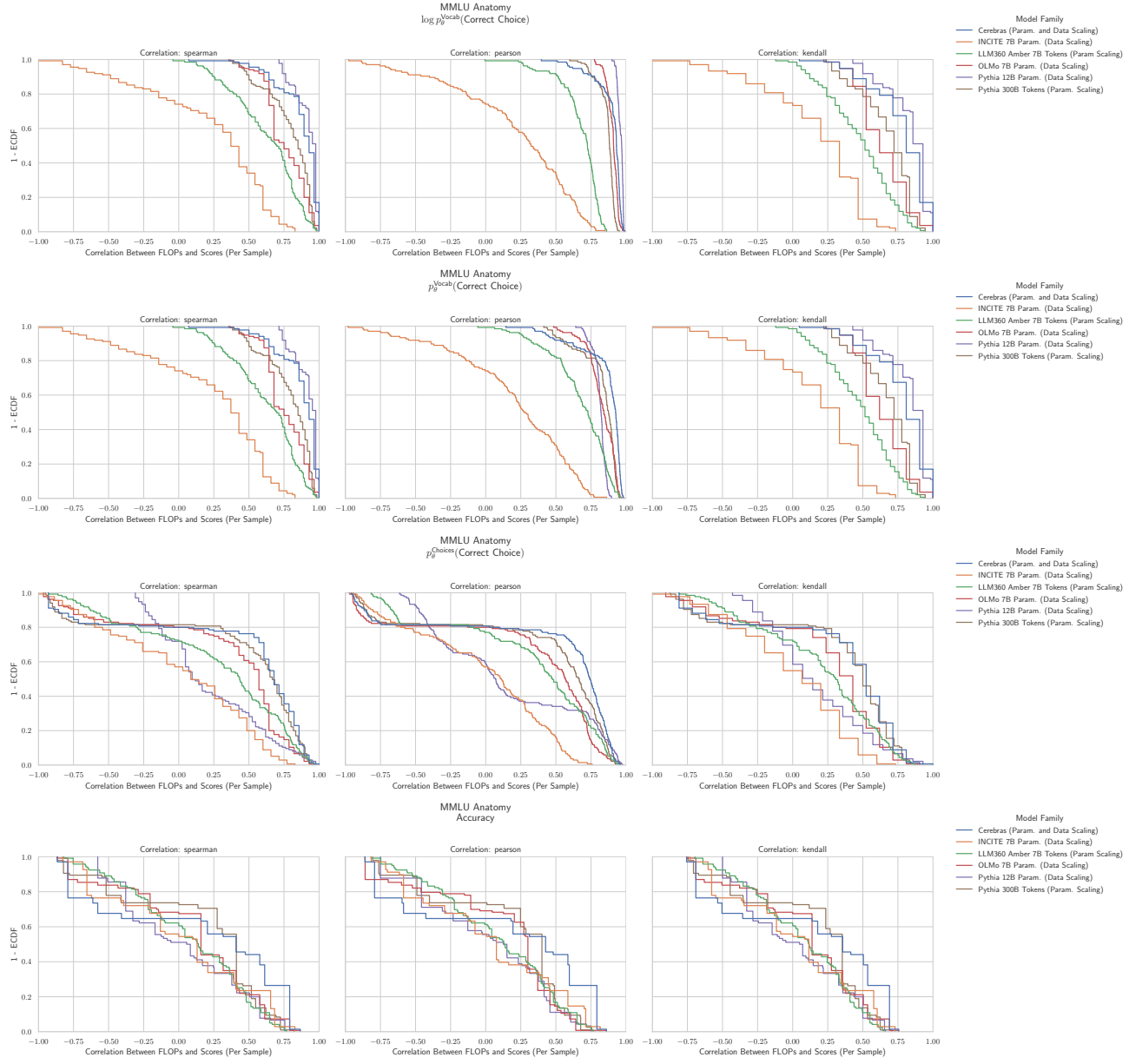
1265 **I.5. NLP Benchmark: MC TACO (Zhou et al., 2019)**
 1266

 1297 **Figure 14. MC TACO: Downstream performance is computed via a sequence of transformations that deteriorate correlations
1298 between scores and pretraining compute.**
 1299

 1300
 1301
 1302
 1303
 1304
 1305
 1306
 1307
 1308
 1309
 1310
 1311
 1312
 1313
 1314
 1315
 1316
 1317
 1318
 1319

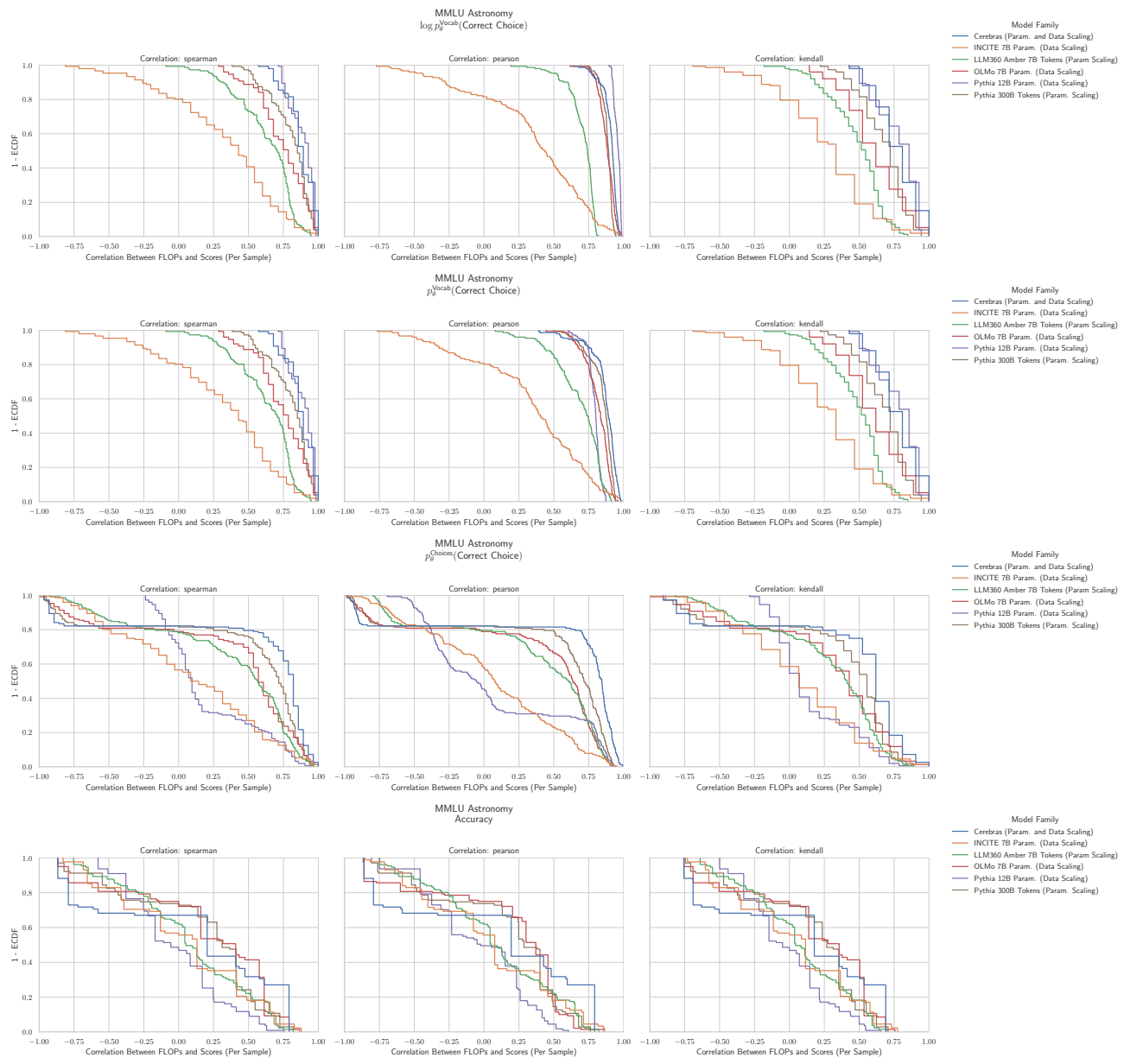
1320 I.6. NLP Benchmark: MMLU Abstract Algebra (Hendrycks et al., 2020)


 1362 **Figure 15. MMLU Abstract Algebra: Downstream performance is computed via a sequence of transformations that deteriorate**
 1363 **correlations between scores and pretraining compute.**

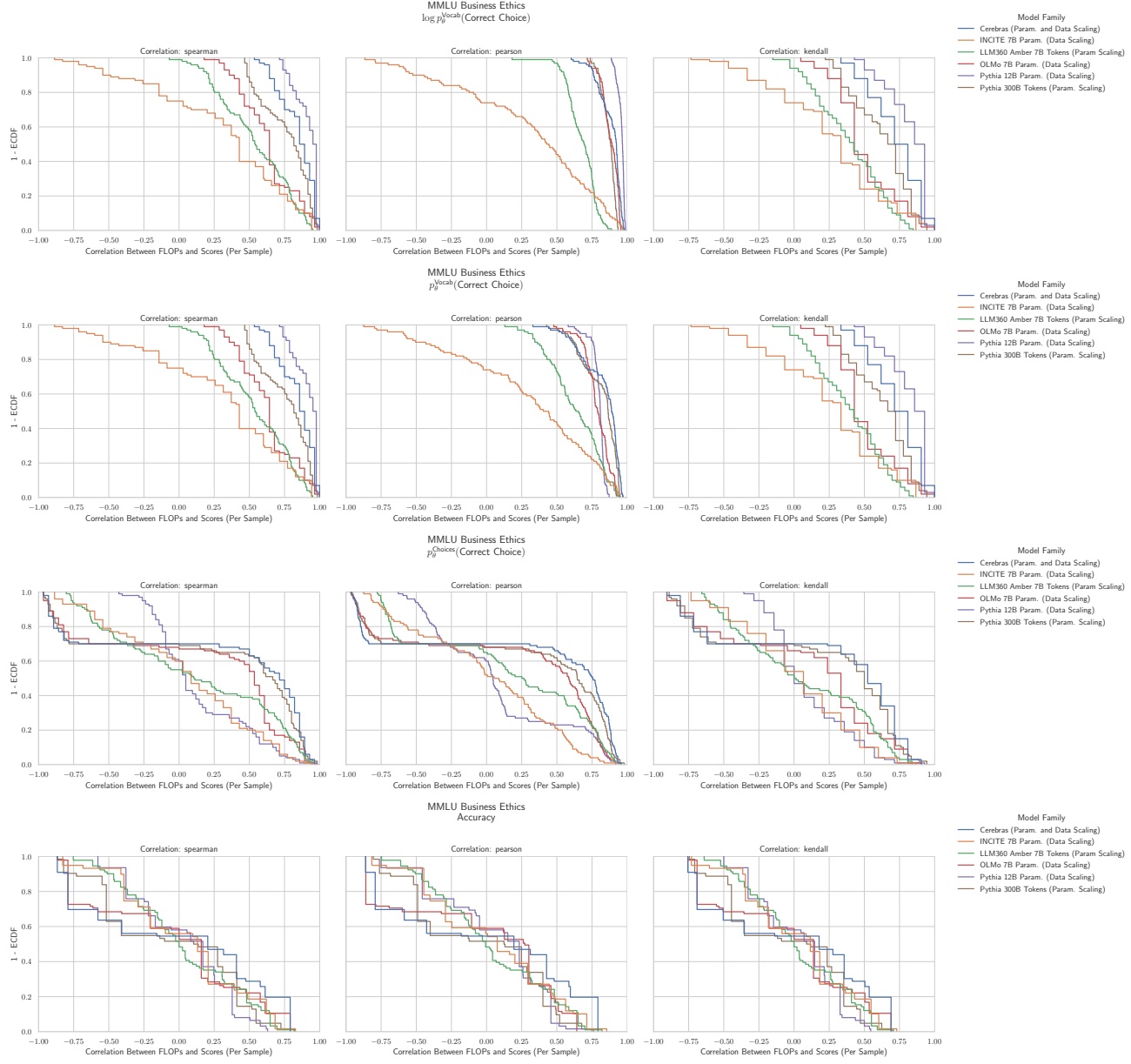
1375 I.7. NLP Benchmark: MMLU Anatomy (Hendrycks et al., 2020)


 1417 **Figure 16. MMLU Anatomy: Downstream performance is computed via a sequence of transformations that deteriorate correlations
1418 between scores and pretraining compute.**
1419

1430 I.8. NLP Benchmark: MMLU Astronomy (Hendrycks et al., 2020)


 1472 **Figure 17. MMLU Astronomy:** Downstream performance is computed via a sequence of transformations that deteriorate correlations between scores and pretraining compute.

1485 I.9. NLP Benchmark: MMLU Business Ethics (Hendrycks et al., 2020)


 1527 **Figure 18. MMLU Business Ethics:** Downstream performance is computed via a sequence of transformations that deteriorate
 1528 correlations between scores and pretraining compute.
 1529

1540 I.10. NLP Benchmark: MMLU Clinical Knowledge (Hendrycks et al., 2020)

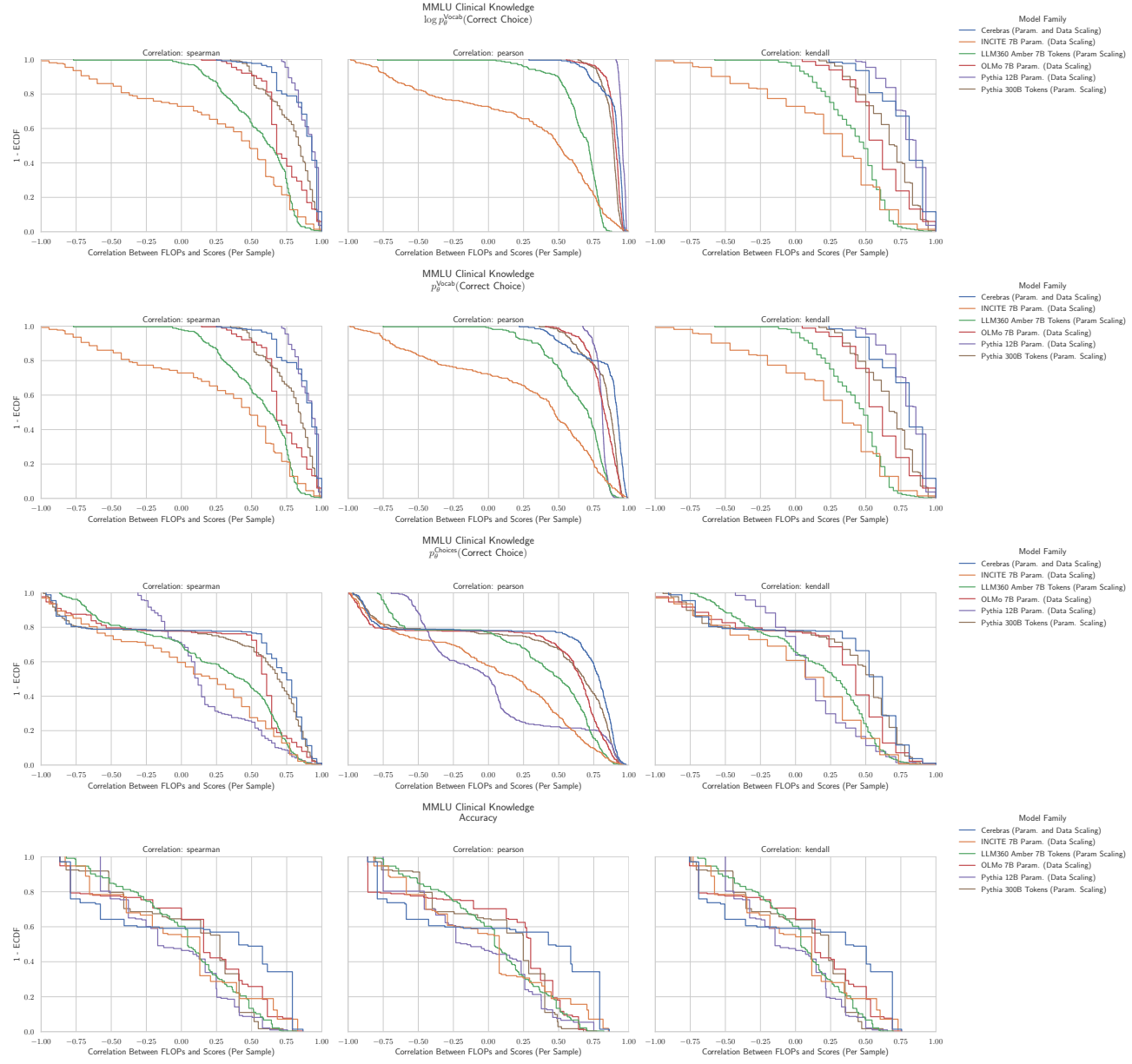

 1541
 1542
 1543
 1544
 1545
 1546
 1547
 1548
 1549
 1550
 1551
 1552
 1553
 1554
 1555
 1556
 1557
 1558
 1559
 1560
 1561
 1562
 1563
 1564
 1565
 1566
 1567
 1568
 1569
 1570
 1571
 1572
 1573
 1574
 1575
 1576
 1577
 1578
 1579
 1580
 1581
 1582
 1583
 1584
 1585
 1586
 1587
 1588
 1589
 1590
 1591
 1592
 1593
 1594

Figure 19. MMLU Clinical Knowledge: Downstream performance is computed via a sequence of transformations that deteriorate correlations between scores and pretraining compute.

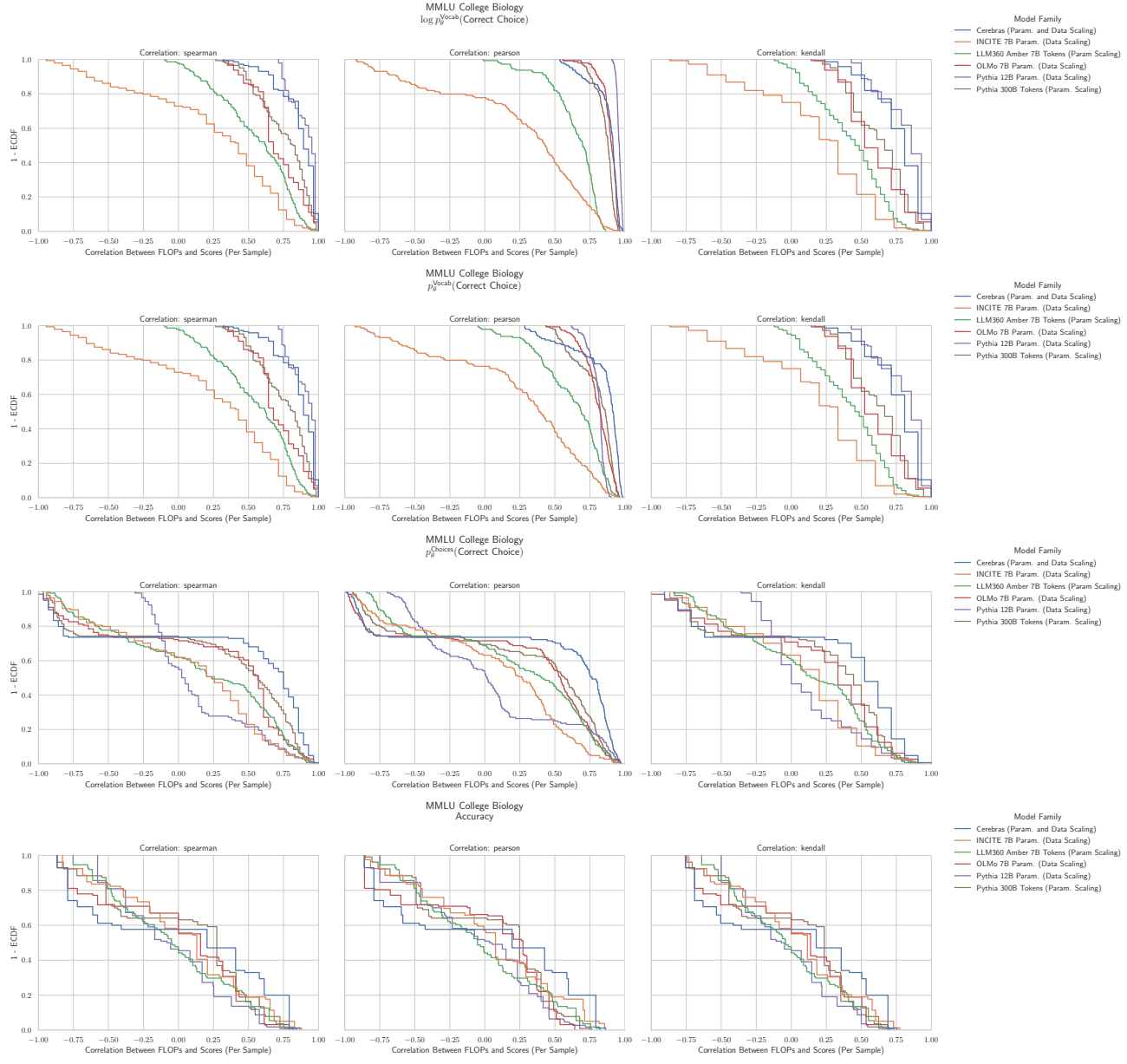
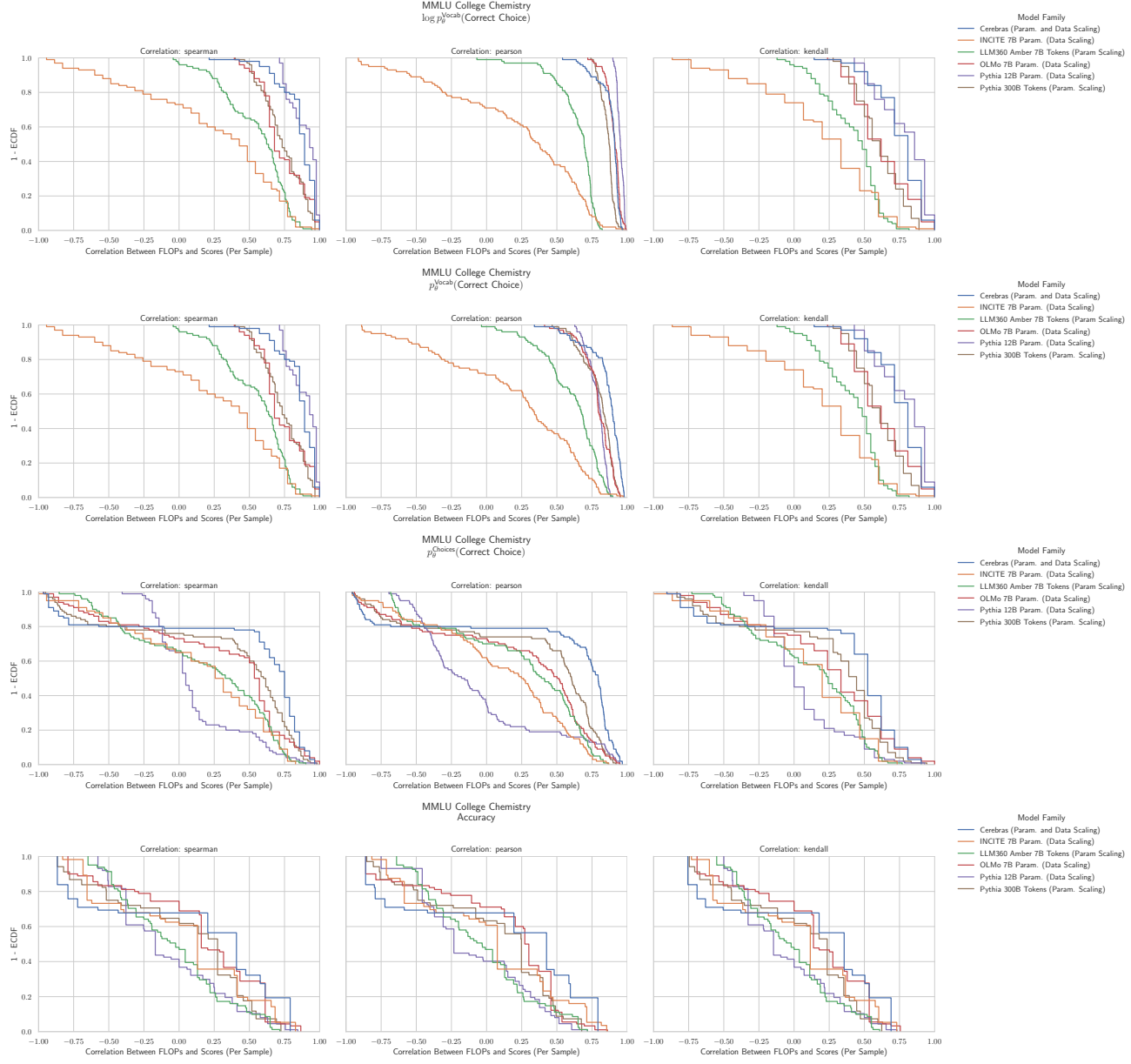
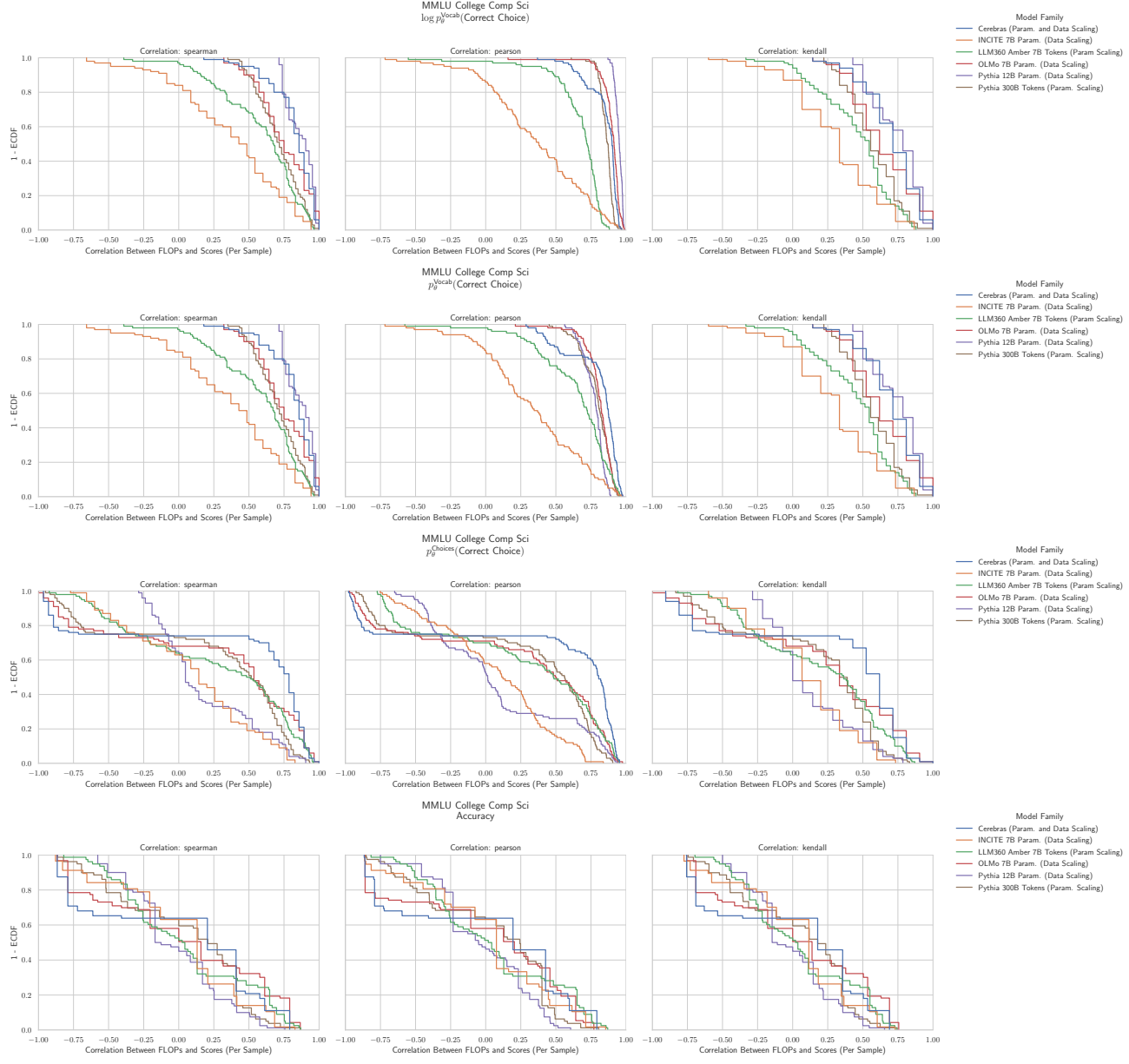
1595 I.11. NLP Benchmark: MMLU College Biology (Hendrycks et al., 2020)
 1596
 1597

 1600
 1601
 1602
 1603
 1604
 1605
 1606
 1607
 1608
 1609
 1610
 1611
 1612
 1613
 1614
 1615
 1616
 1617
 1618
 1619
 1620
 1621
 1622
 1623
 1624
 1625
 1626
 1627
 1628
 1629
 1630
 1631
 1632
 1633
 1634
 1635
 1636
 1637
 1638
 1639
 1640
 1641
 1642
 1643
 1644
 1645
 1646
 1647
 1648
 1649

Figure 20. MMLU College Biology: Downstream performance is computed via a sequence of transformations that deteriorate correlations between scores and pretraining compute.

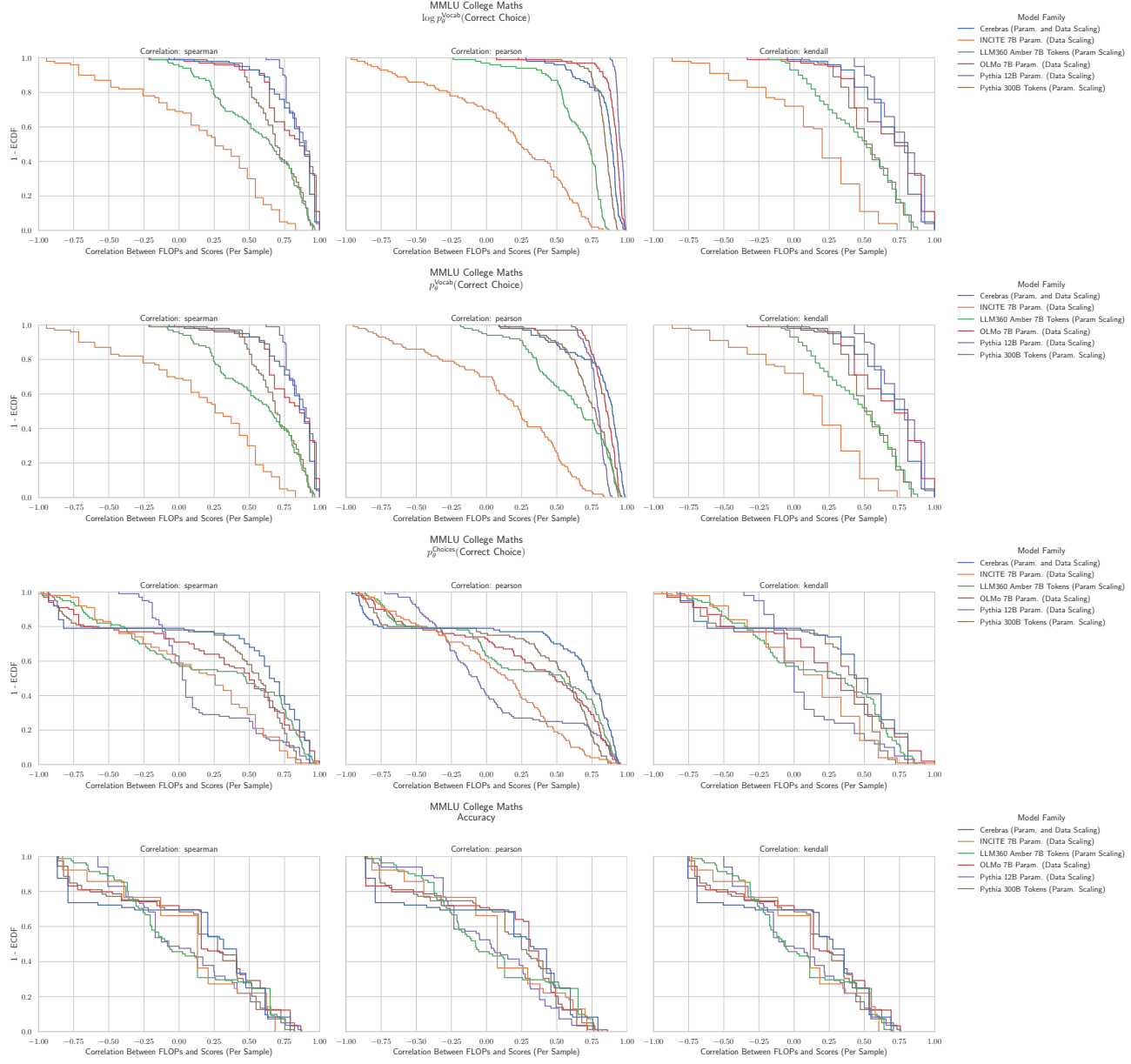
1650 I.12. NLP Benchmark: MMLU College Chemistry (Hendrycks et al., 2020)


 1692 **Figure 21. MMLU College Chemistry: Downstream performance is computed via a sequence of transformations that deteriorate**
 1693 **correlations between scores and pretraining compute.**

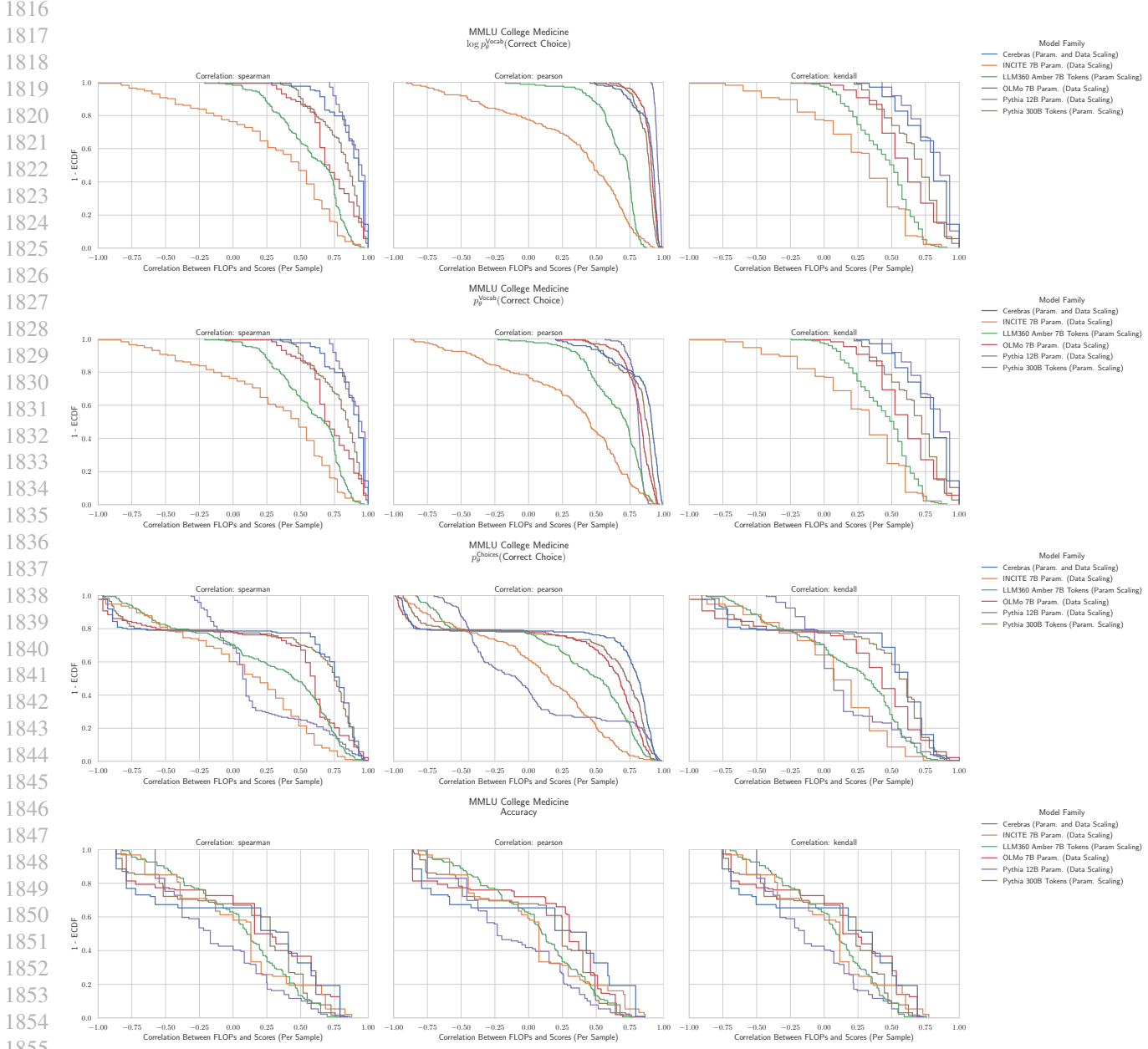
1705 I.13. NLP Benchmark: MMLU College Computer Science (Hendrycks et al., 2020)


 1747 **Figure 22. MMLU College Computer Science: Downstream performance is computed via a sequence of transformations that**
 1748 **deteriorate correlations between scores and pretraining compute.**

1760 I.14. NLP Benchmark: MMLU College Mathematics (Hendrycks et al., 2020)


 1802 **Figure 23. MMLU College Mathematics: Downstream performance is computed via a sequence of transformations that deteriorate**
 1803 **correlations between scores and pretraining compute.**

1815 I.15. NLP Benchmark: MMLU College Medicine (Hendrycks et al., 2020)


 1857 **Figure 24. MMLU College Medicine: Downstream performance is computed via a sequence of transformations that deteriorate**
 1858 **correlations between scores and pretraining compute.**

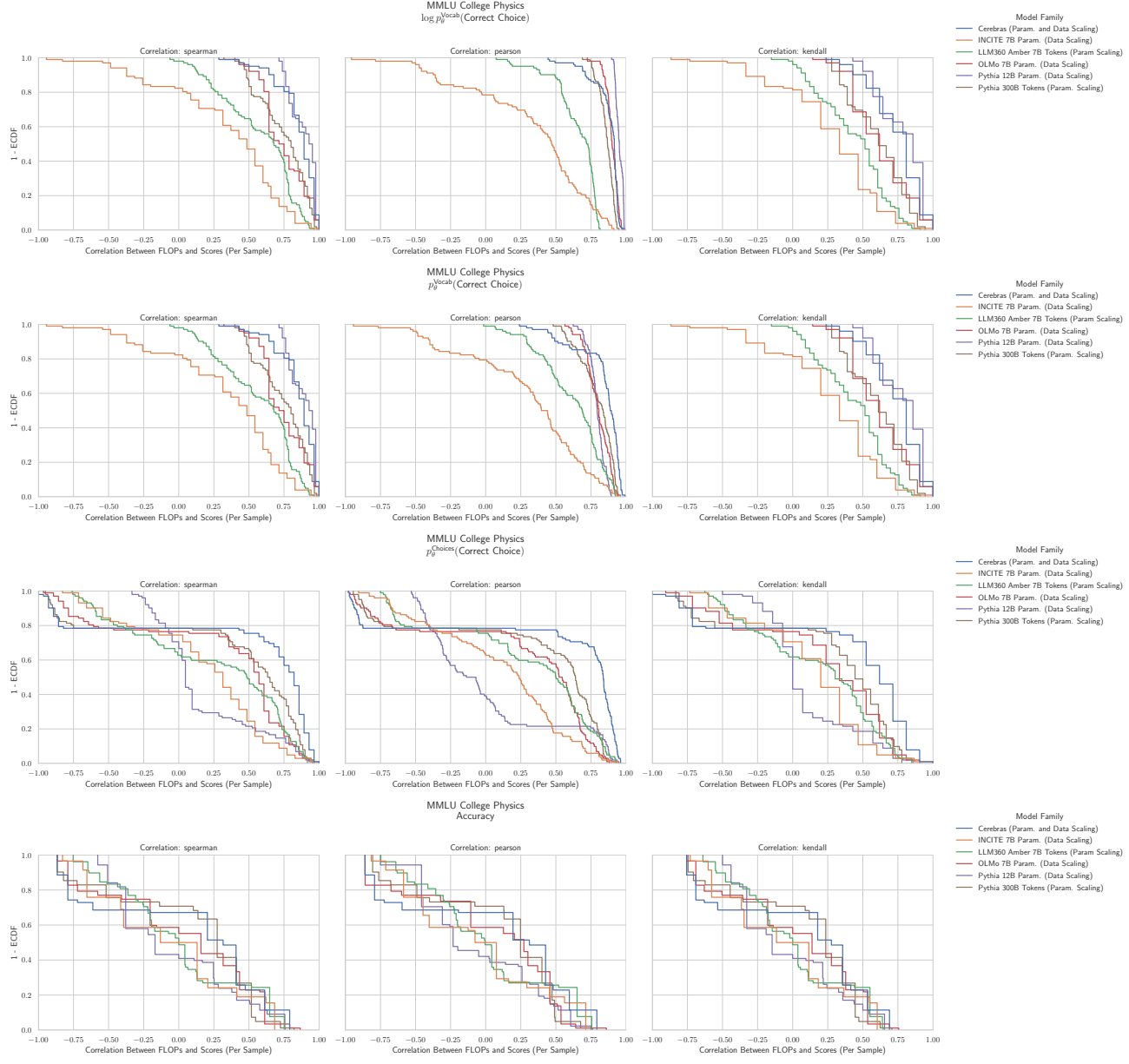
I.16. NLP Benchmark: MMLU College Physics (Hendrycks et al., 2020)


Figure 25. MMLU College Physics: Downstream performance is computed via a sequence of transformations that deteriorate correlations between scores and pretraining compute.

I.17. NLP Benchmark: MMLU Computer Security (Hendrycks et al., 2020)

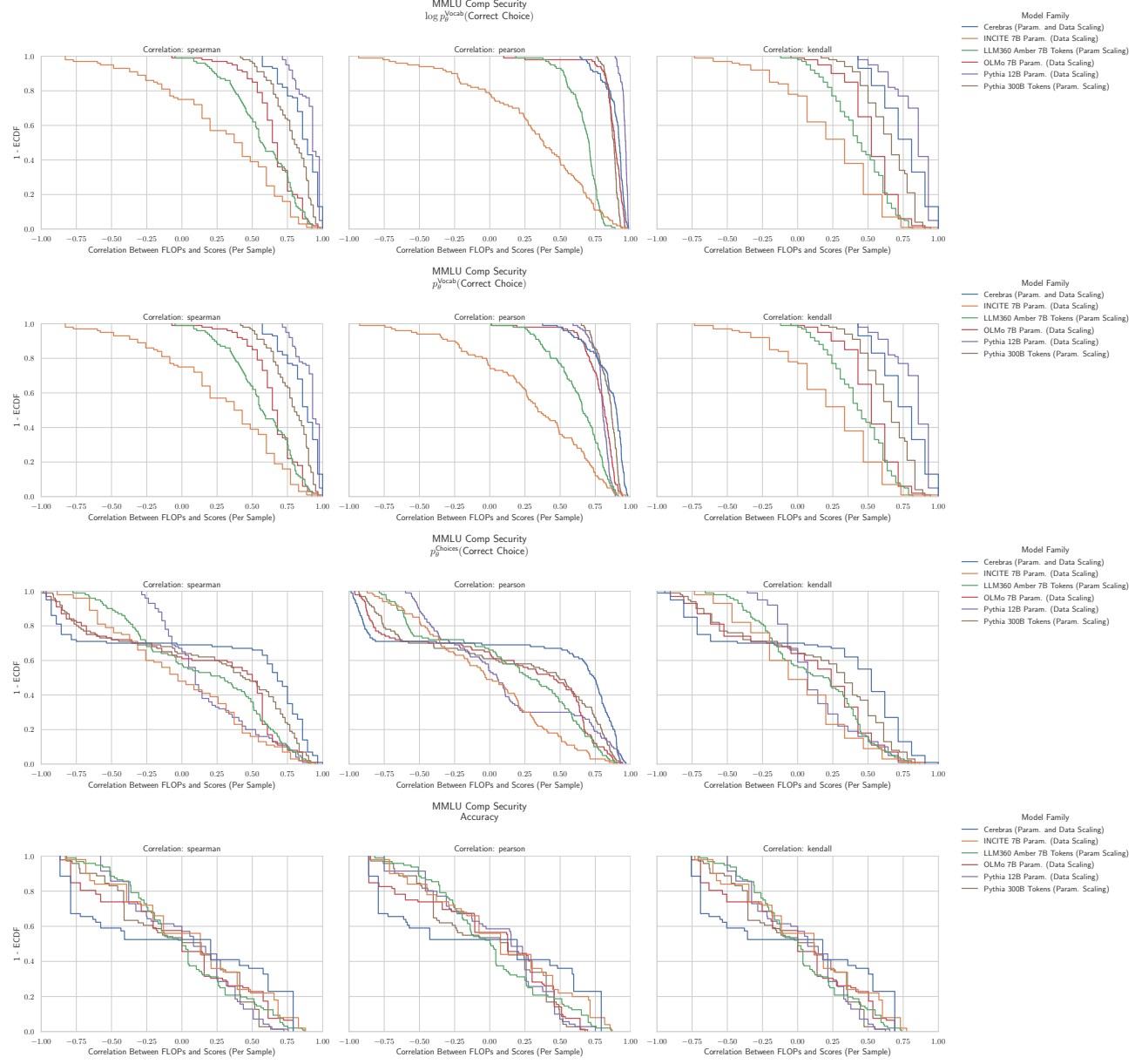


Figure 26. MMLU Computer Security: Downstream performance is computed via a sequence of transformations that deteriorate correlations between scores and pretraining compute.

I.18. NLP Benchmark: MMLU Conceptual Physics (Hendrycks et al., 2020)

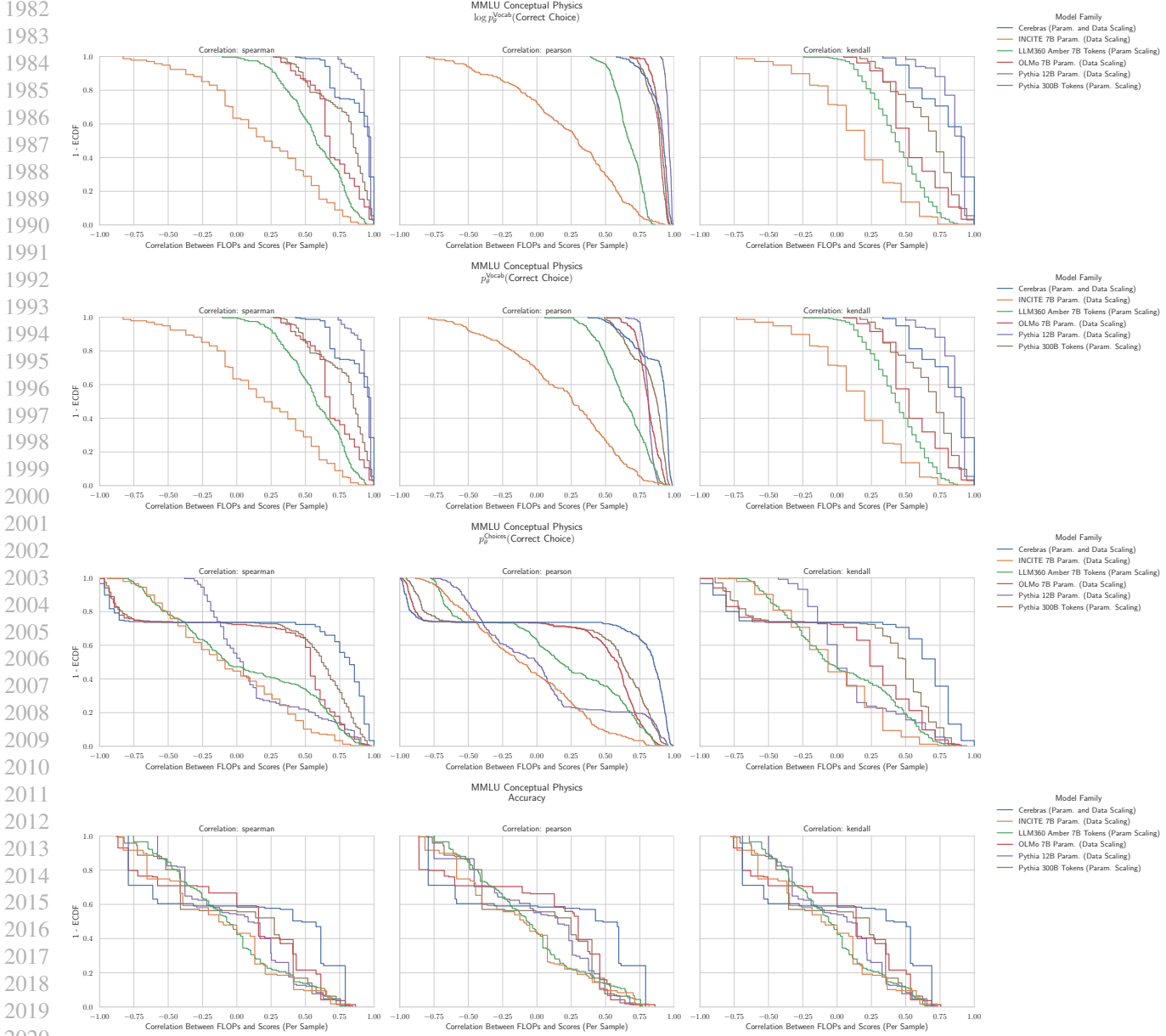


Figure 27. MMLU Conceptual Physics: Downstream performance is computed via a sequence of transformations that deteriorate correlations between scores and pretraining compute.

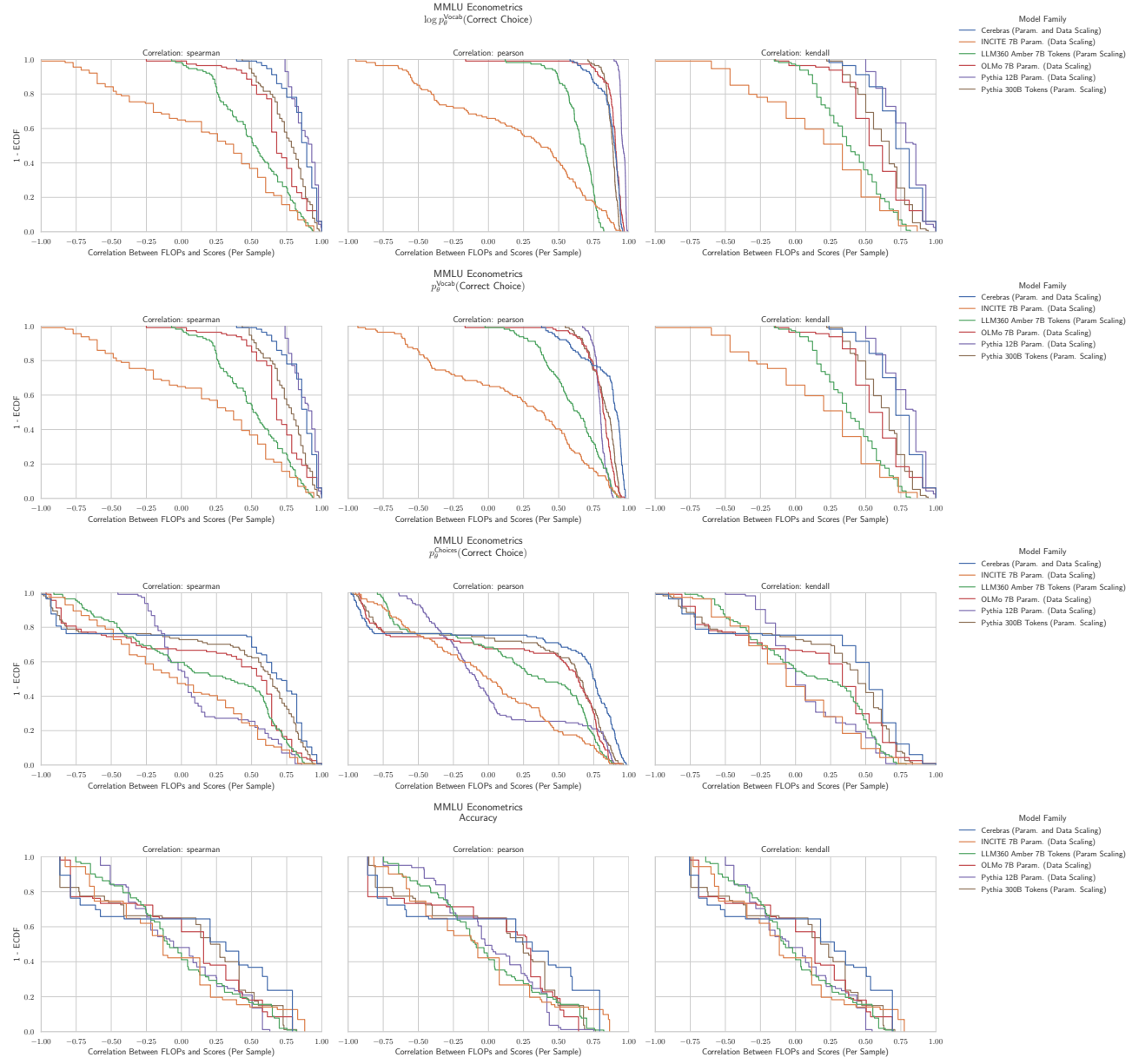
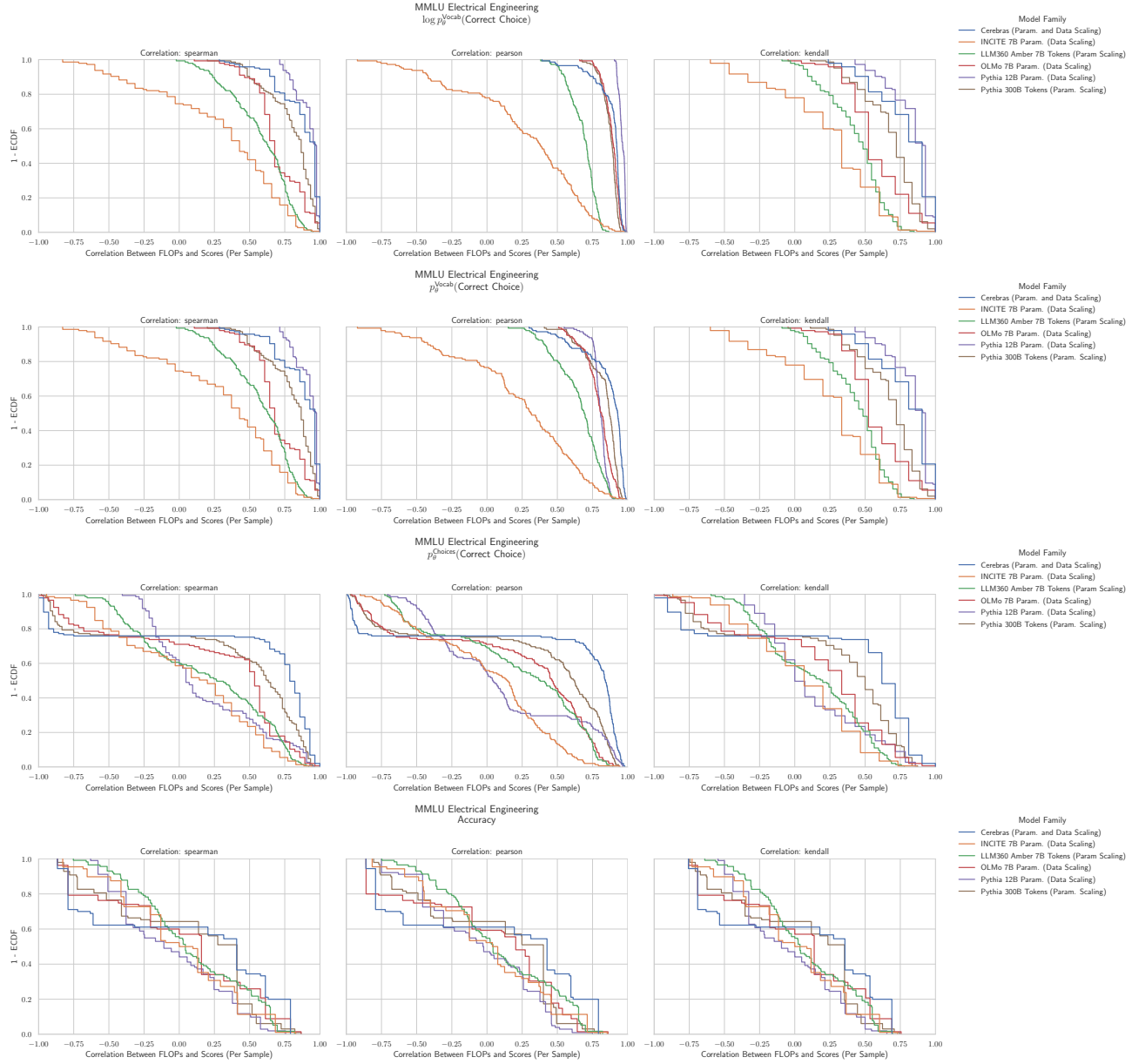
I.19. NLP Benchmark: MMLU Econometrics (Hendrycks et al., 2020)


Figure 28. MMLU Econometrics: Downstream performance is computed via a sequence of transformations that deteriorate correlations between scores and pretraining compute.

2090 I.20. NLP Benchmark: MMLU Electrical Engineering (Hendrycks et al., 2020)


 2132 **Figure 29. MMLU Electrical Engineering:** Downstream performance is computed via a sequence of transformations that deteriorate correlations between scores and pretraining compute.

2145 I.21. NLP Benchmark: MMLU Elementary Mathematics (Hendrycks et al., 2020)

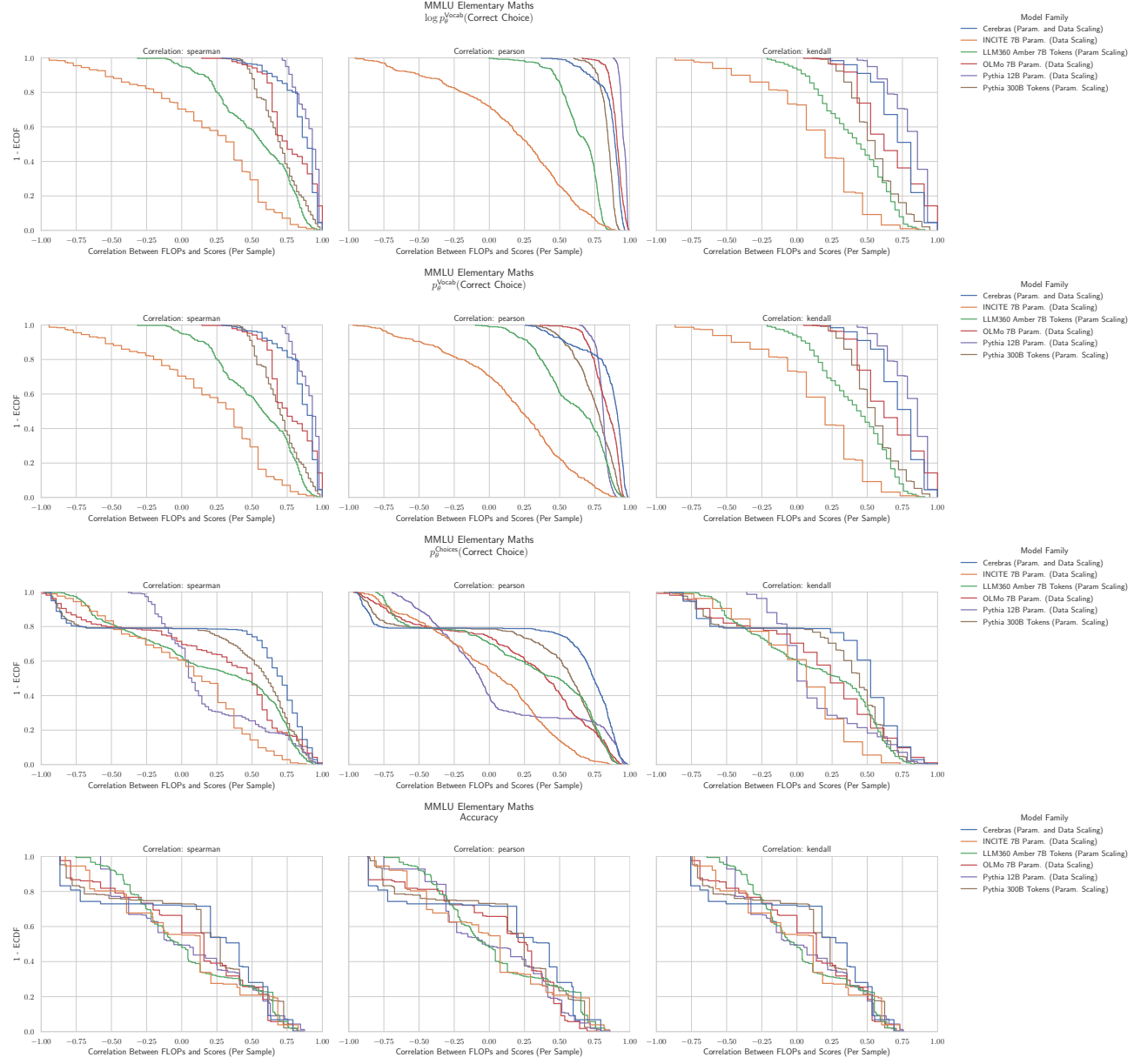

 2146
 2147
 2148
 2149
 2150
 2151
 2152
 2153
 2154
 2155
 2156
 2157
 2158
 2159
 2160
 2161
 2162
 2163
 2164
 2165
 2166
 2167
 2168
 2169
 2170
 2171
 2172
 2173
 2174
 2175
 2176
 2177
 2178
 2179
 2180
 2181
 2182
 2183
 2184
 2185
 2186
 2187
 2188
 2189
 2190
 2191
 2192
 2193
 2194
 2195
 2196
 2197
 2198
 2199

Figure 30. MMLU Elementary Mathematics: Downstream performance is computed via a sequence of transformations that deteriorate correlations between scores and pretraining compute.

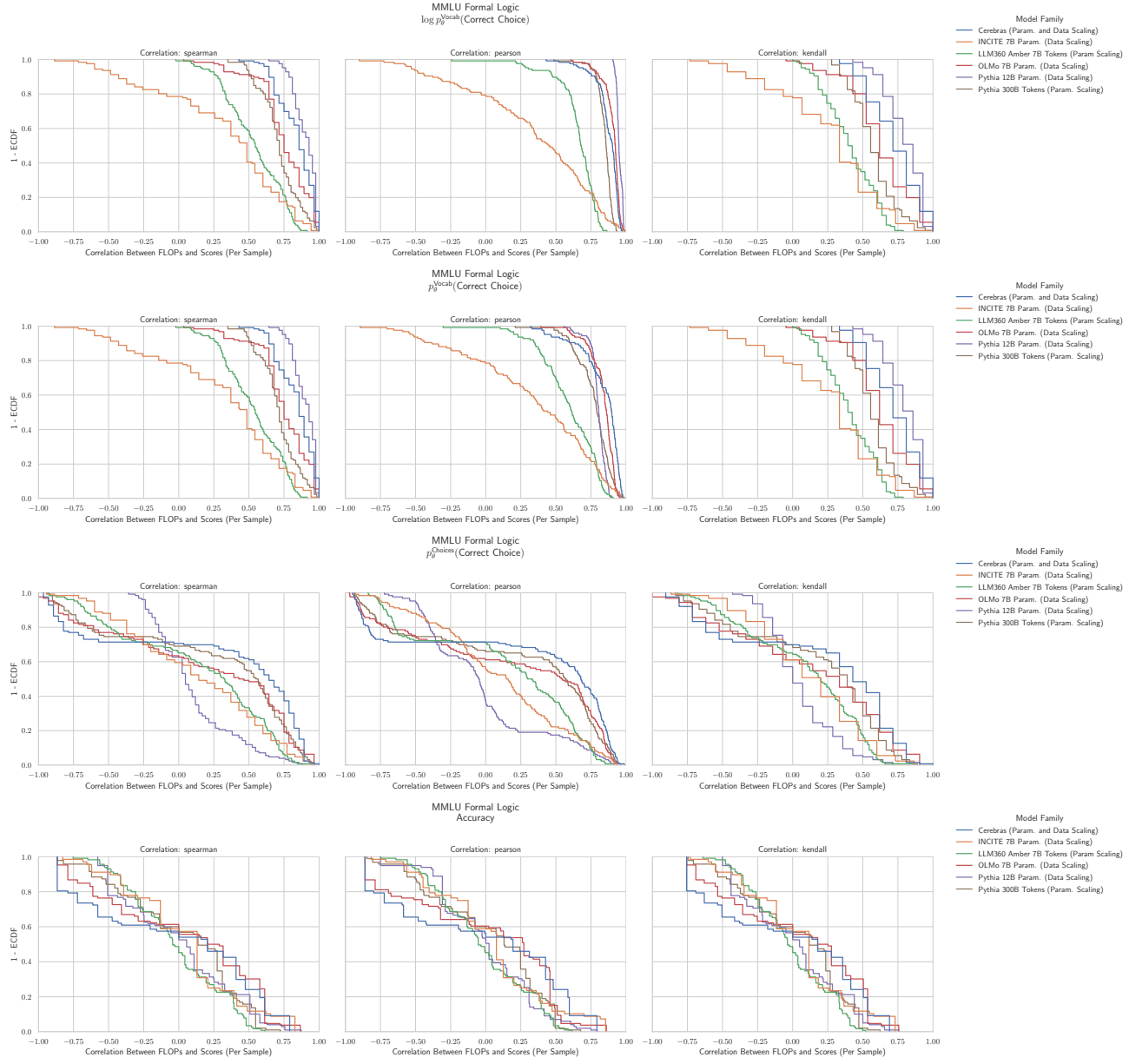
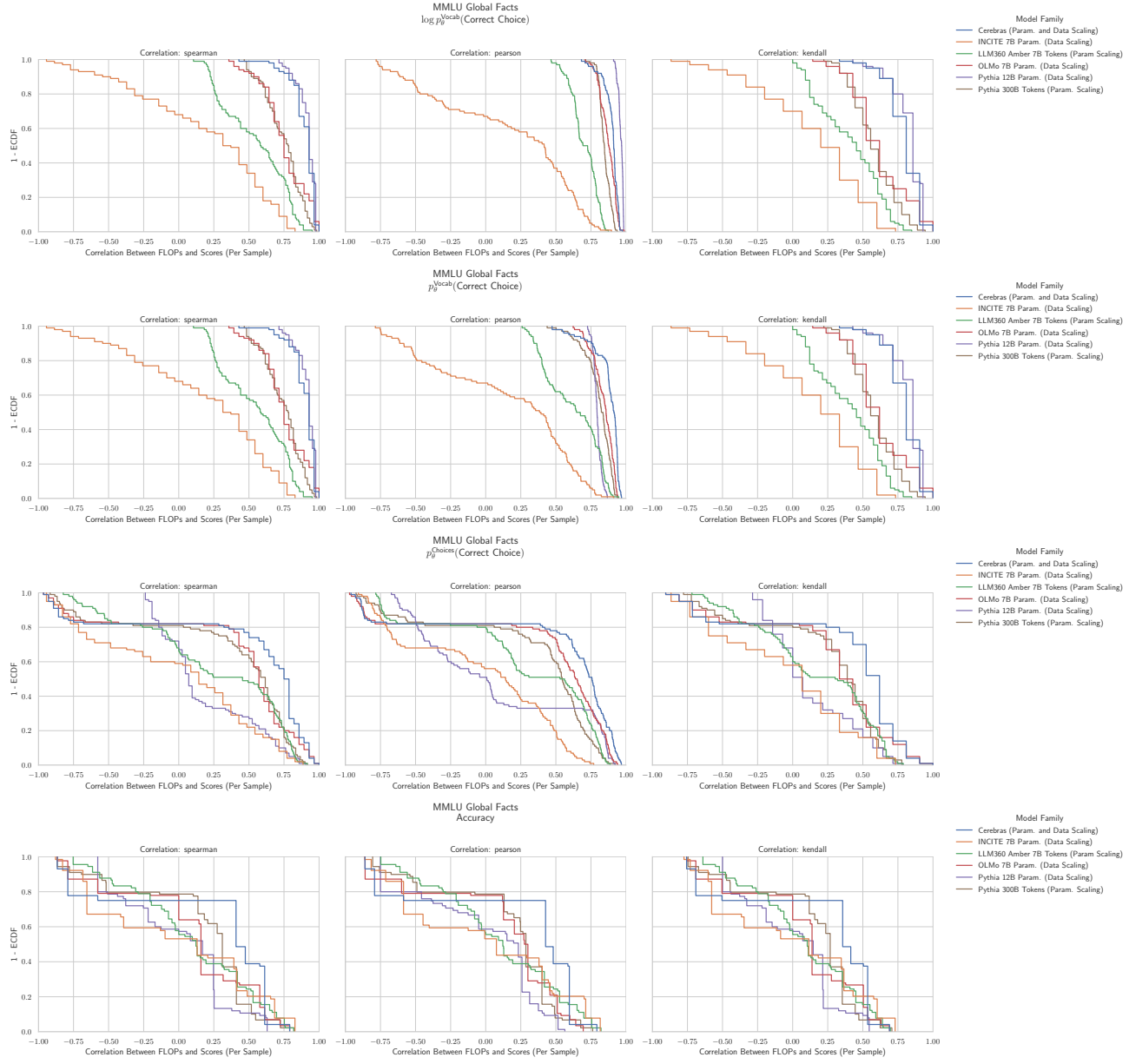
I.22. NLP Benchmark: MMLU Formal Logic (Hendrycks et al., 2020)


Figure 31. MMLU Formal Logic: Downstream performance is computed via a sequence of transformations that deteriorate correlations between scores and pretraining compute.

2255 I.23. NLP Benchmark: MMLU Global Facts (Hendrycks et al., 2020)


 2297 **Figure 32. MMLU Global Facts: Downstream performance is computed via a sequence of transformations that deteriorate**
 2298 **correlations between scores and pretraining compute.**

I.24. NLP Benchmark: MMLU High School Biology (Hendrycks et al., 2020)

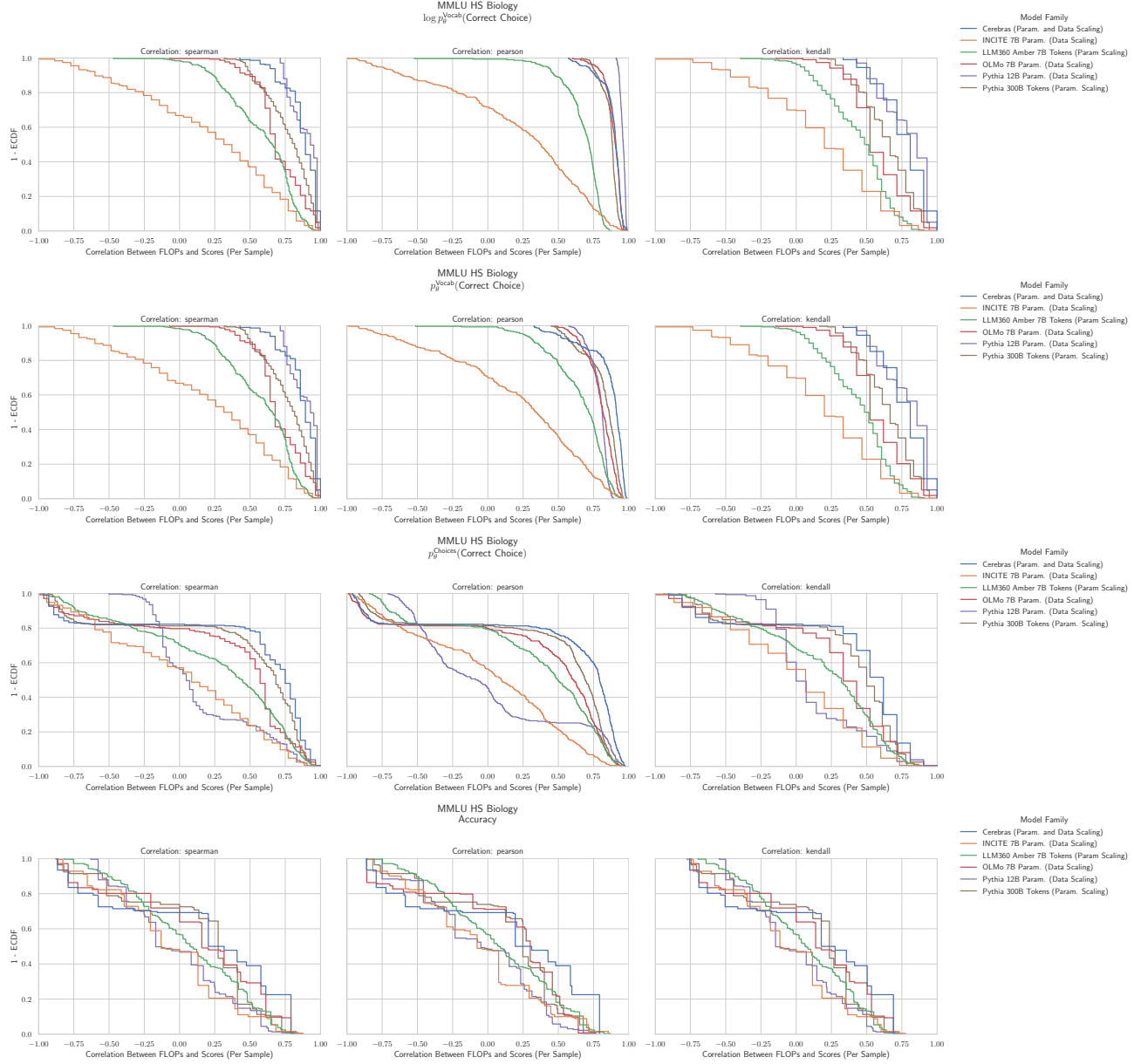


Figure 33. MMLU High School Biology: Downstream performance is computed via a sequence of transformations that deteriorate correlations between scores and pretraining compute.

I.25. NLP Benchmark: MMLU High School Chemistry (Hendrycks et al., 2020)

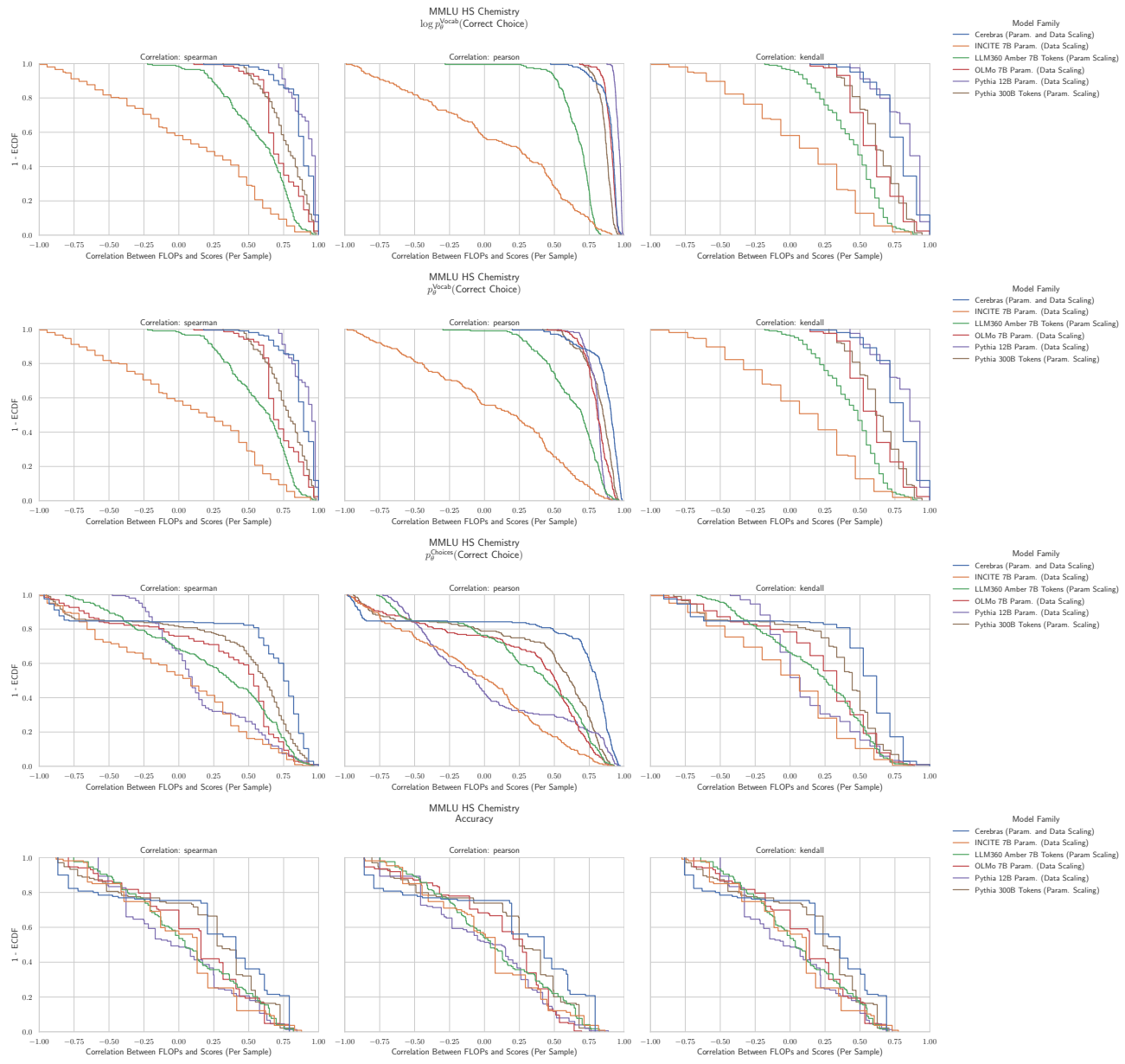


Figure 34. MMLU High School Chemistry: Downstream performance is computed via a sequence of transformations that deteriorate correlations between scores and pretraining compute.

I.26. NLP Benchmark: MMLU High School Computer Science (Hendrycks et al., 2020)

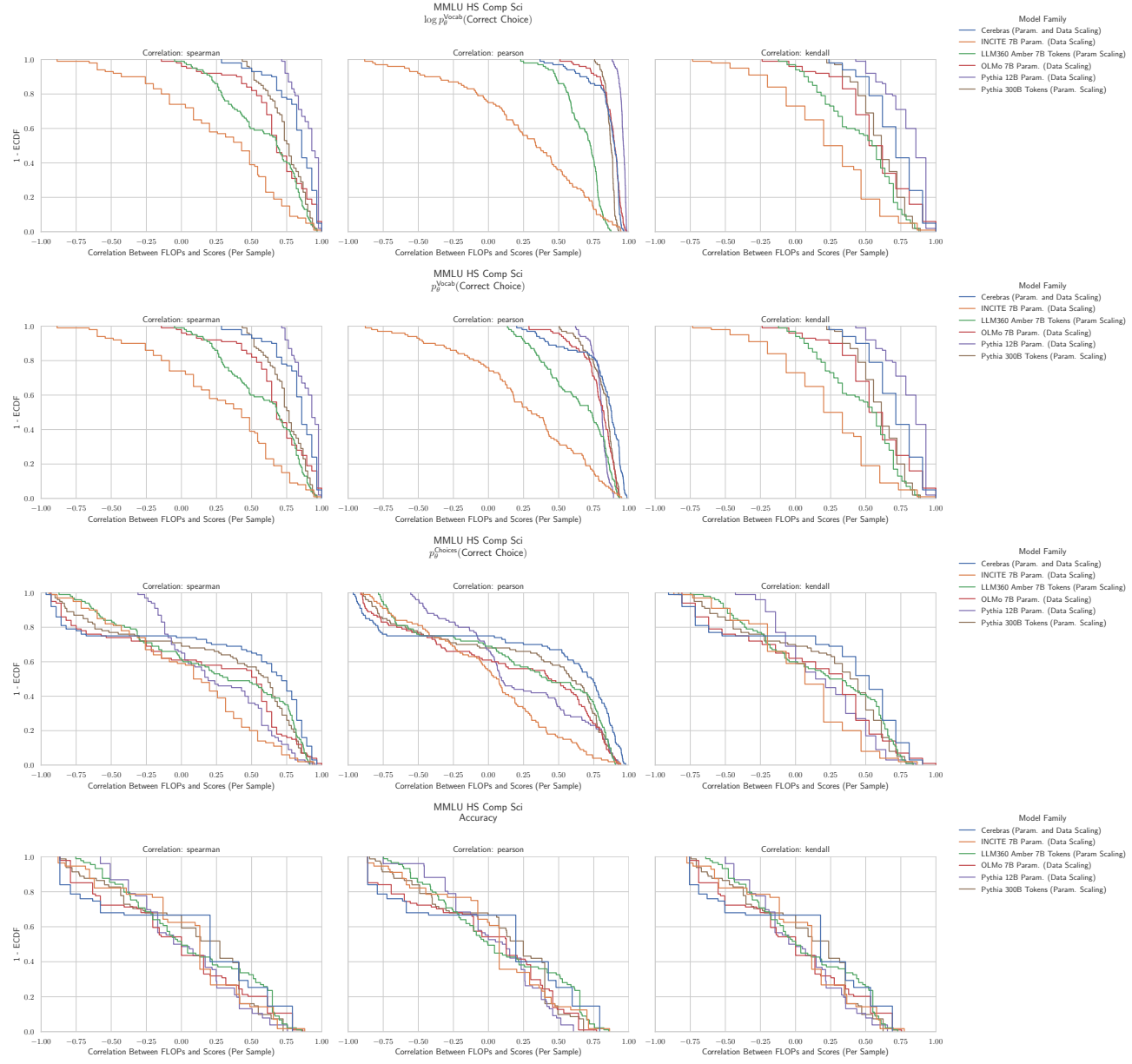


Figure 35. MMLU High School Computer Science: Downstream performance is computed via a sequence of transformations that deteriorate correlations between scores and pretraining compute.

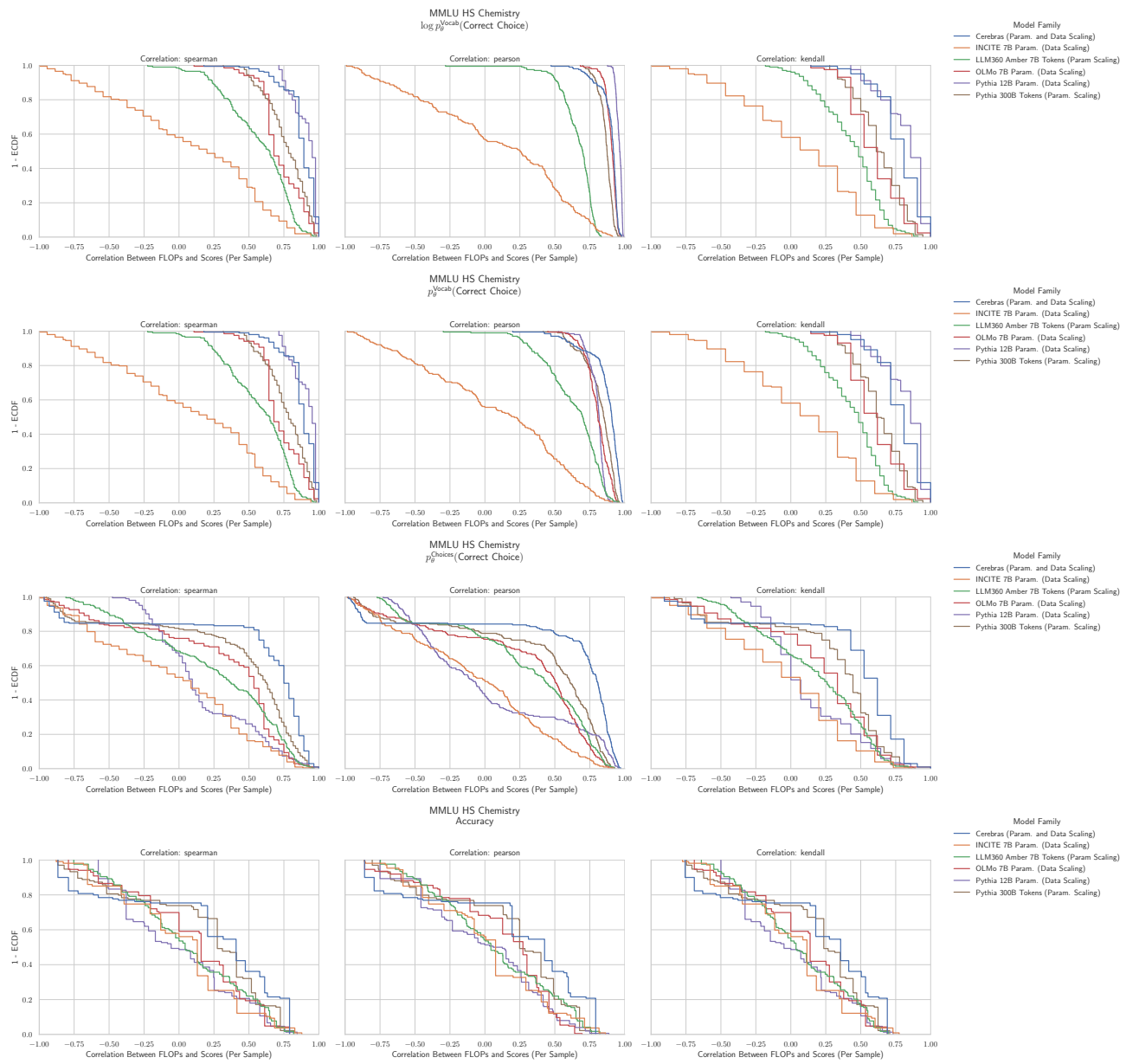
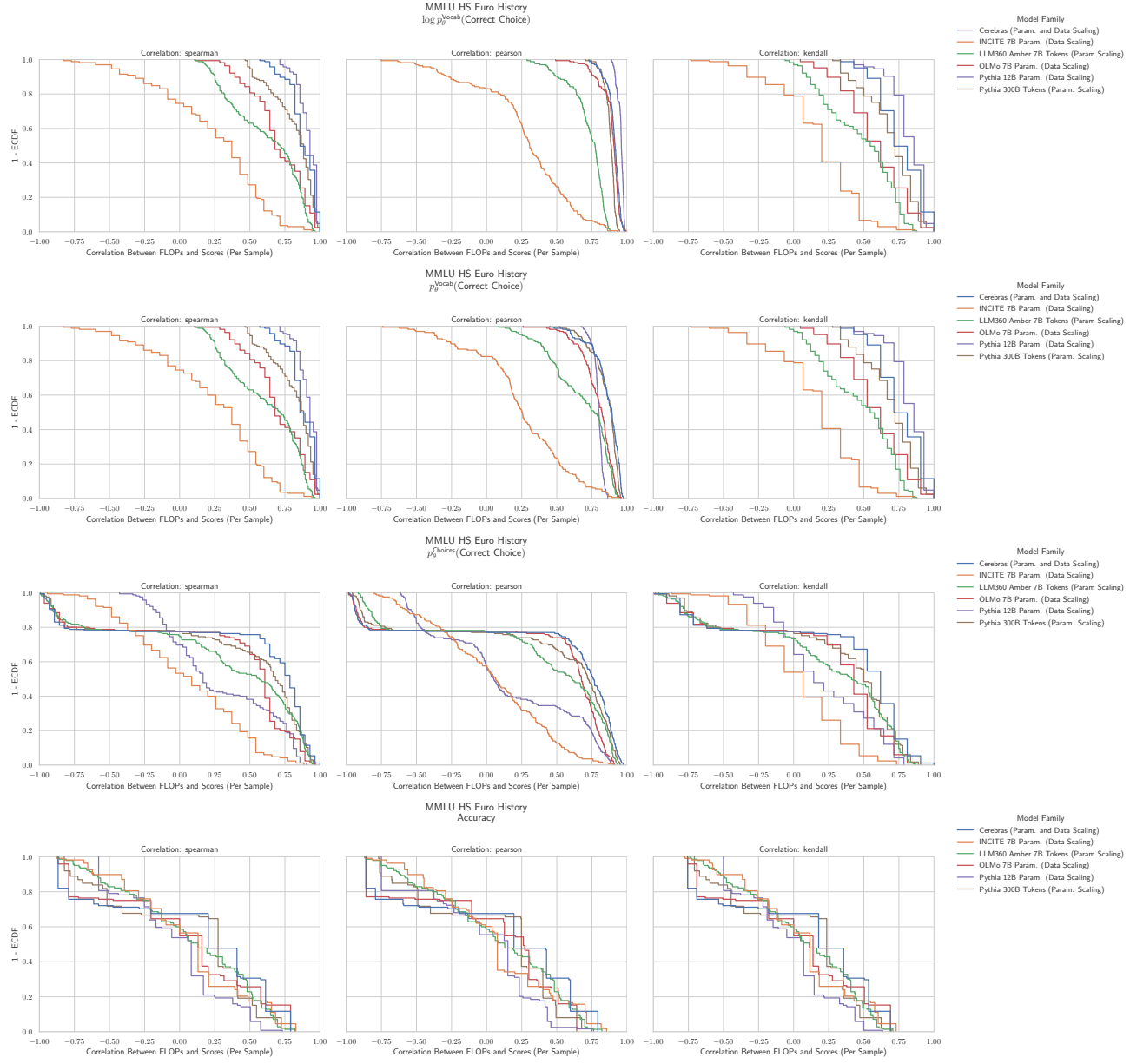
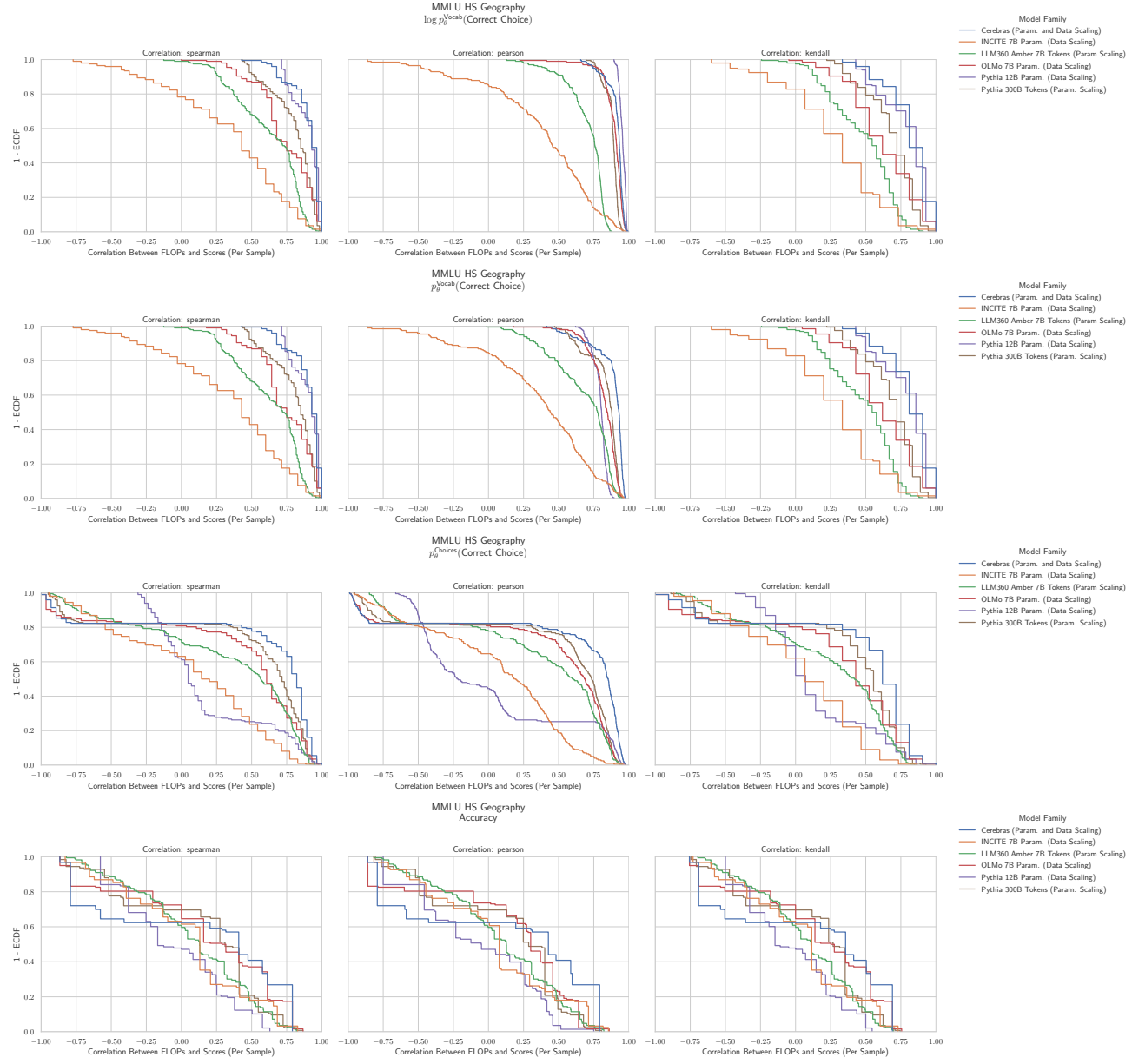
I.27. NLP Benchmark: MMLU High School Chemistry (Hendrycks et al., 2020)


Figure 36. MMLU High School Chemistry: Downstream performance is computed via a sequence of transformations that deteriorate correlations between scores and pretraining compute.

2530 I.28. NLP Benchmark: MMLU High School European History (Hendrycks et al., 2020)
 2531
 2532

 2533
 2534 Figure 37. MMLU High School European History: Downstream performance is computed via a sequence of transformations that
 2535 deteriorate correlations between scores and pretraining compute.
 2536
 2537
 2538
 2539
 2540
 2541
 2542
 2543
 2544
 2545
 2546
 2547
 2548
 2549
 2550
 2551
 2552
 2553
 2554
 2555
 2556
 2557
 2558
 2559
 2560
 2561
 2562
 2563
 2564
 2565
 2566
 2567
 2568
 2569
 2570
 2571
 2572
 2573
 2574
 2575
 2576
 2577
 2578
 2579
 2580
 2581
 2582
 2583
 2584

2585 I.29. NLP Benchmark: MMLU High School Geography (Hendrycks et al., 2020)


 2627 **Figure 38. MMLU High School Geography: Downstream performance is computed via a sequence of transformations that**
 2628 **deteriorate correlations between scores and pretraining compute.**

I.30. NLP Benchmark: MMLU High School Government & Politics (Hendrycks et al., 2020)

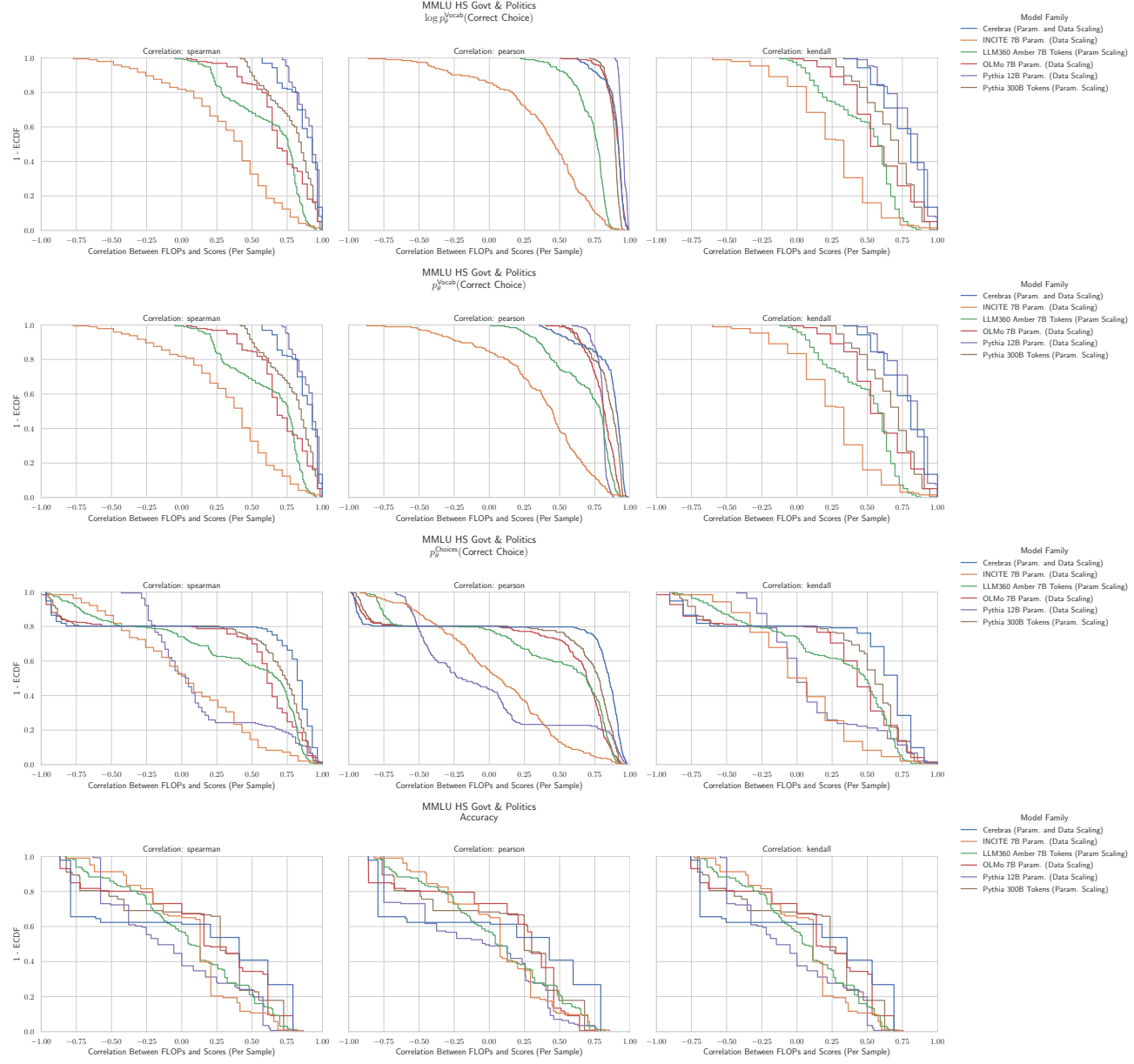
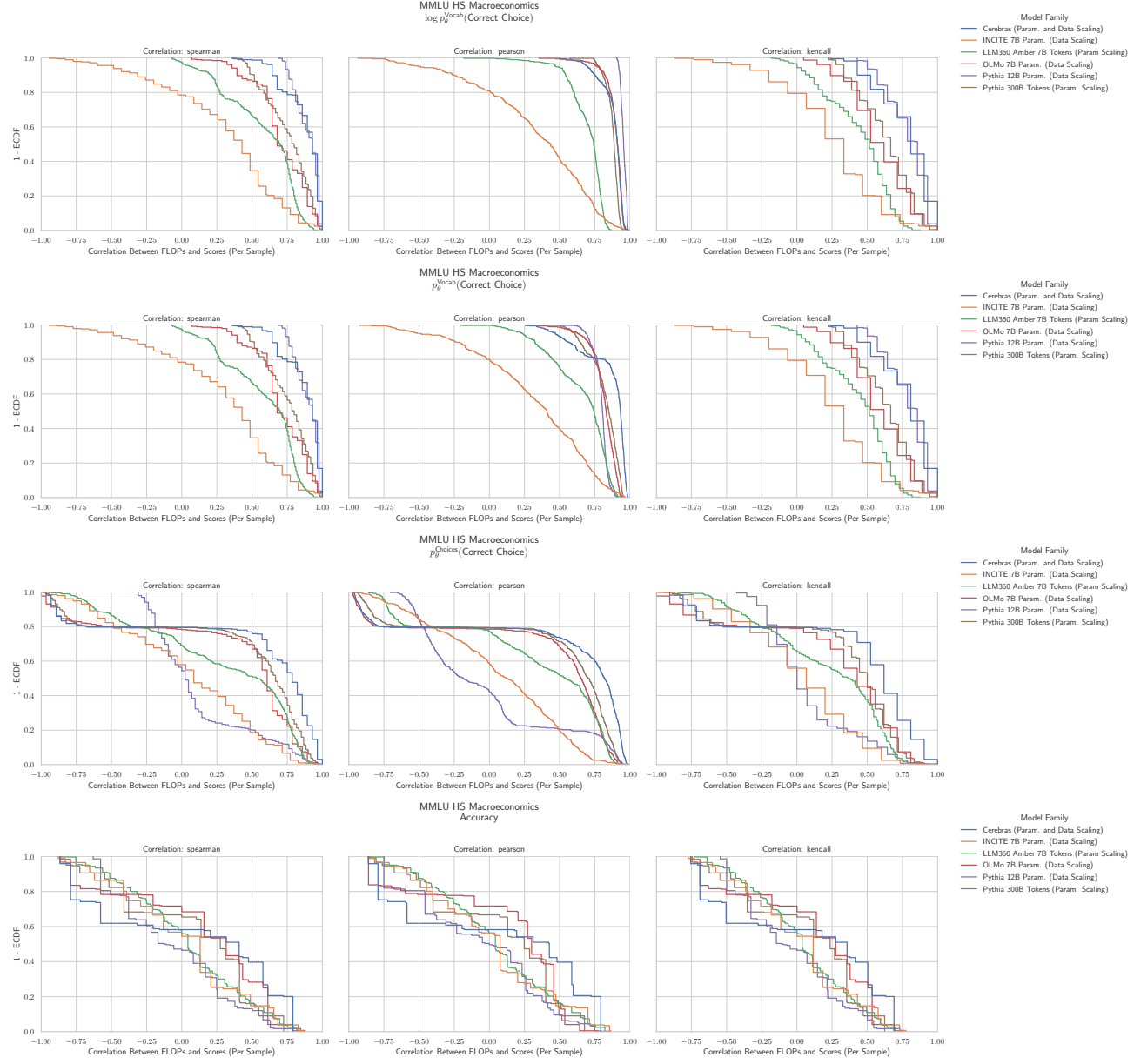


Figure 39. MMLU High School Government & Politics: Downstream performance is computed via a sequence of transformations that deteriorate correlations between scores and pretraining compute.

2695 I.31. NLP Benchmark: MMLU High School Macroeconomics (Hendrycks et al., 2020)


 2737 **Figure 40. MMLU High School Macroeconomics: Downstream performance is computed via a sequence of transformations that**
 2738 **deteriorate correlations between scores and pretraining compute.**

I.32. NLP Benchmark: MMLU High School Mathematics (Hendrycks et al., 2020)

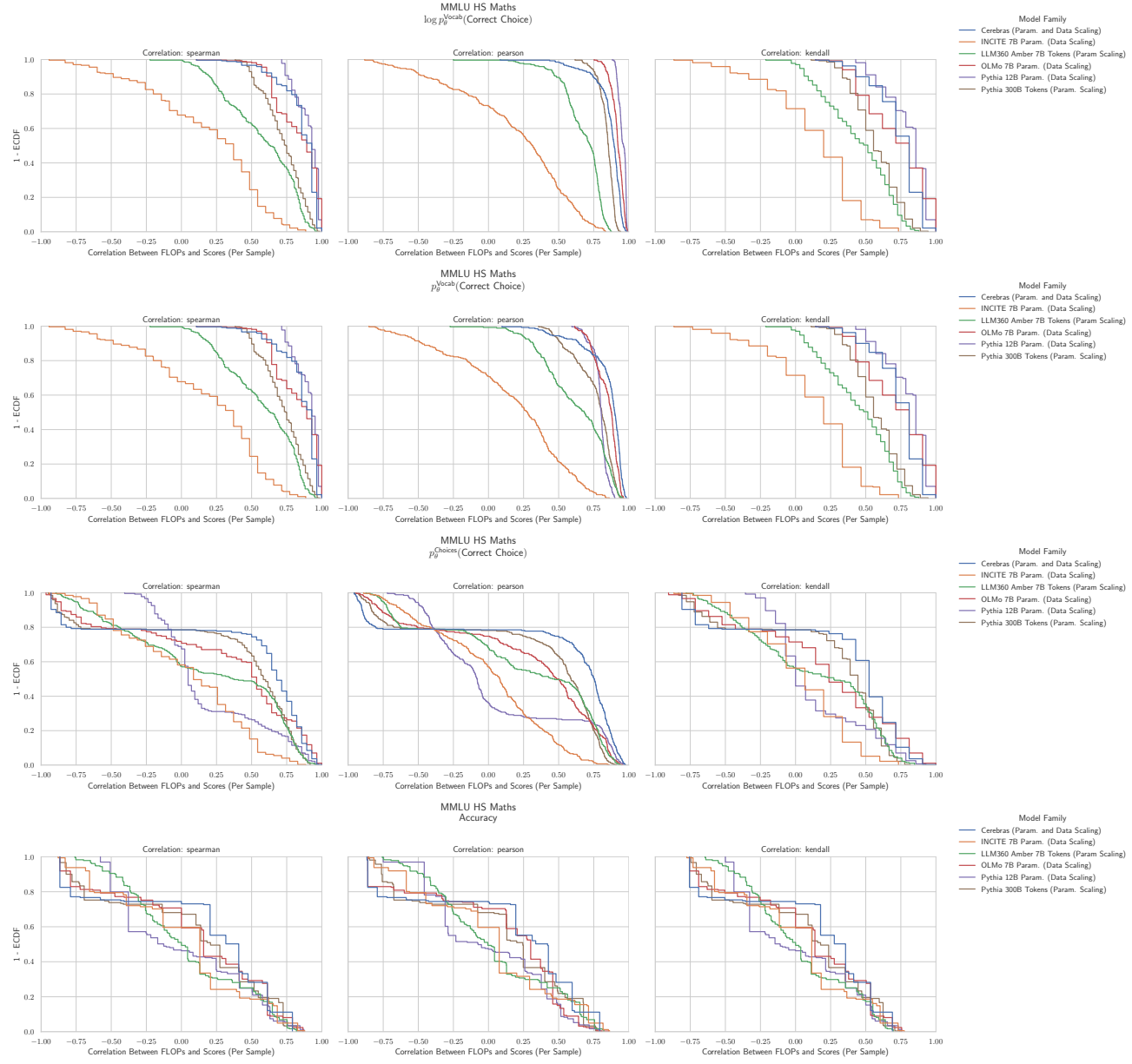
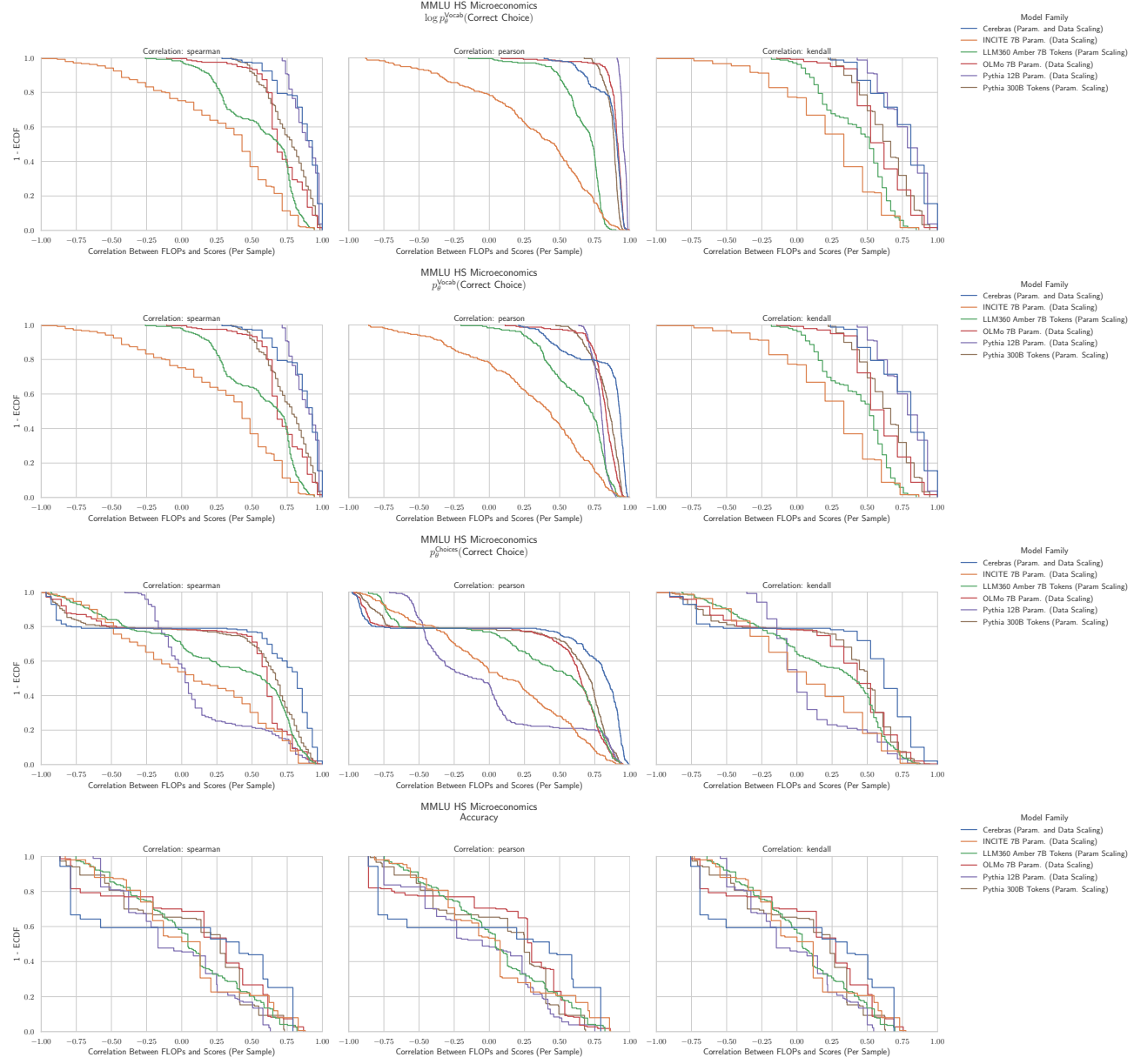
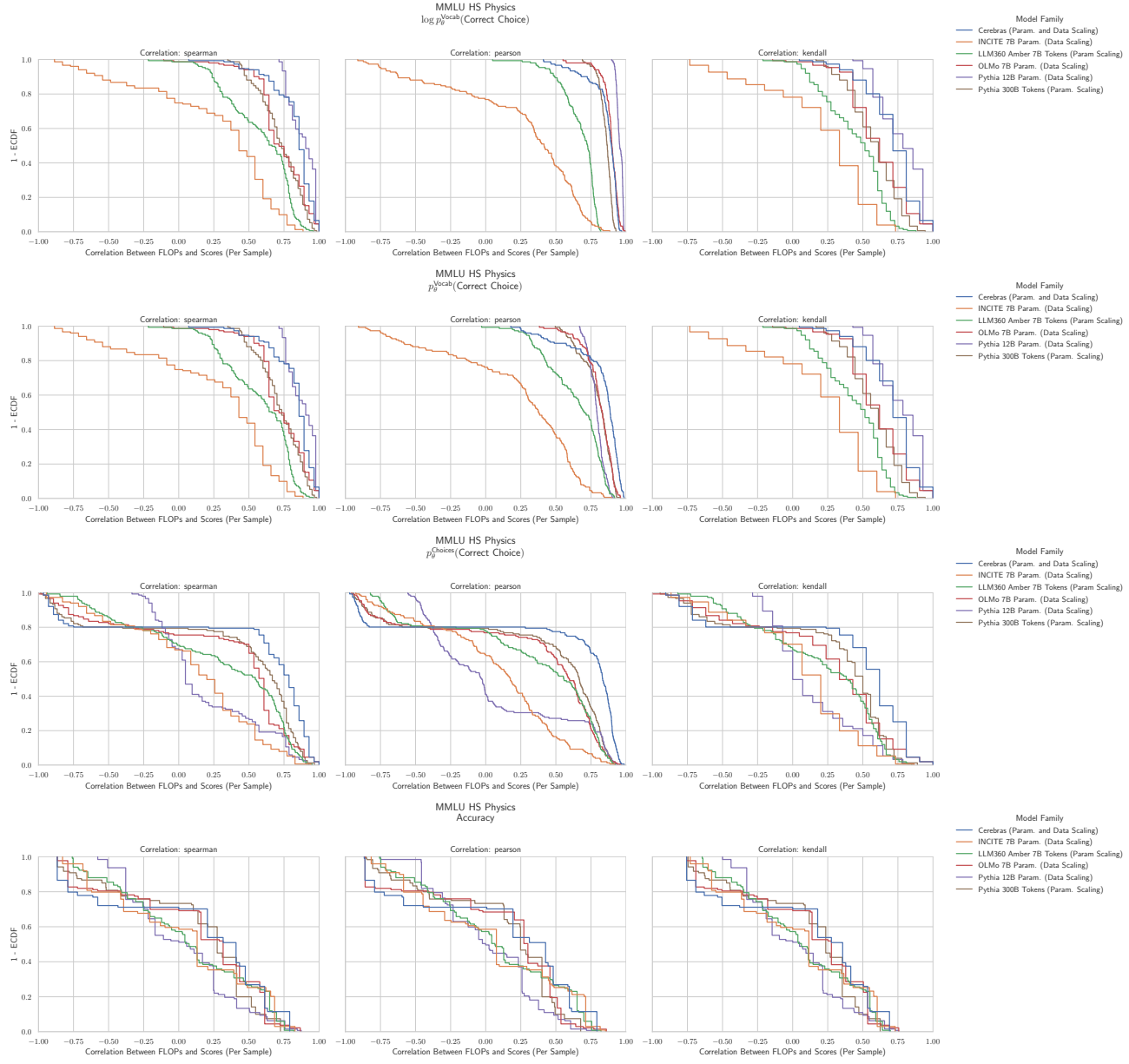


Figure 41. MMLU High School Mathematics: Downstream performance is computed via a sequence of transformations that deteriorate correlations between scores and pretraining compute.

2805 I.33. NLP Benchmark: MMLU High School Microeconomics (Hendrycks et al., 2020)


 2847 **Figure 42. MMLU High School Microeconomics: Downstream performance is computed via a sequence of transformations that**
 2848 **deteriorate correlations between scores and pretraining compute.**

2860 I.34. NLP Benchmark: MMLU High School Physics (Hendrycks et al., 2020)


 2902 **Figure 43. MMLU High School Physics: Downstream performance is computed via a sequence of transformations that deteriorate**
 2903 **correlations between scores and pretraining compute.**

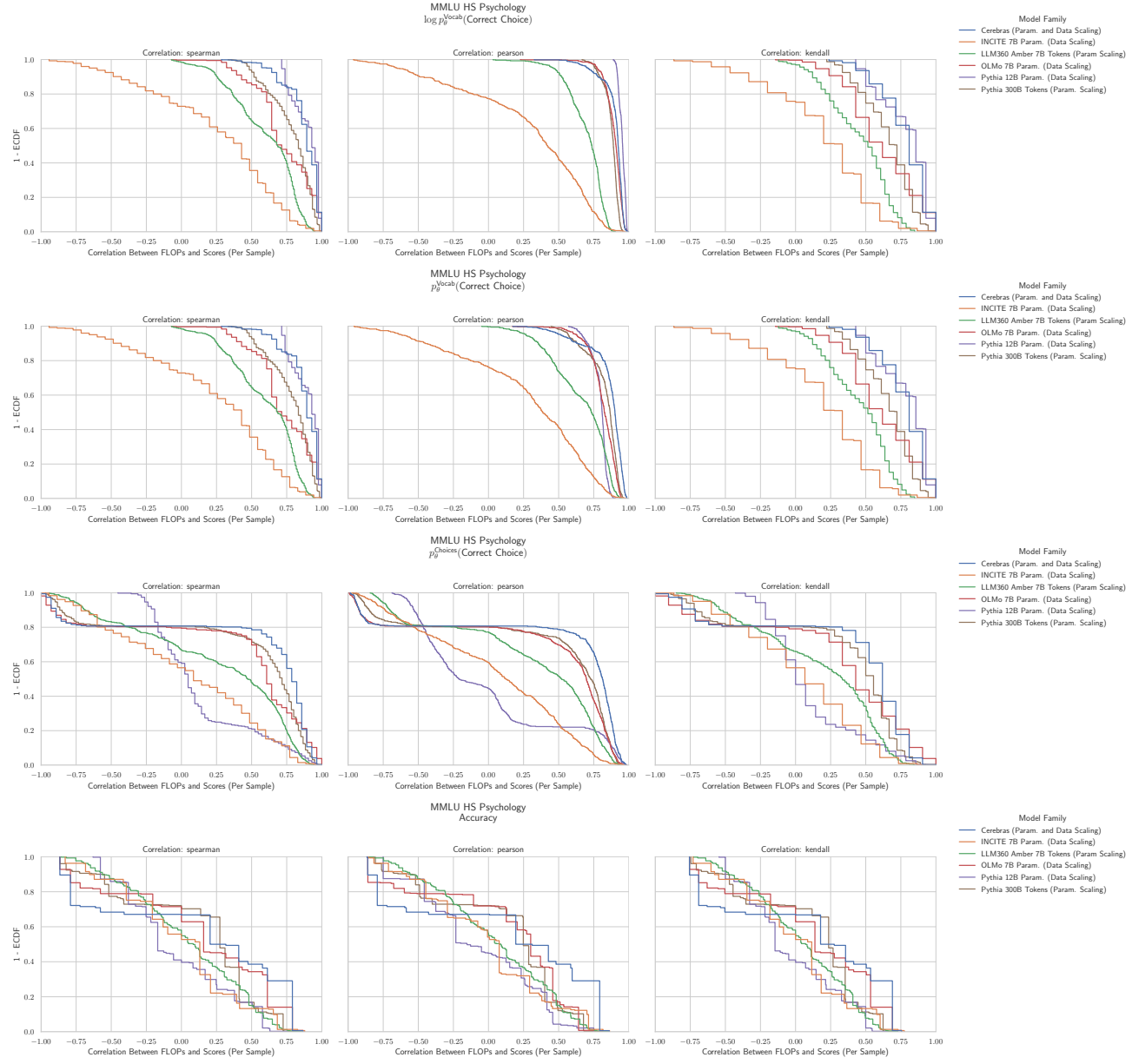
I.35. NLP Benchmark: MMLU High School Psychology (Hendrycks et al., 2020)


Figure 44. MMLU High School Psychology: Downstream performance is computed via a sequence of transformations that deteriorate correlations between scores and pretraining compute.

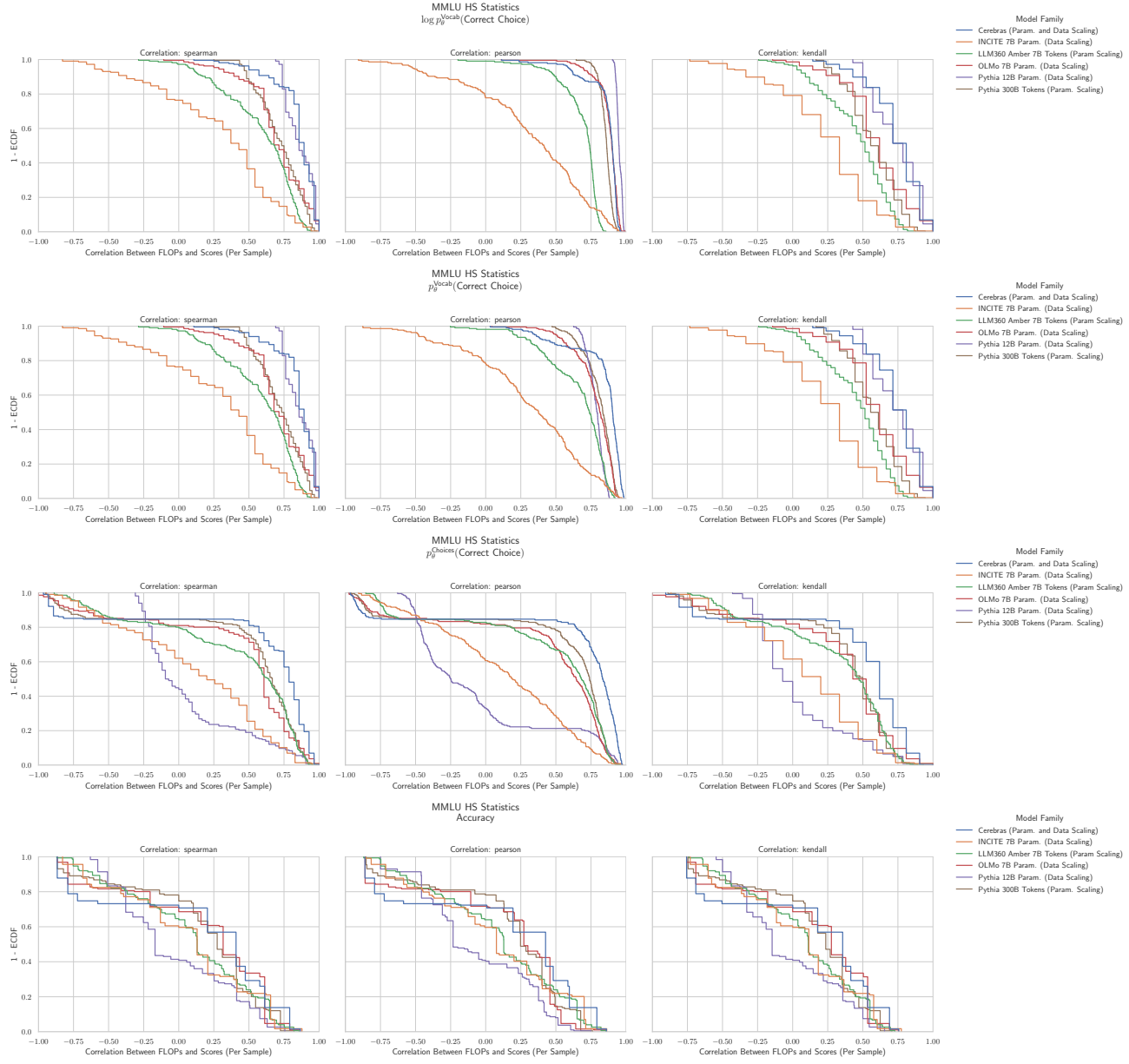
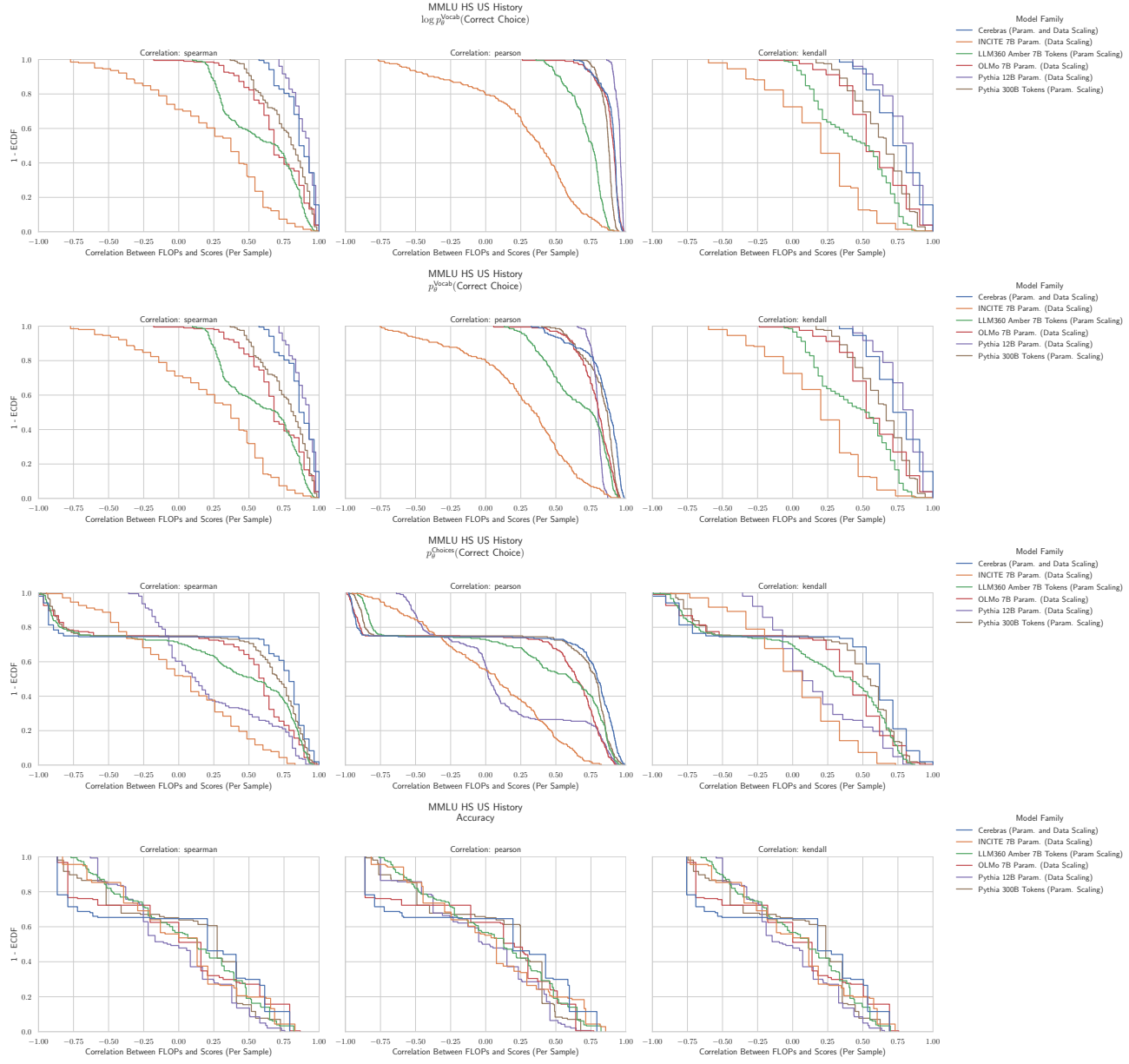
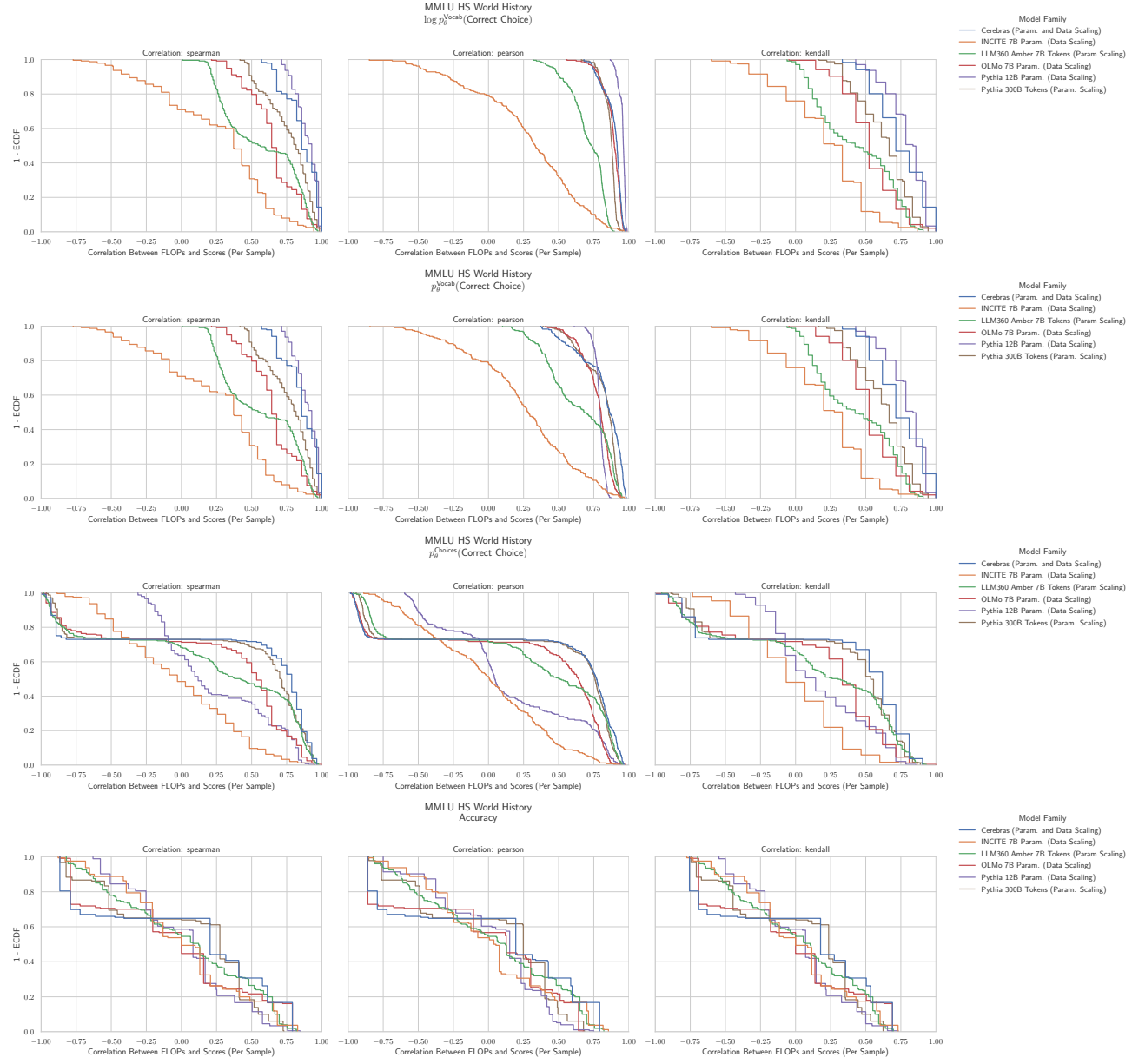
I.36. NLP Benchmark: MMLU High School Statistics (Hendrycks et al., 2020)


Figure 45. MMLU High School Statistics: Downstream performance is computed via a sequence of transformations that deteriorate correlations between scores and pretraining compute.

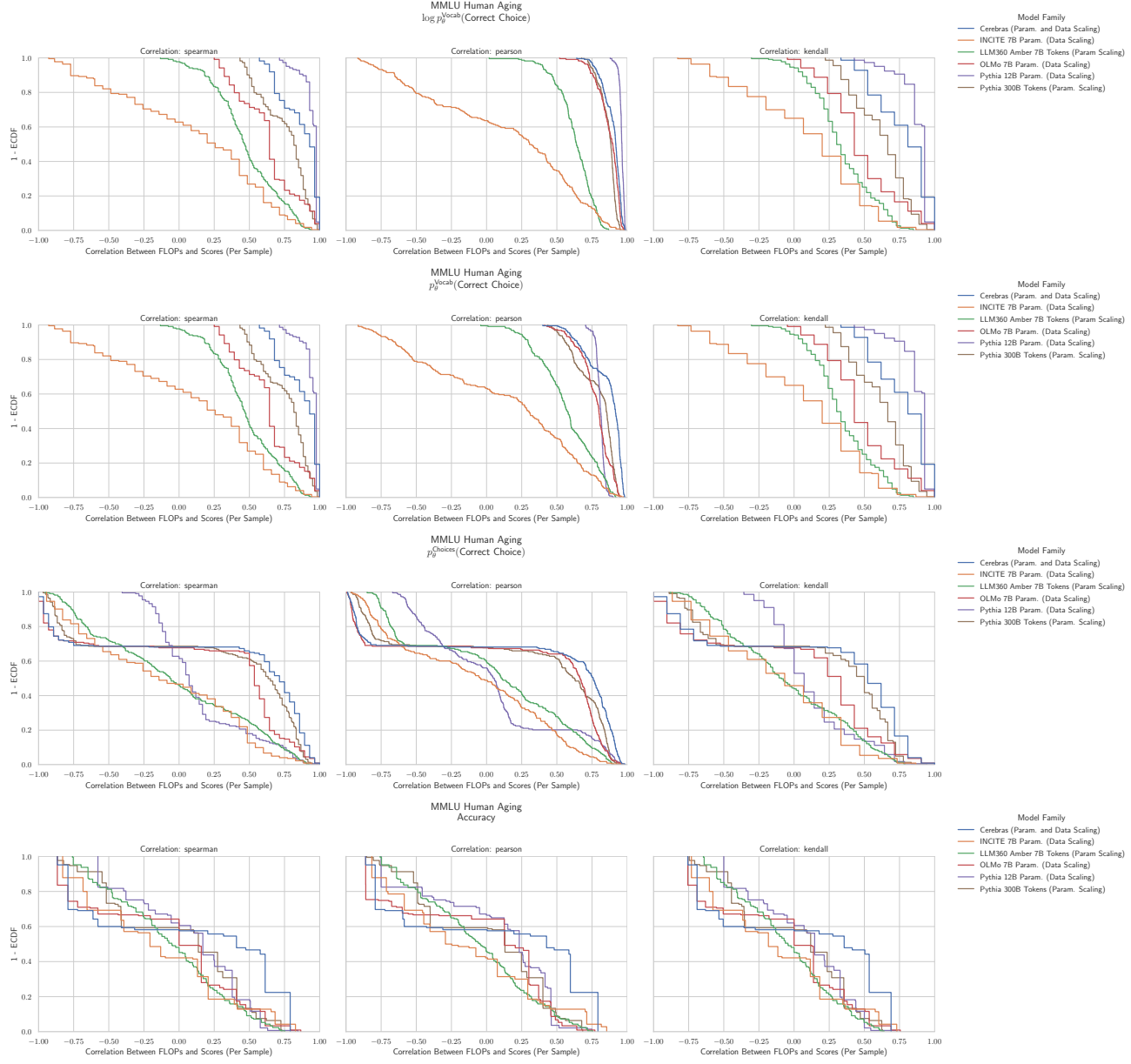
3025 I.37. NLP Benchmark: MMLU High School US History (Hendrycks et al., 2020)


 3067 **Figure 46. MMLU High School US History: Downstream performance is computed via a sequence of transformations that
3068 deteriorate correlations between scores and pretraining compute.**

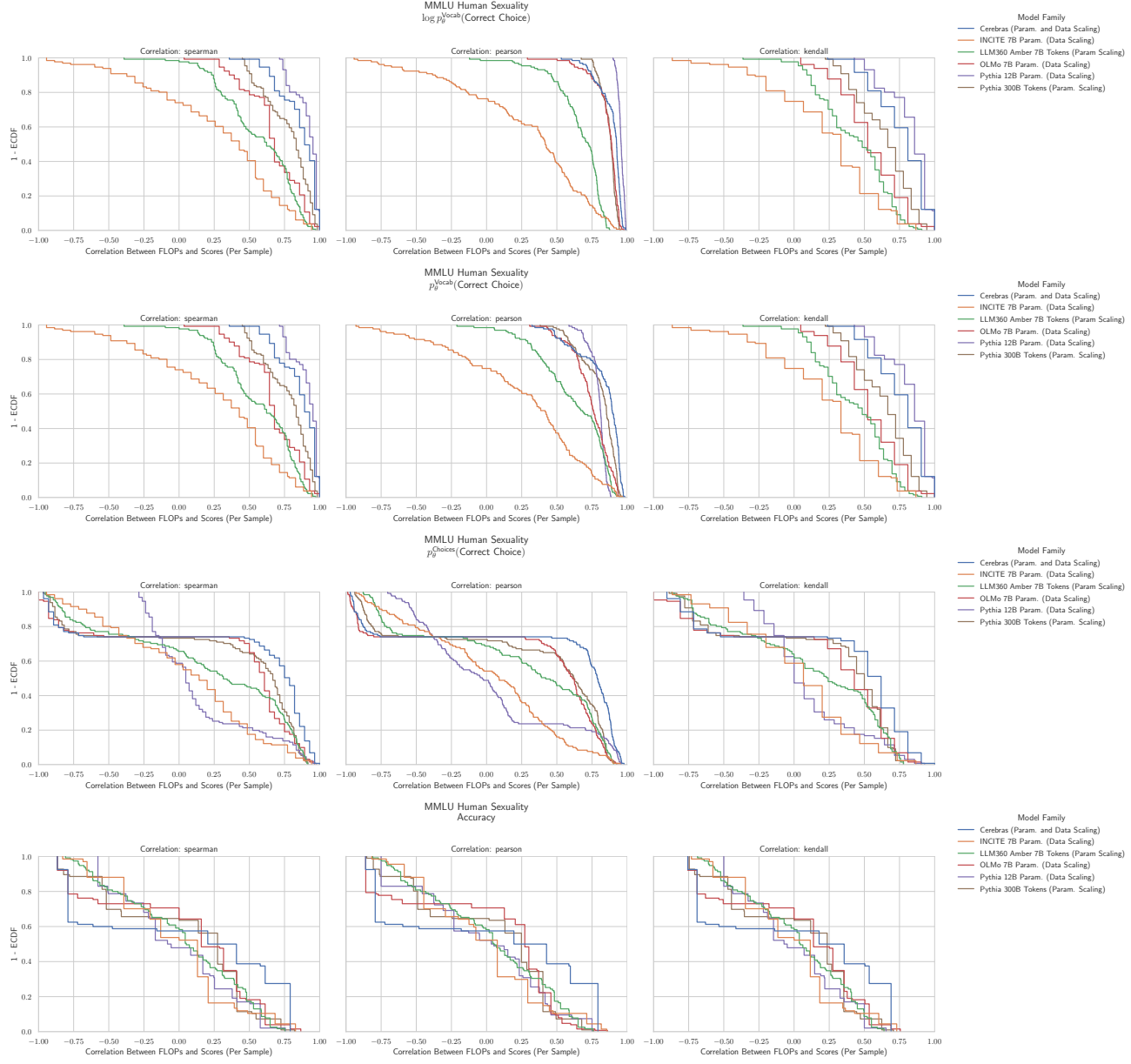
3080 I.38. NLP Benchmark: MMLU High School World History (Hendrycks et al., 2020)


 3122 Figure 47. MMLU High School World History: Downstream performance is computed via a sequence of transformations that
 3123 deteriorate correlations between scores and pretraining compute.
 3124

3135 I.39. NLP Benchmark: MMLU Human Aging (Hendrycks et al., 2020)


 3177 **Figure 48. MMLU Human Aging: Downstream performance is computed via a sequence of transformations that deteriorate**
 3178 **correlations between scores and pretraining compute.**

3190 I.40. NLP Benchmark: MMLU Human Sexuality (Hendrycks et al., 2020)


 3232 **Figure 49. MMLU Human Sexuality: Downstream performance is computed via a sequence of transformations that deteriorate**
 3233 **correlations between scores and pretraining compute.**

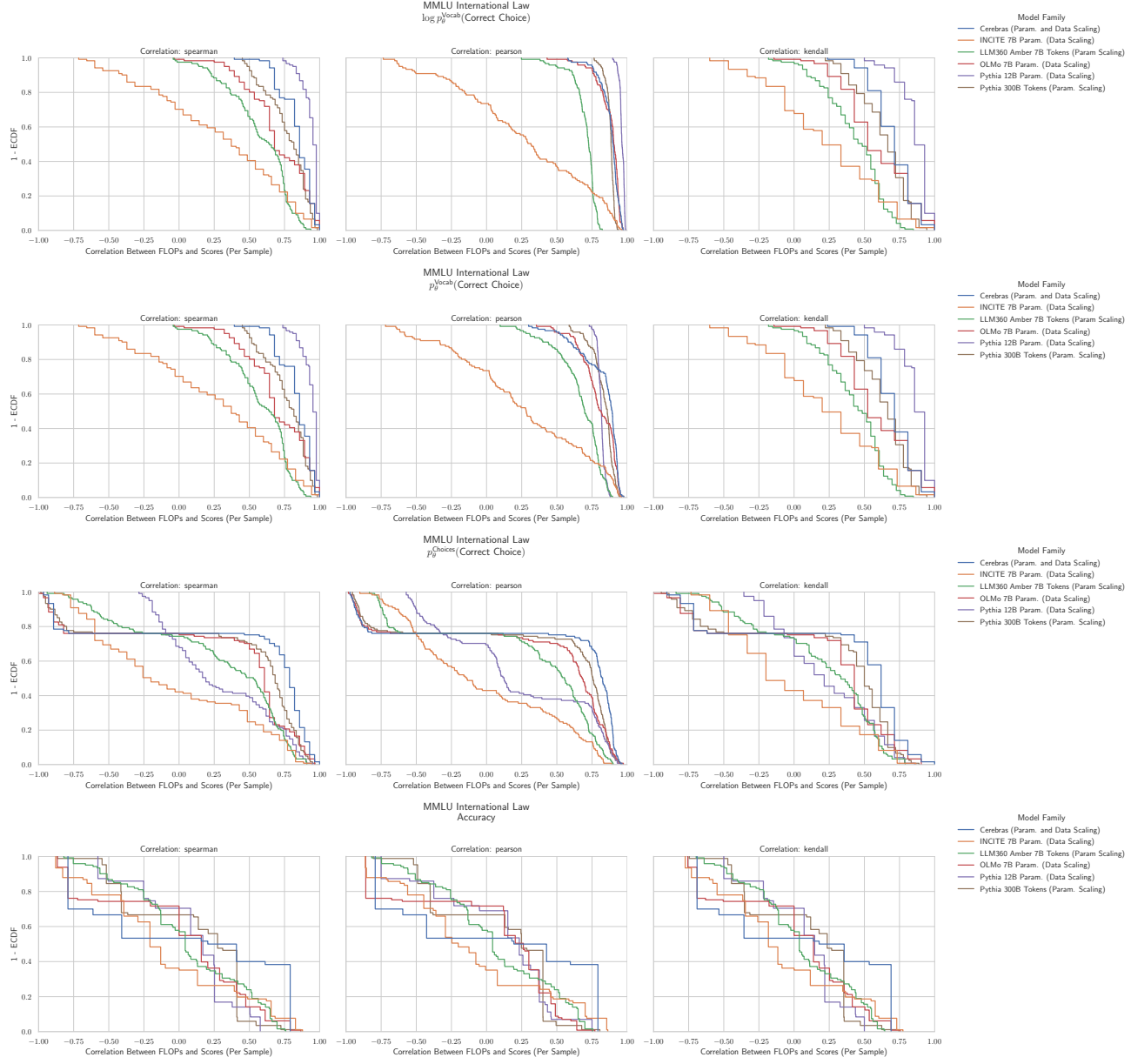
I.41. NLP Benchmark: MMLU International Law (Hendrycks et al., 2020)


Figure 50. MMLU International Law: Downstream performance is computed via a sequence of transformations that deteriorate correlations between scores and pretraining compute.

I.42. NLP Benchmark: MMLU Jurisprudence (Hendrycks et al., 2020)

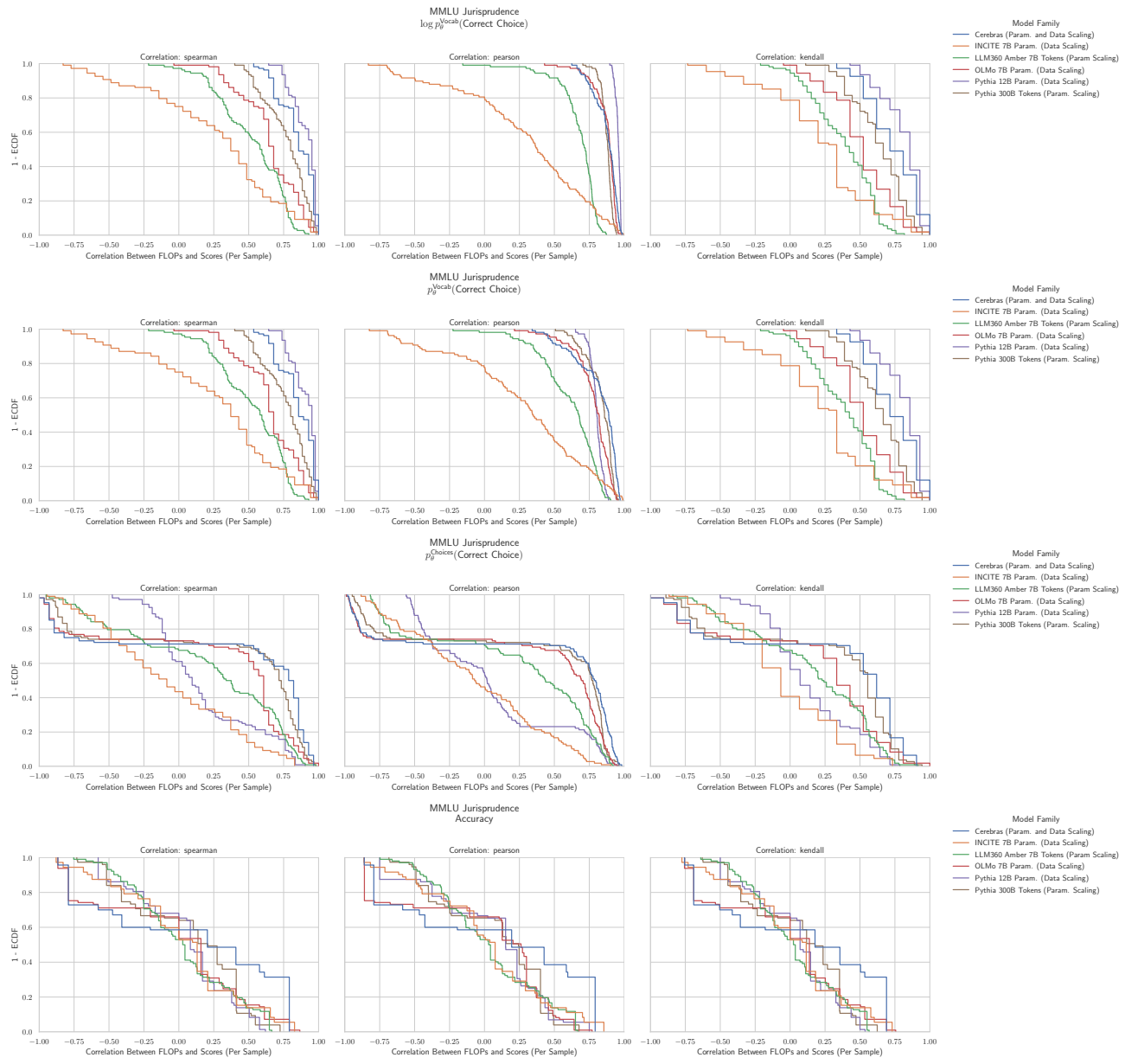
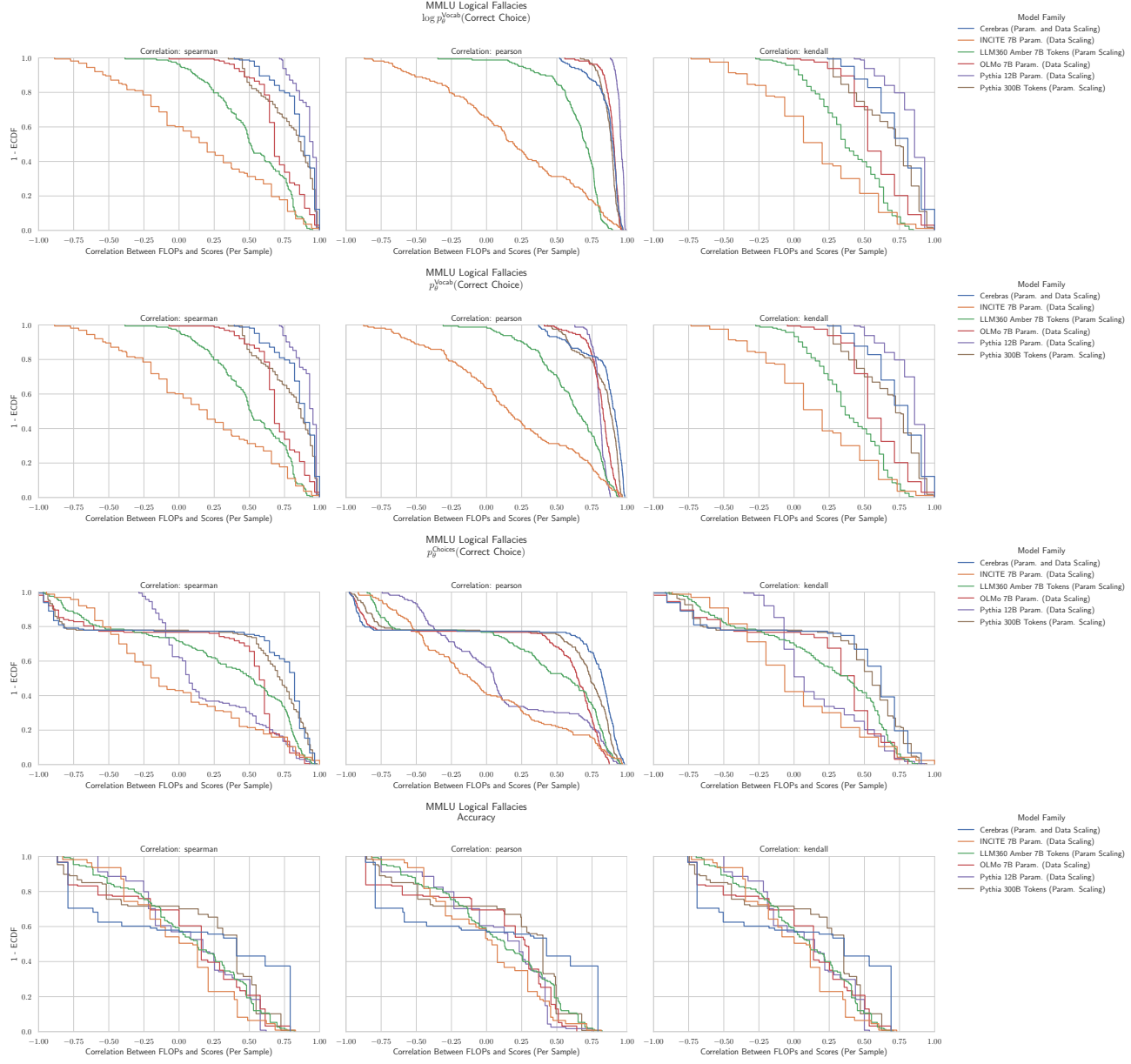


Figure 51. MMLU Jurisprudence: Downstream performance is computed via a sequence of transformations that deteriorate correlations between scores and pretraining compute.

3355 I.43. NLP Benchmark: MMLU Logical Fallacies (Hendrycks et al., 2020)


 3397 **Figure 52. MMLU Logical Fallacies:** Downstream performance is computed via a sequence of transformations that deteriorate
 3398 correlations between scores and pretraining compute.
 3399

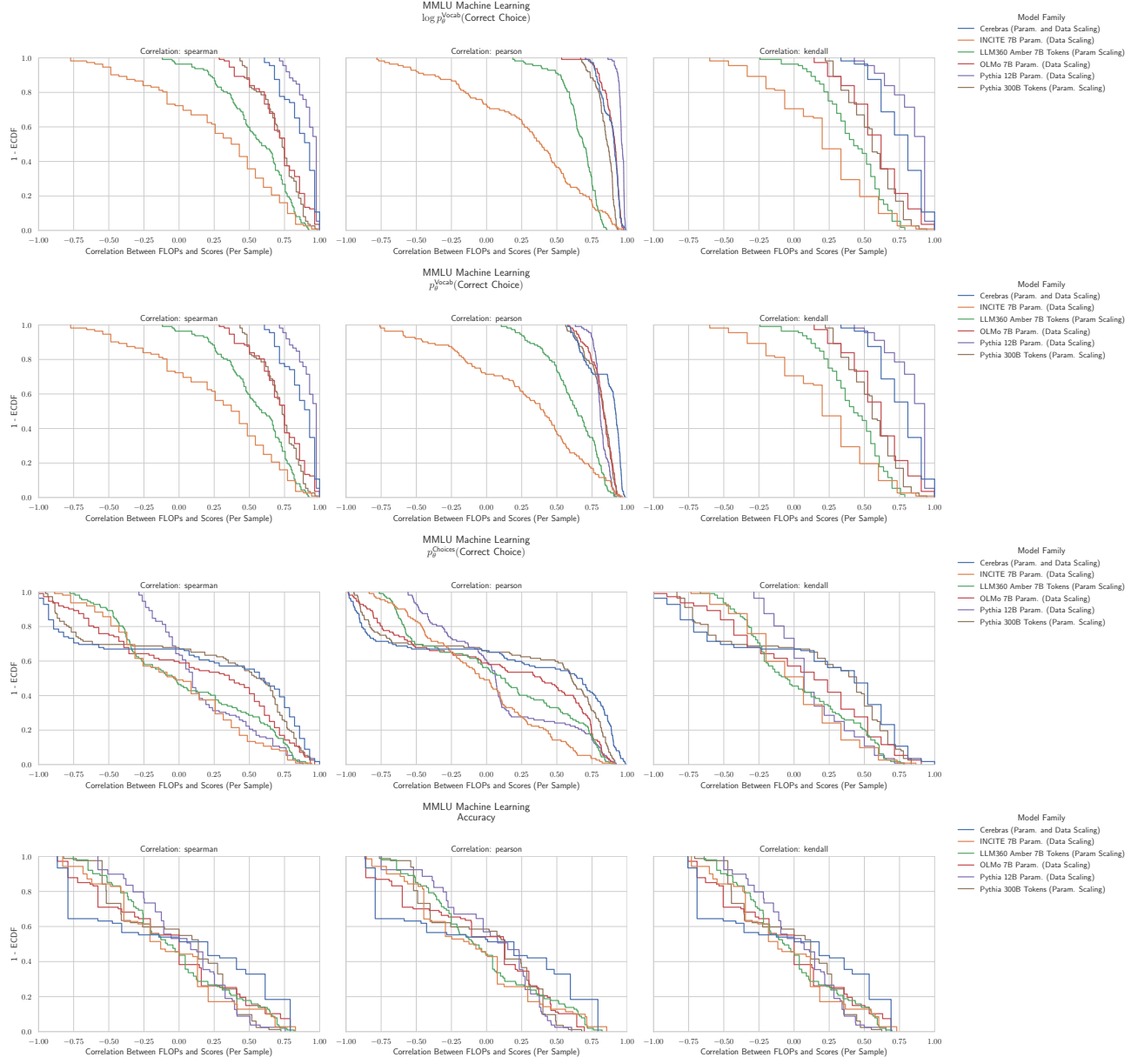
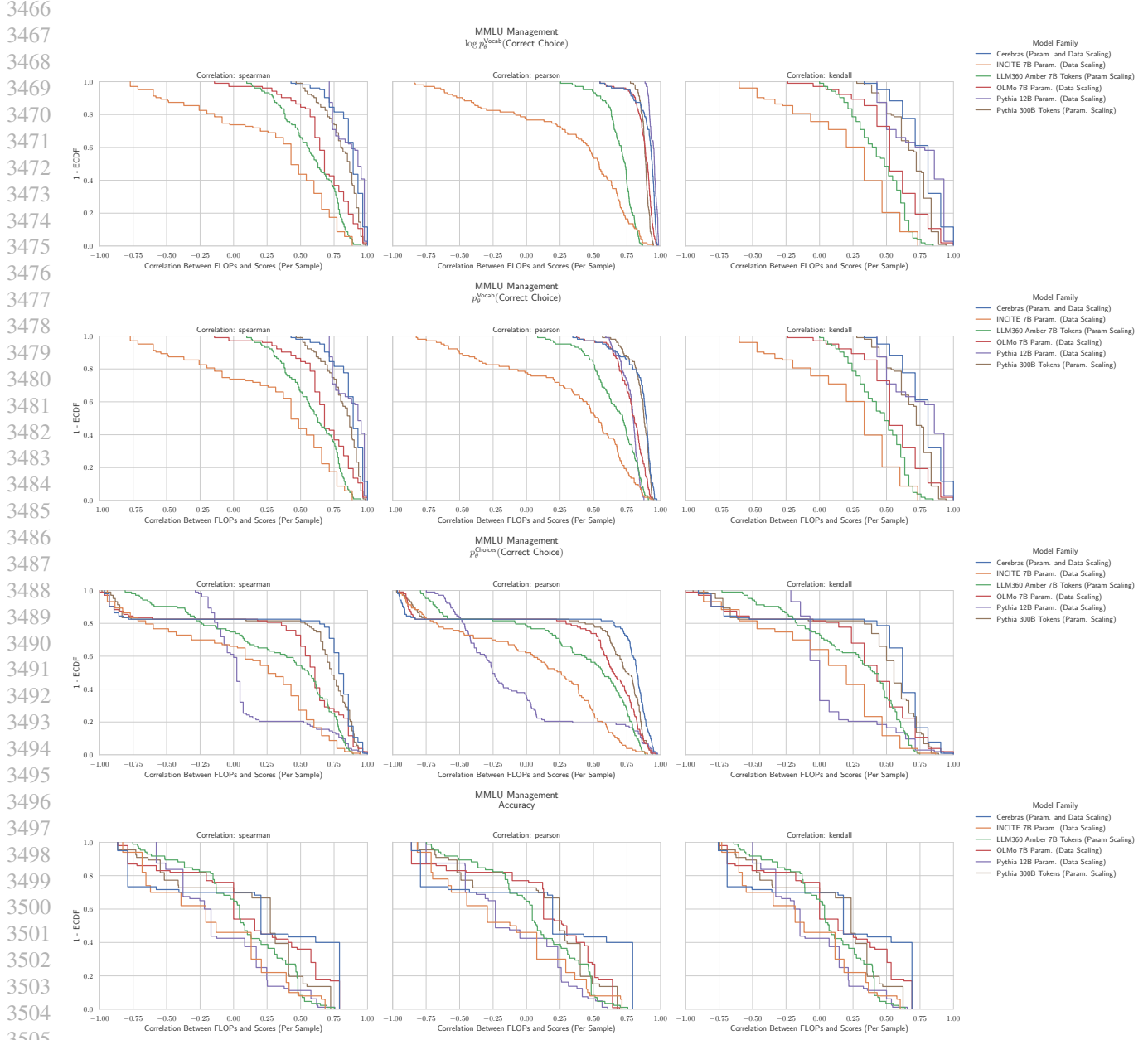
I.44. NLP Benchmark: MMLU Machine Learning (Hendrycks et al., 2020)


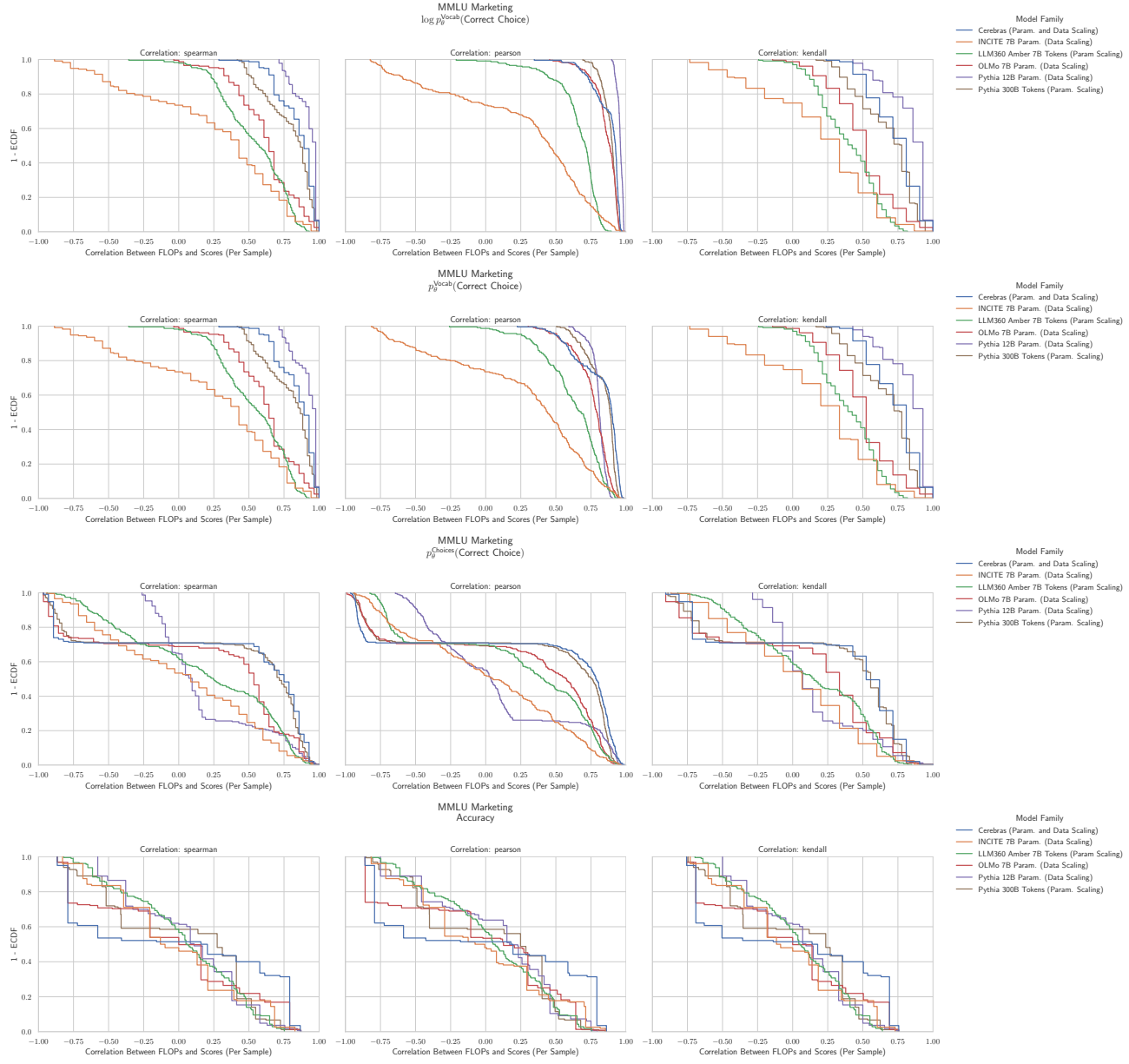
Figure 53. MMLU Machine Learning: Downstream performance is computed via a sequence of transformations that deteriorate correlations between scores and pretraining compute.

3465 I.45. NLP Benchmark: MMLU Management (Hendrycks et al., 2020)

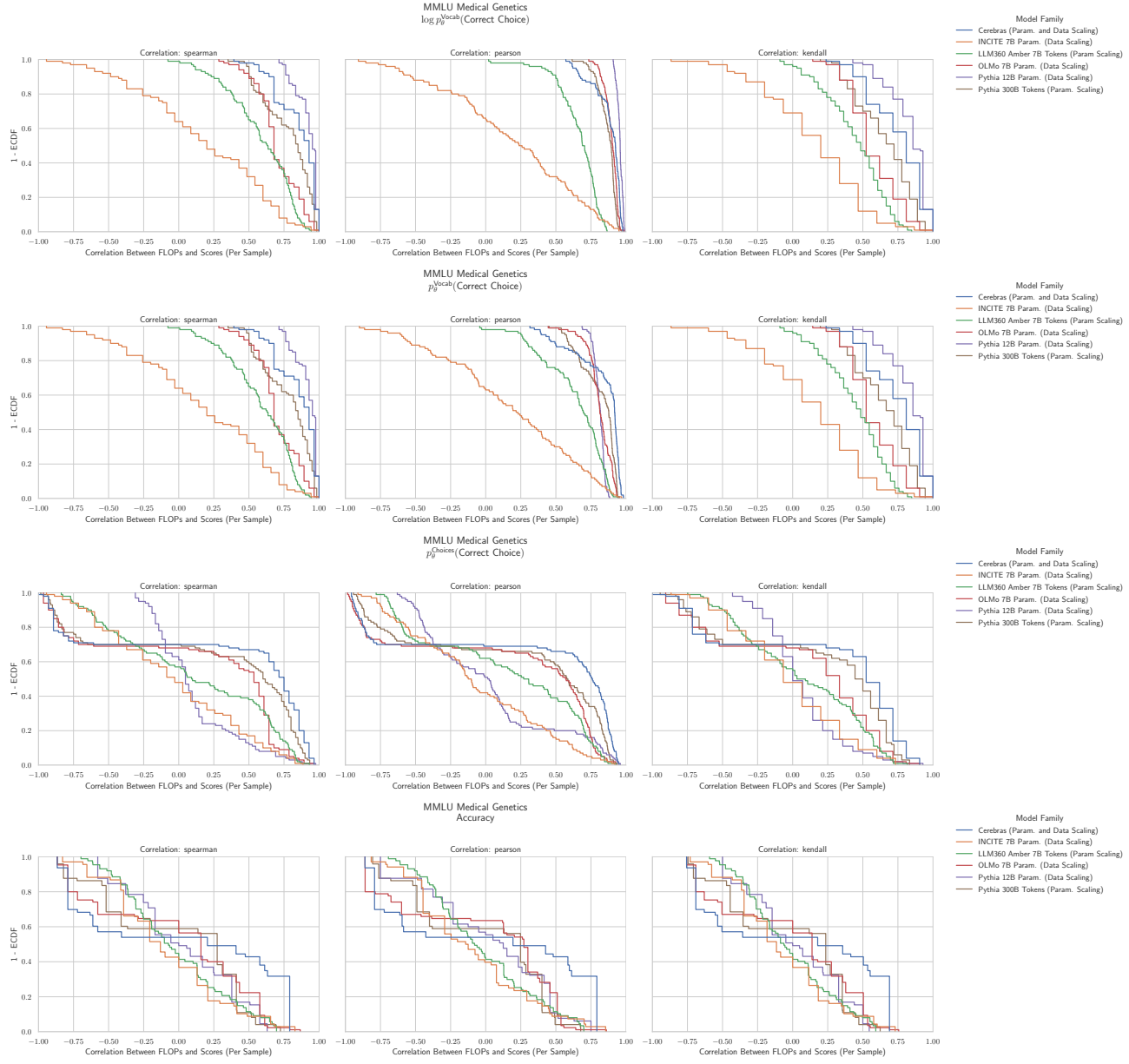

 3507 **Figure 54. MMLU Management:** Downstream performance is computed via a sequence of transformations that deteriorate
 3508 correlations between scores and pretraining compute.
 3509

 3510
 3511
 3512
 3513
 3514
 3515
 3516
 3517
 3518
 3519

3520 I.46. NLP Benchmark: MMLU Marketing (Hendrycks et al., 2020)


 3562 **Figure 55. MMLU Marketing:** Downstream performance is computed via a sequence of transformations that deteriorate correlations between scores and pretraining compute.

3575 I.47. NLP Benchmark: MMLU Medical Genetics (Hendrycks et al., 2020)


 3617 **Figure 56. MMLU Medical Genetics: Downstream performance is computed via a sequence of transformations that deteriorate**
 3618 **correlations between scores and pretraining compute.**

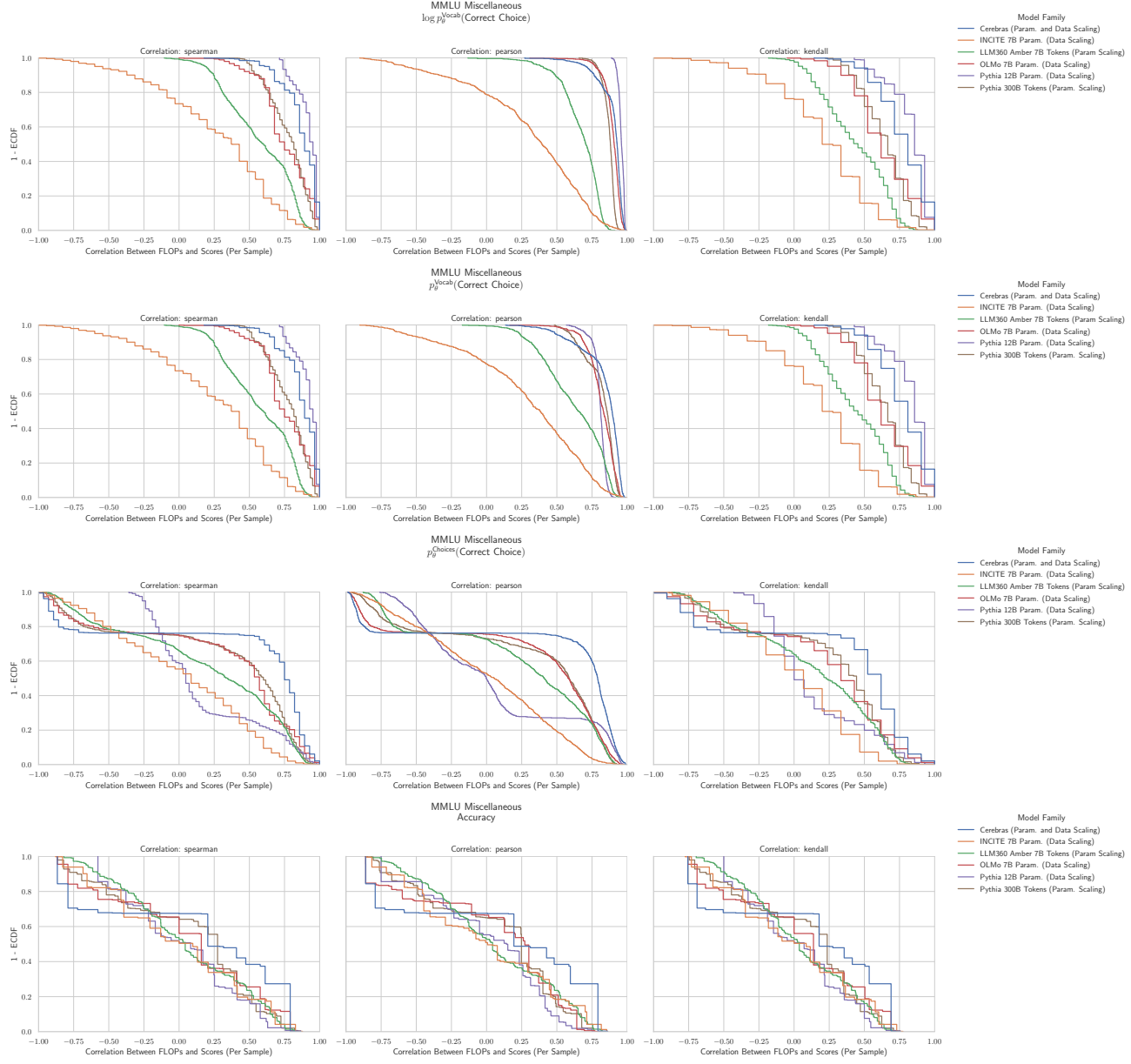
I.48. NLP Benchmark: MMLU Miscellaneous (Hendrycks et al., 2020)


Figure 57. MMLU Miscellaneous: Downstream performance is computed via a sequence of transformations that deteriorate correlations between scores and pretraining compute.

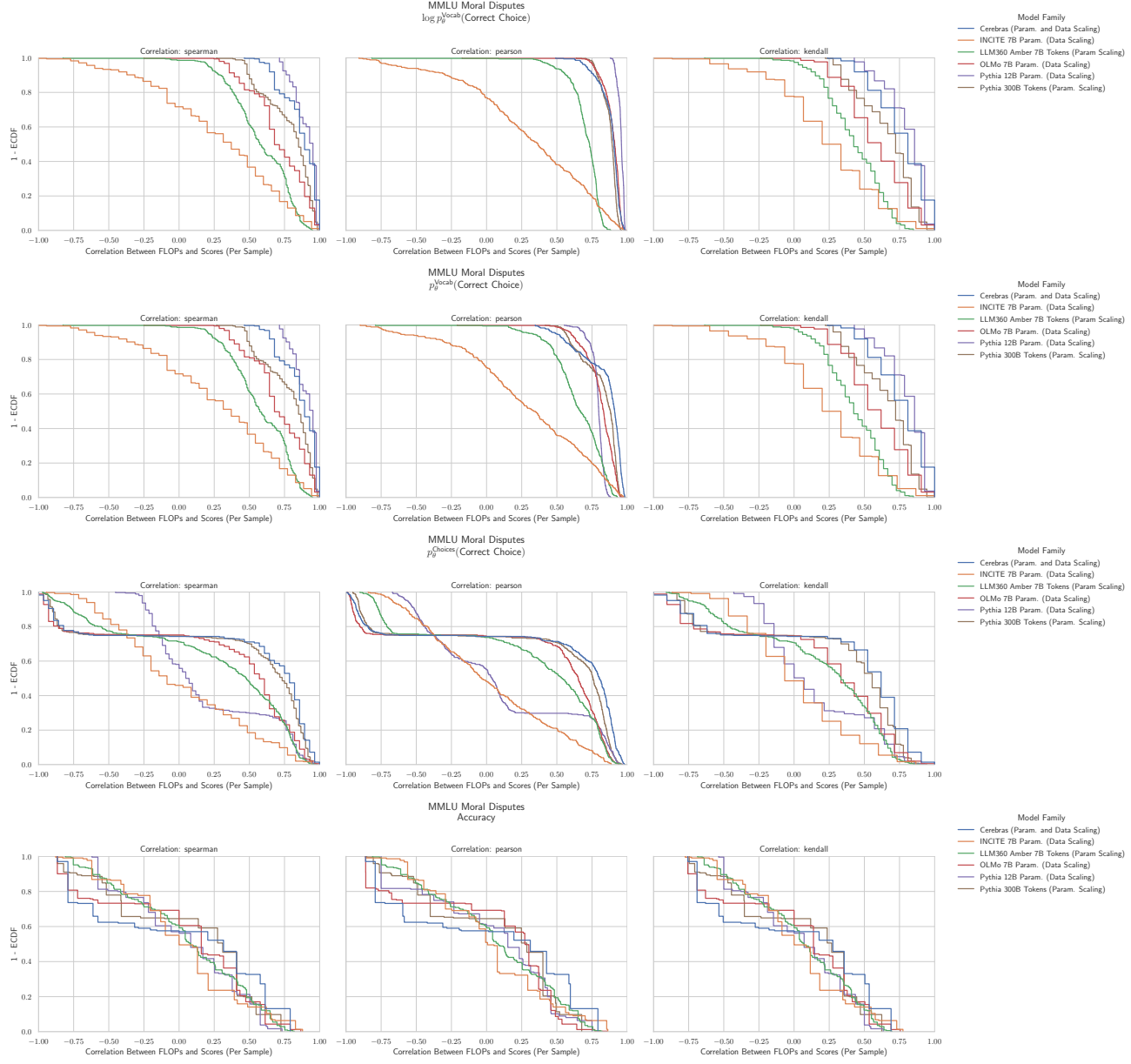
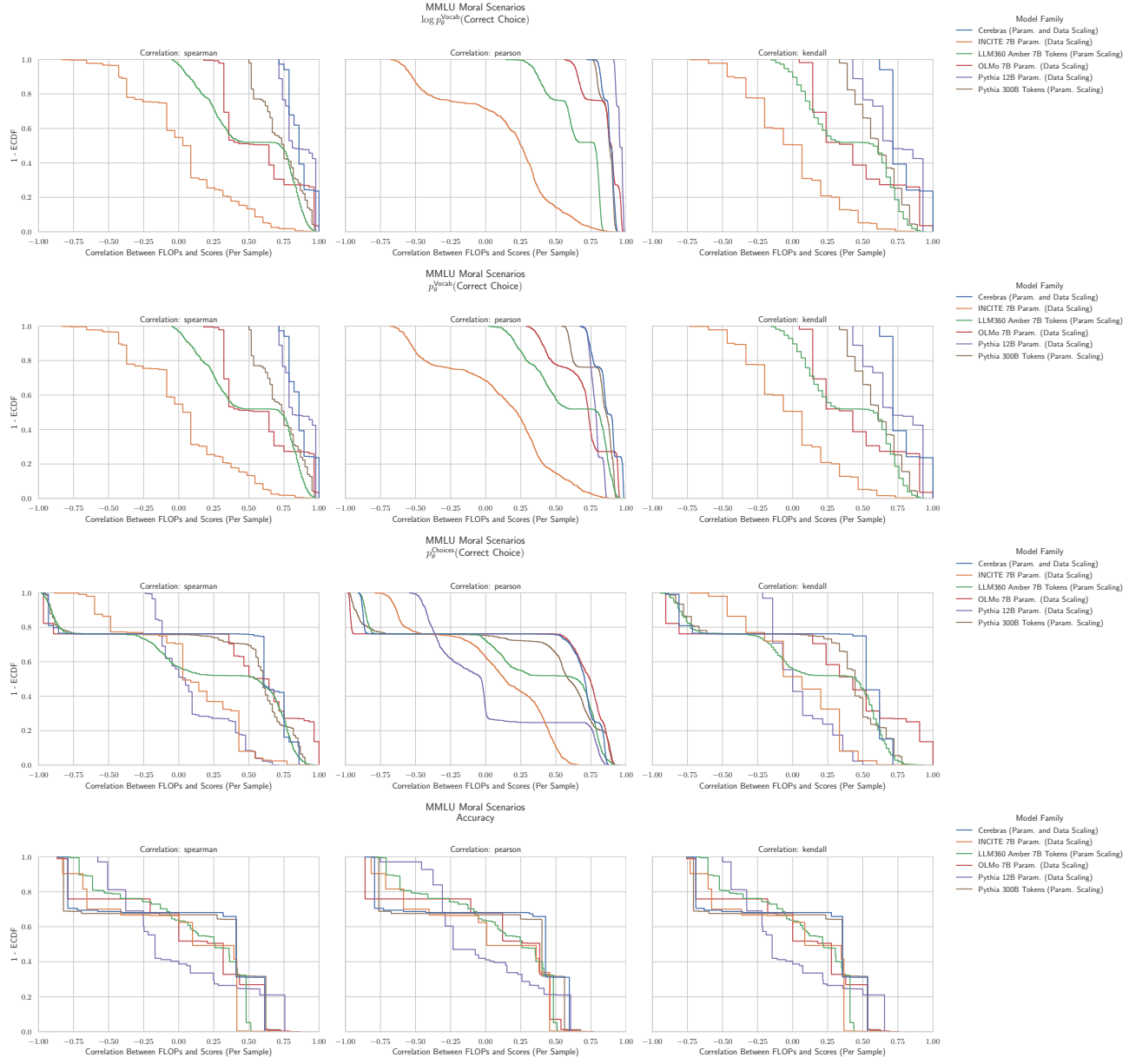
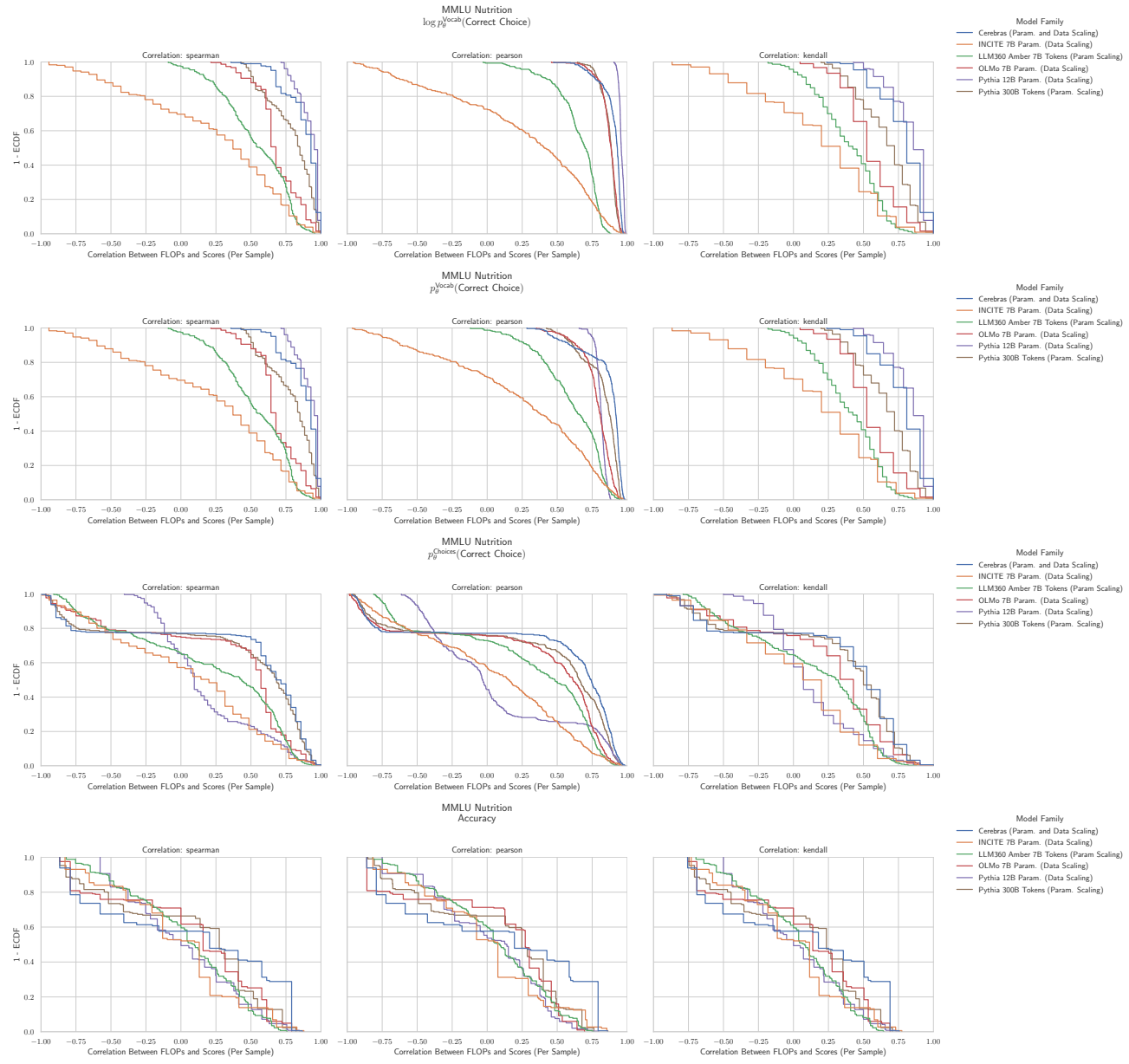
I.49. NLP Benchmark: MMLU Moral Disputes (Hendrycks et al., 2020)


Figure 58. MMLU Moral Disputes: Downstream performance is computed via a sequence of transformations that deteriorate correlations between scores and pretraining compute.

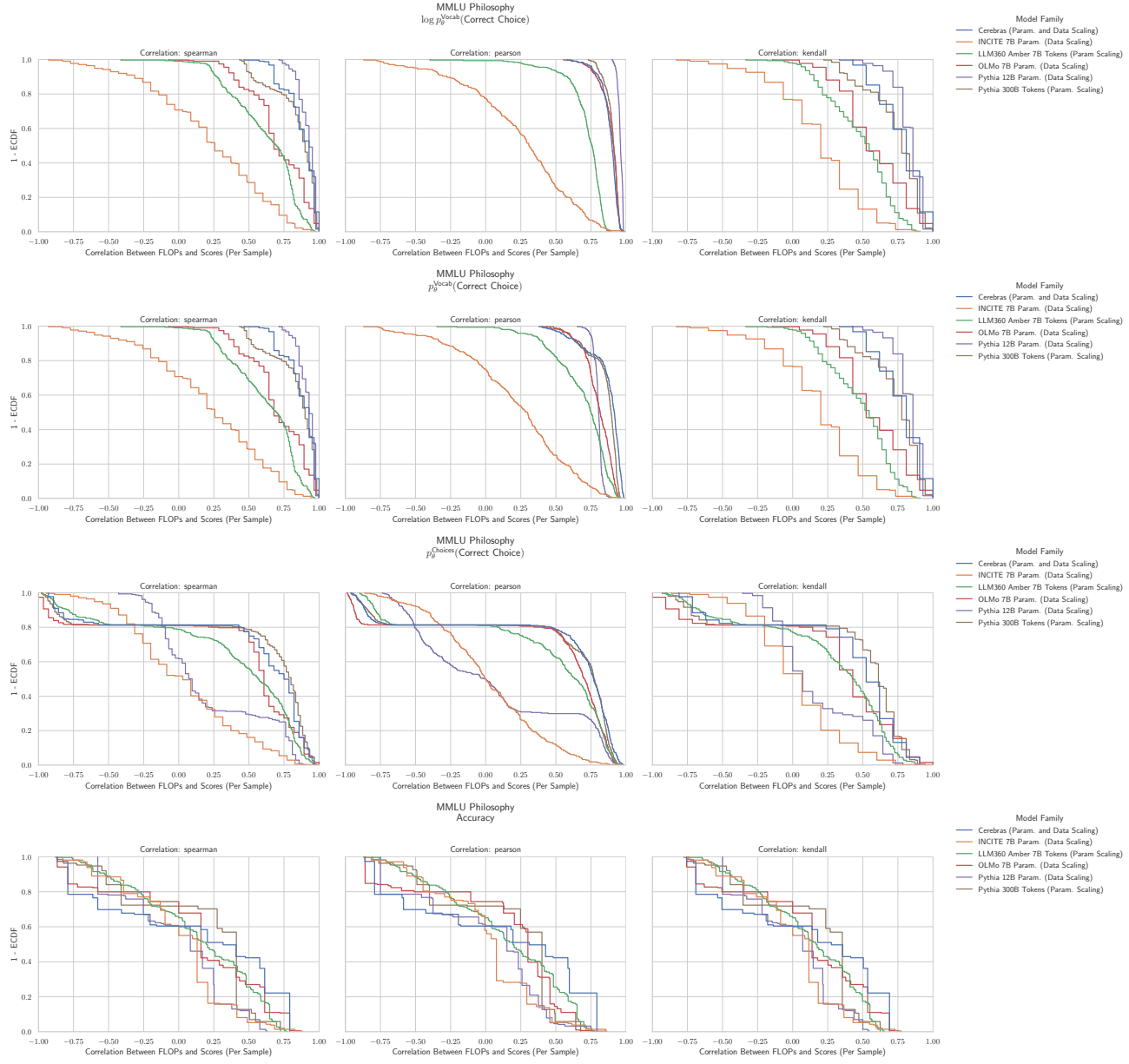
3740 I.50. NLP Benchmark: MMLU Moral Scenarios (Hendrycks et al., 2020)


 3782 **Figure 59. MMLU Moral Scenarios: Downstream performance is computed via a sequence of transformations that deteriorate**
 3783 **correlations between scores and pretraining compute.**

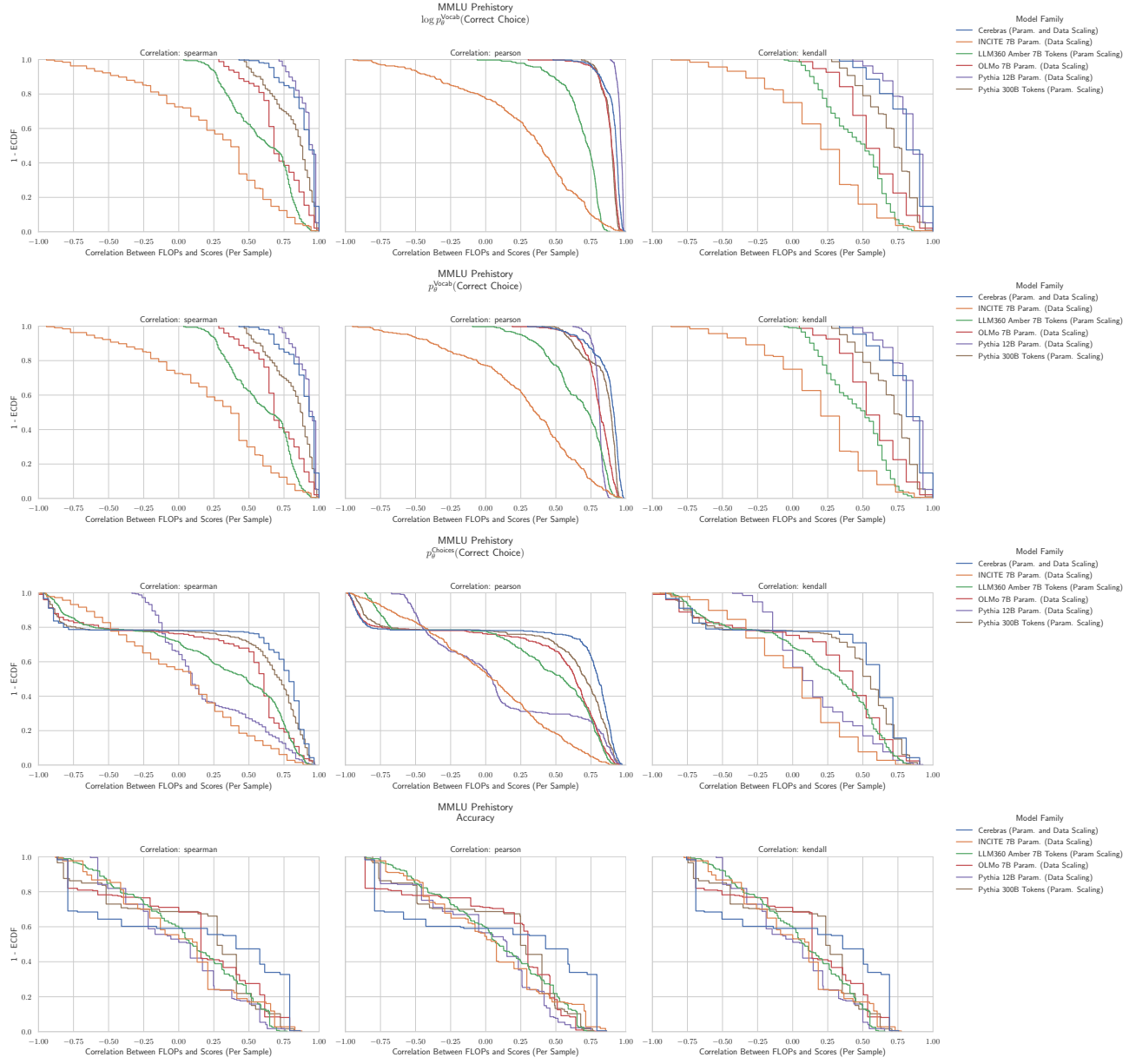
3795 I.51. NLP Benchmark: MMLU Nutrition (Hendrycks et al., 2020)


 3837 **Figure 60. MMLU Nutrition: Downstream performance is computed via a sequence of transformations that deteriorate correlations
3838 between scores and pretraining compute.**

3850 I.52. NLP Benchmark: MMLU Philosophy (Hendrycks et al., 2020)


 3892 **Figure 61. MMLU Philosophy:** Downstream performance is computed via a sequence of transformations that deteriorate correlations between scores and pretraining compute.

3905 I.53. NLP Benchmark: MMLU Prehistory (Hendrycks et al., 2020)


 3947 **Figure 62. MMLU Prehistory: Downstream performance is computed via a sequence of transformations that deteriorate correlations between scores and pretraining compute.**

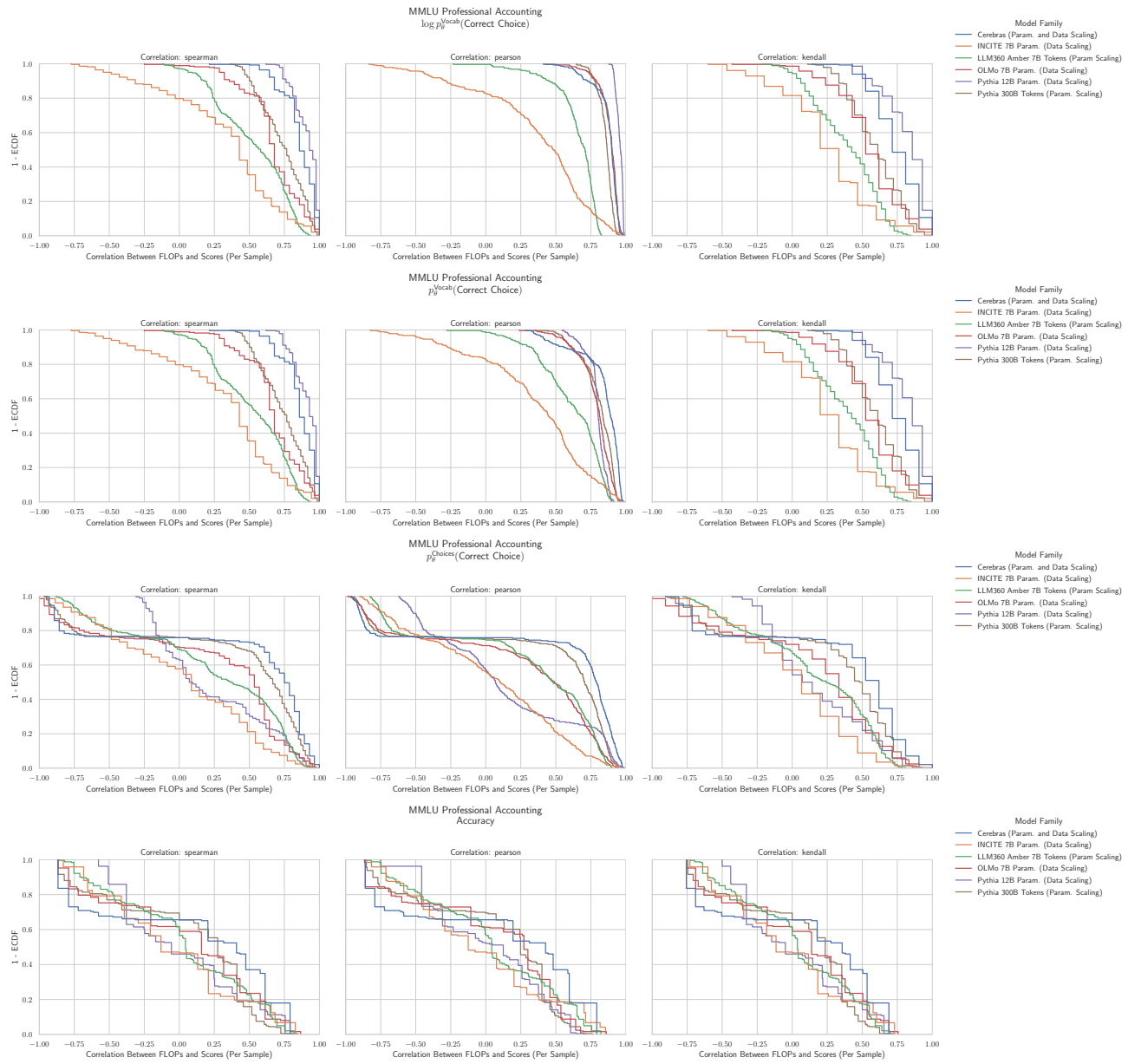
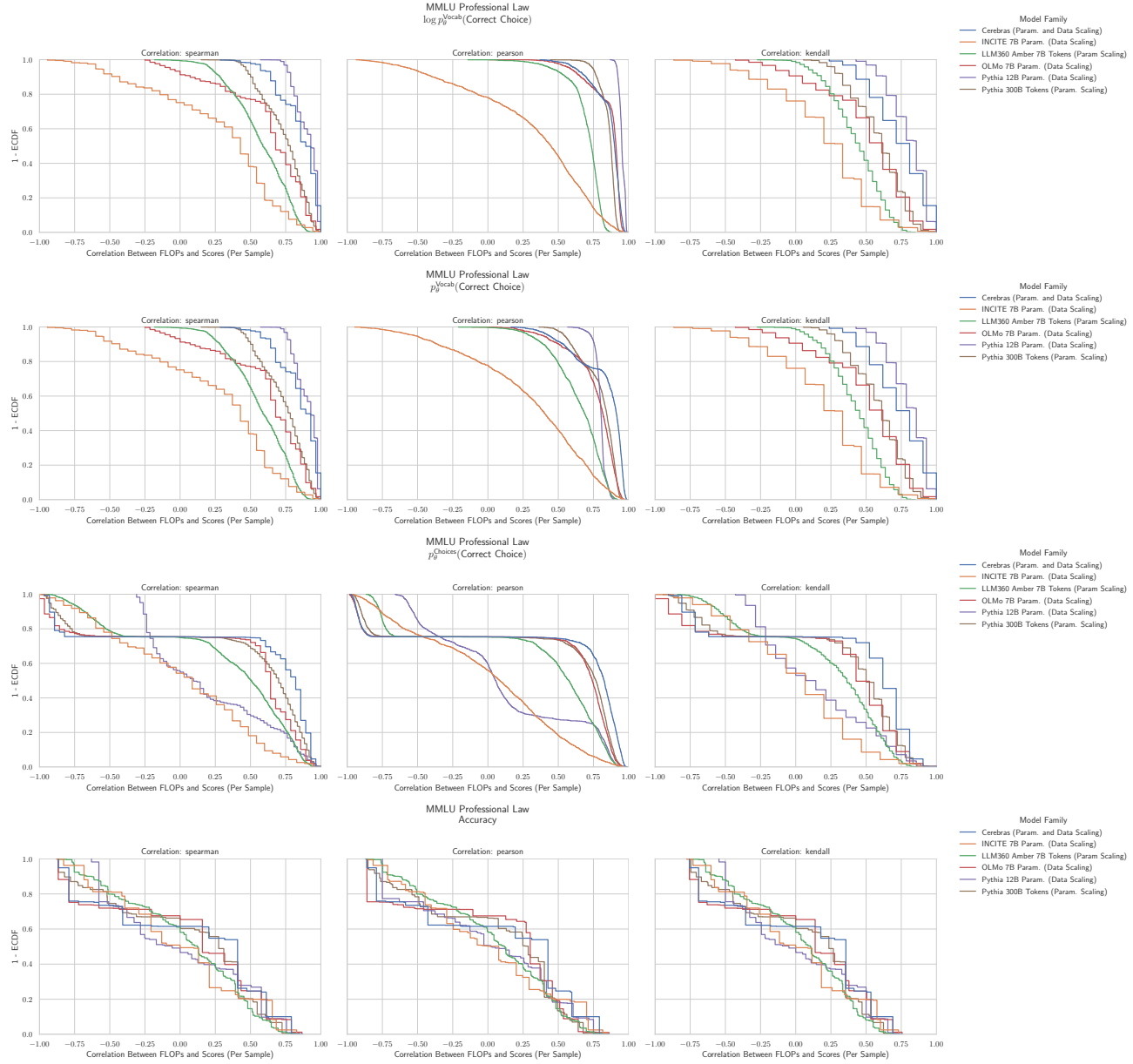
I.54. NLP Benchmark: MMLU Professional Accounting (Hendrycks et al., 2020)


Figure 63. MMLU Professional Accounting: Downstream performance is computed via a sequence of transformations that deteriorate correlations between scores and pretraining compute.

4015 I.55. NLP Benchmark: MMLU Professional Law (Hendrycks et al., 2020)
 4016
 4017

 4057 Figure 64. MMLU Professional Law: Downstream performance is computed via a sequence of transformations that deteriorate
 4058 correlations between scores and pretraining compute.
 4059
 4060
 4061
 4062
 4063
 4064
 4065
 4066
 4067
 4068
 4069

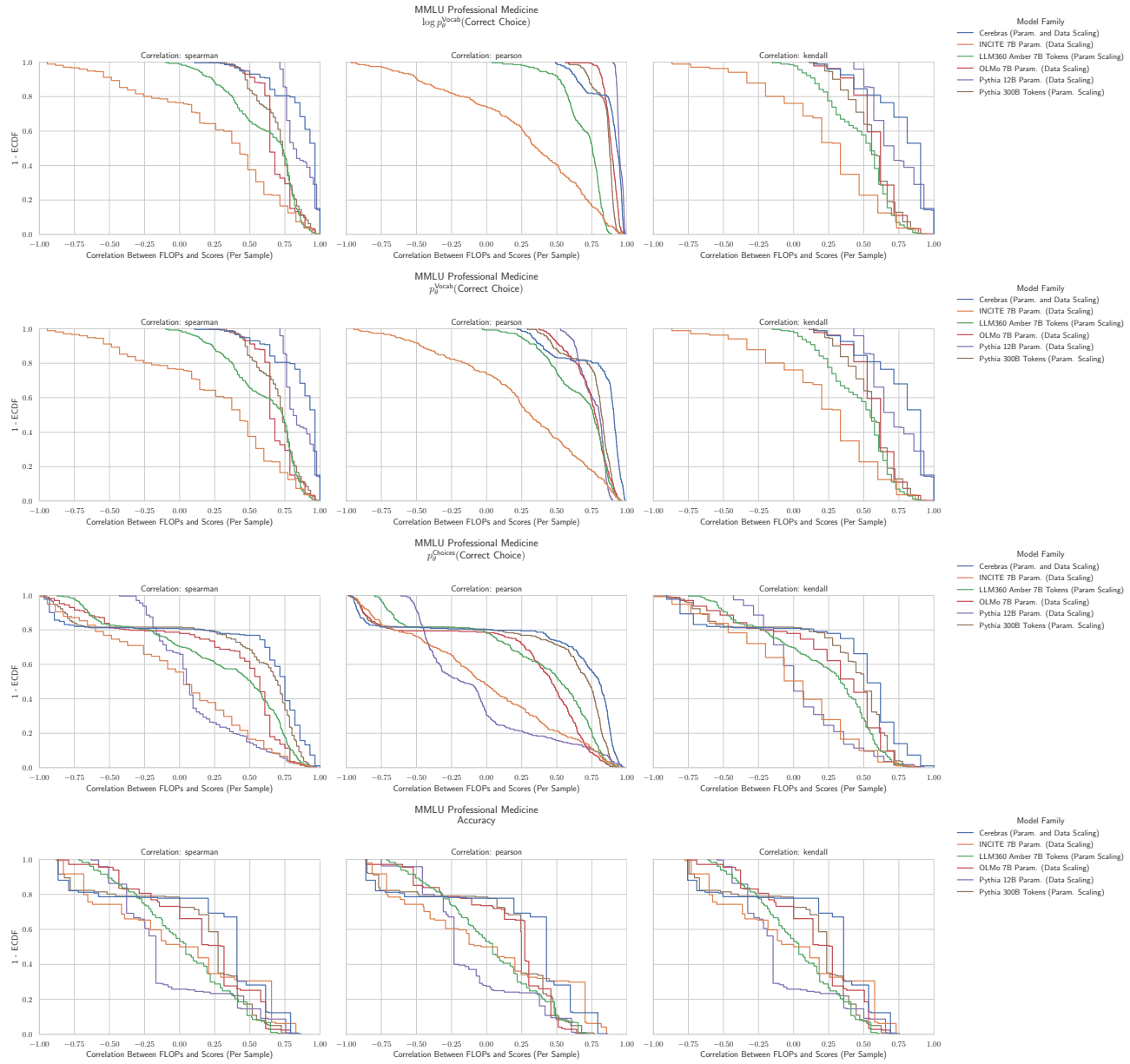
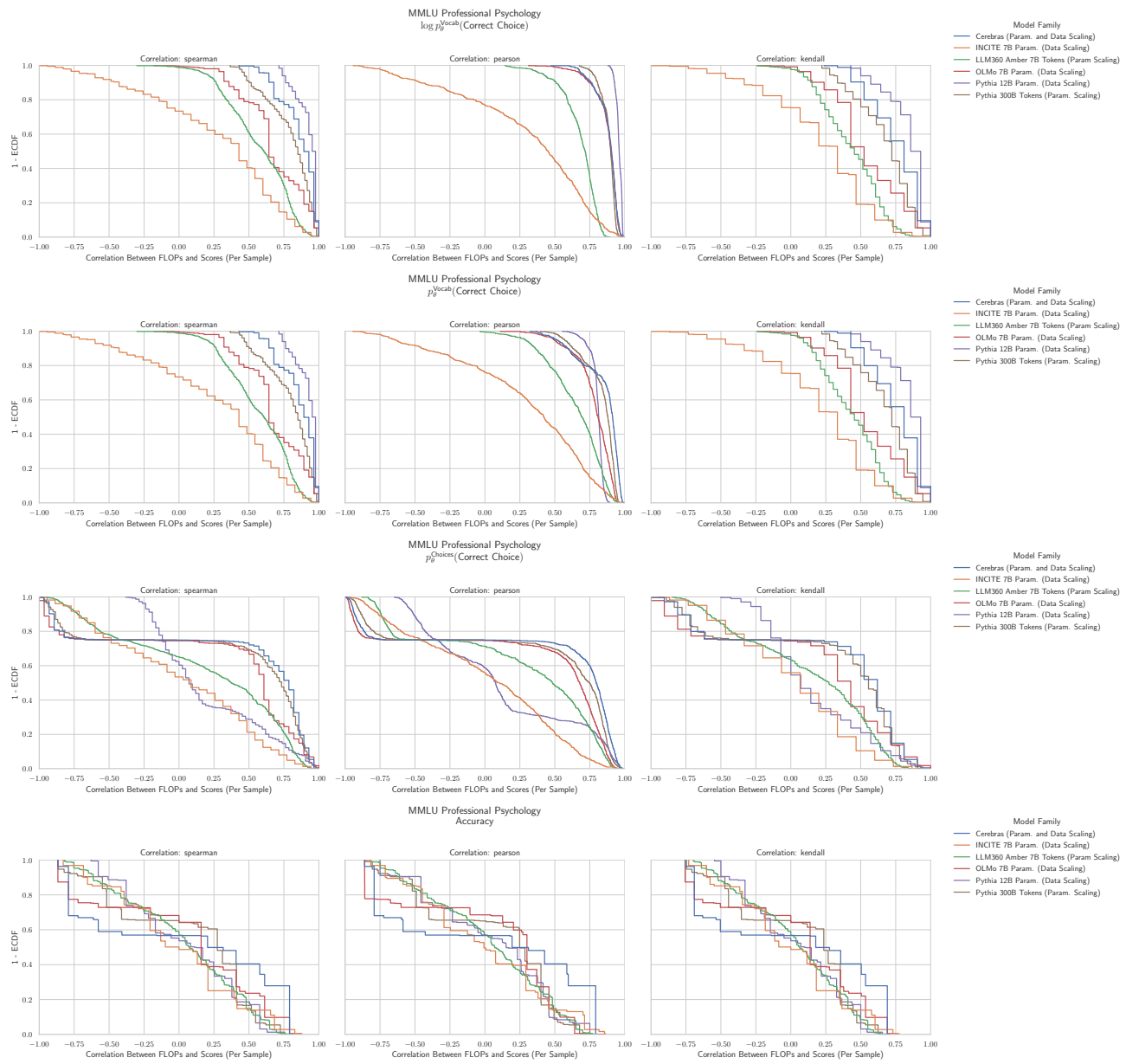
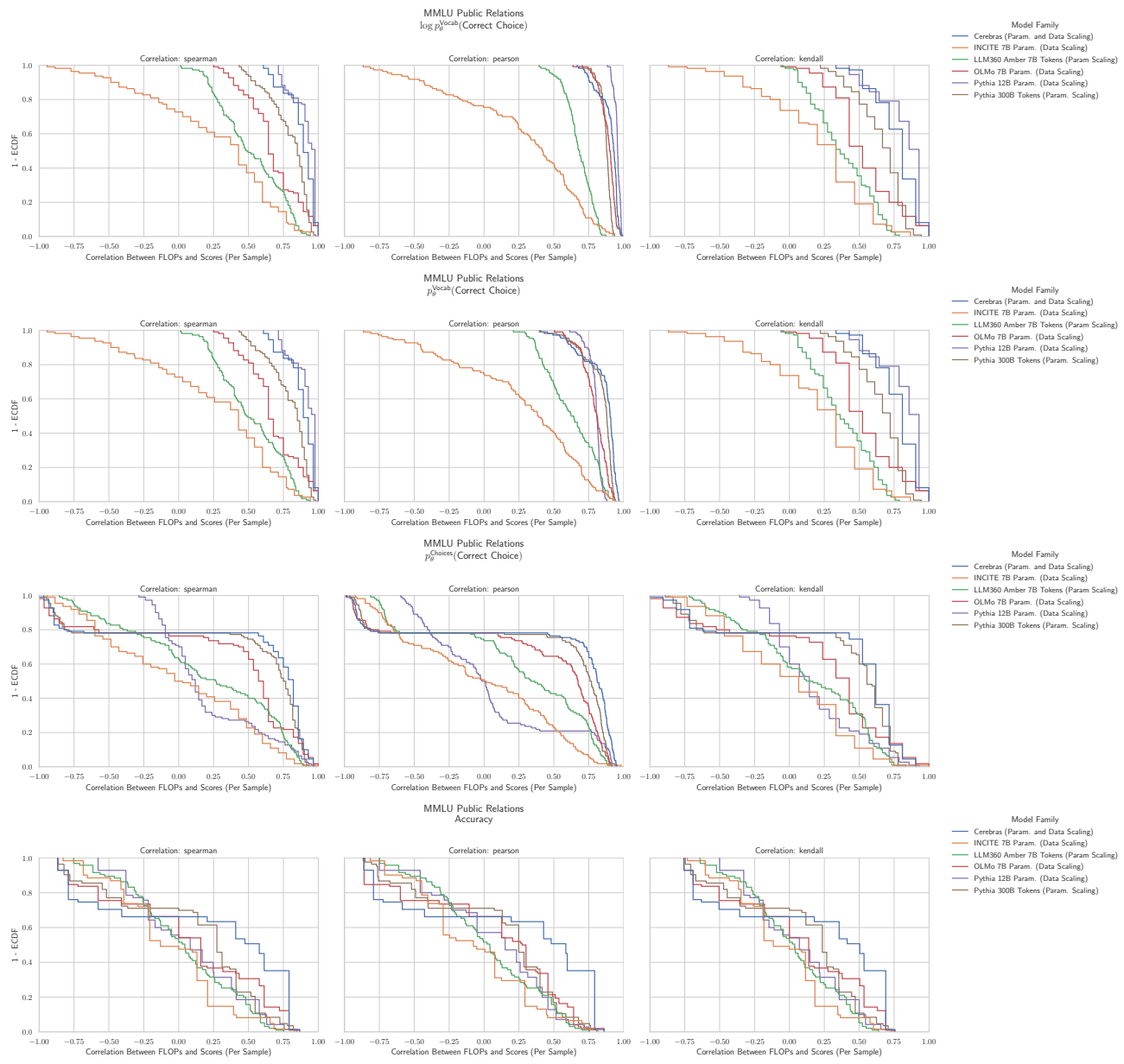
I.56. NLP Benchmark: MMLU Professional Medicine (Hendrycks et al., 2020)


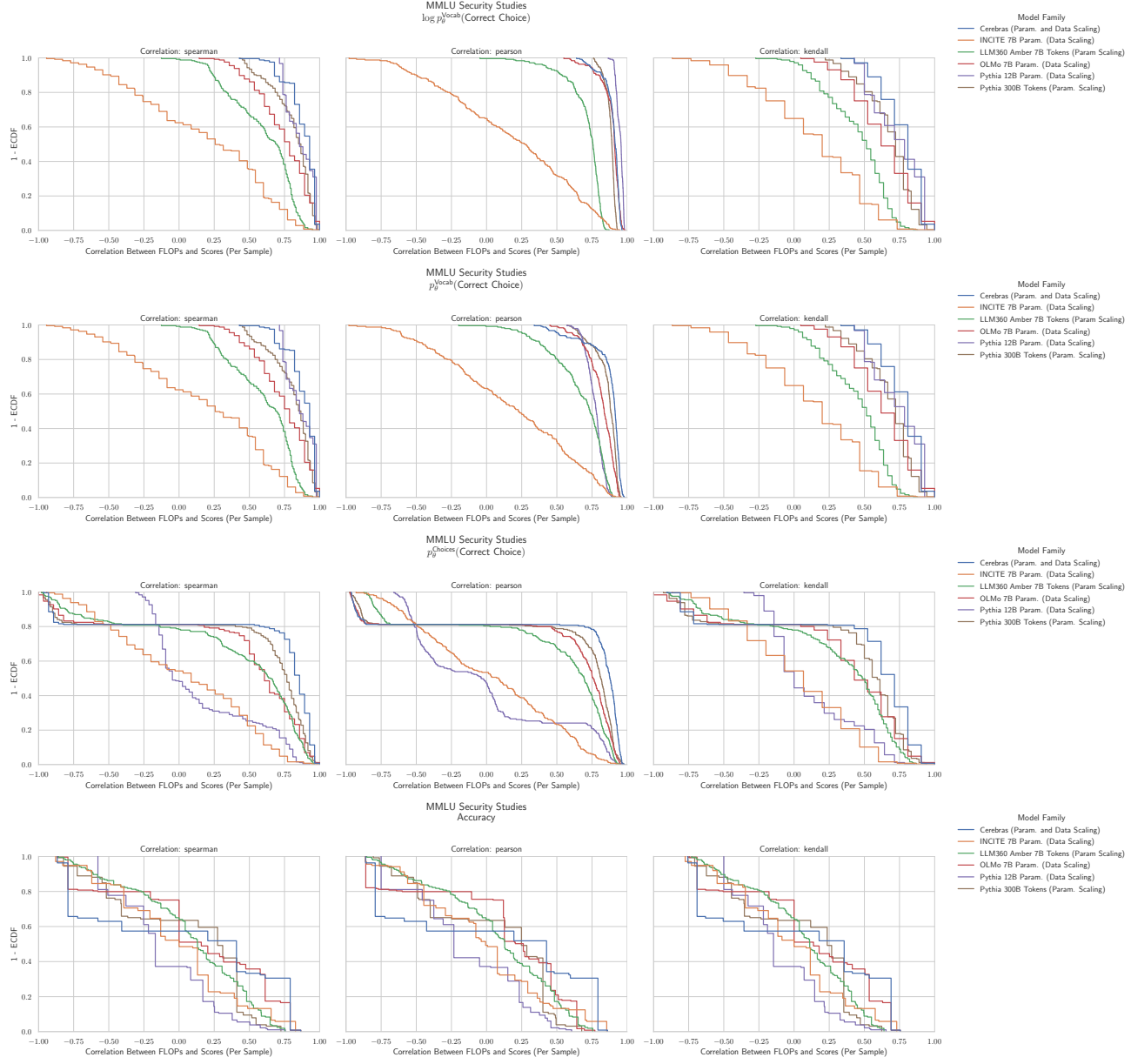
Figure 65. MMLU Professional Medicine: Downstream performance is computed via a sequence of transformations that deteriorate correlations between scores and pretraining compute.

4125 **I.57. NLP Benchmark: MMLU Professional Psychology (Hendrycks et al., 2020)**
 4126
 4127
 4128


4180 I.58. NLP Benchmark: MMLU Public Relations (Hendrycks et al., 2020)


 4222 **Figure 67. MMLU Public Relations: Downstream performance is computed via a sequence of transformations that deteriorate**
 4223 **correlations between scores and pretraining compute.**

4235 I.59. NLP Benchmark: MMLU Security Studies (Hendrycks et al., 2020)


 4277 **Figure 68. MMLU Security Studies: Downstream performance is computed via a sequence of transformations that deteriorate**
 4278 **correlations between scores and pretraining compute.**

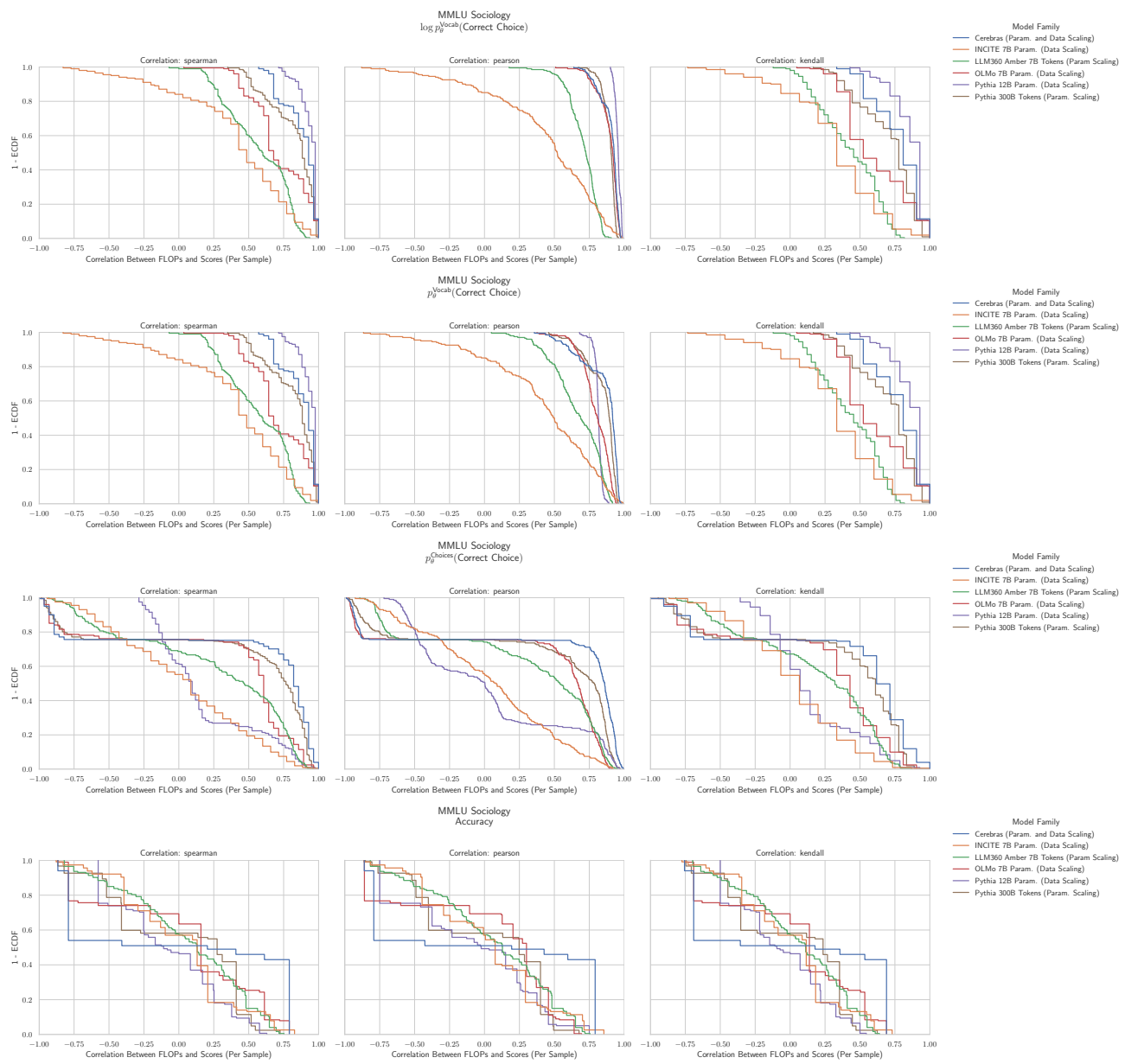
I.60. NLP Benchmark: MMLU Sociology (Hendrycks et al., 2020)


Figure 69. MMLU Sociology: Downstream performance is computed via a sequence of transformations that deteriorate correlations between scores and pretraining compute.

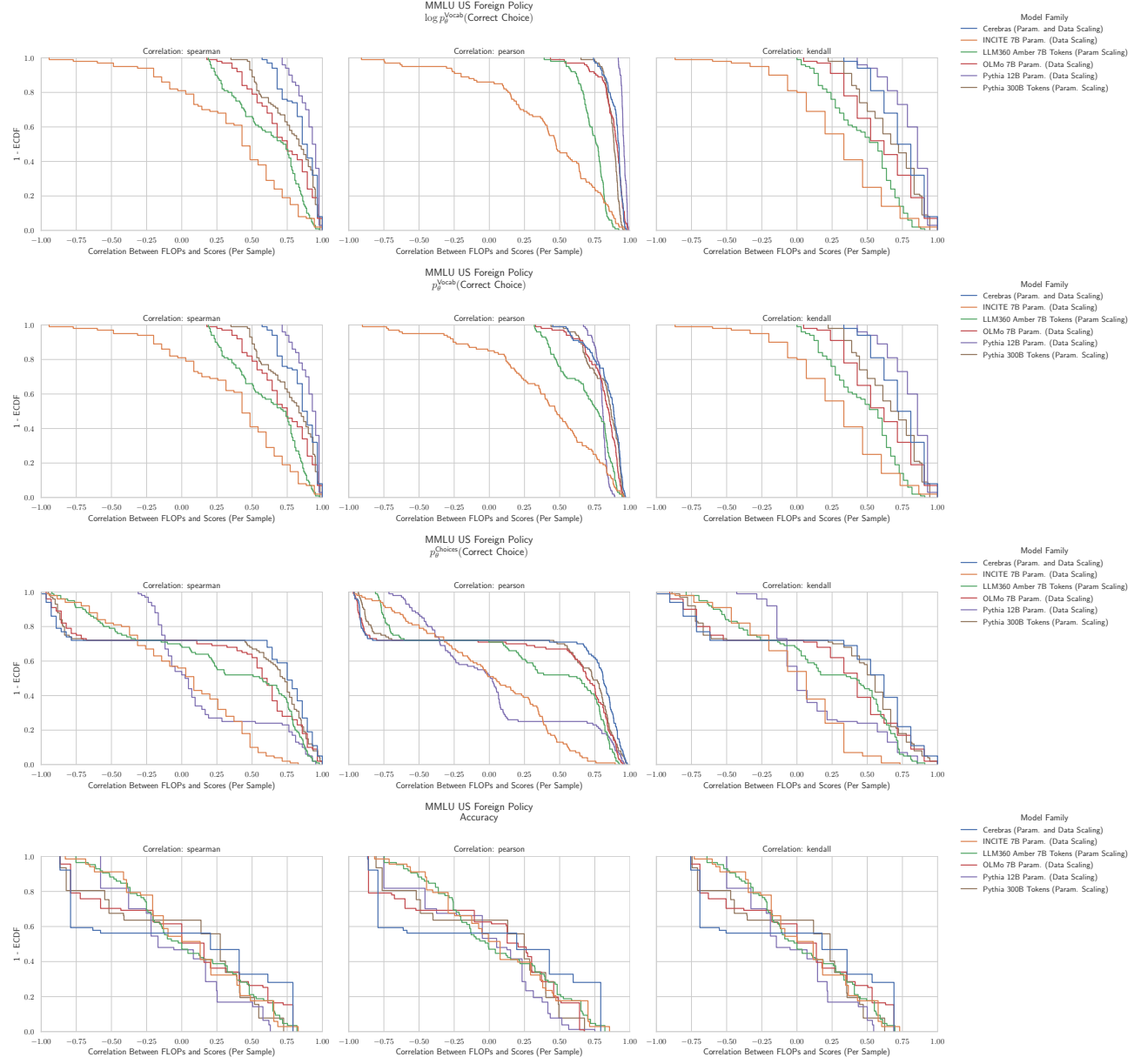
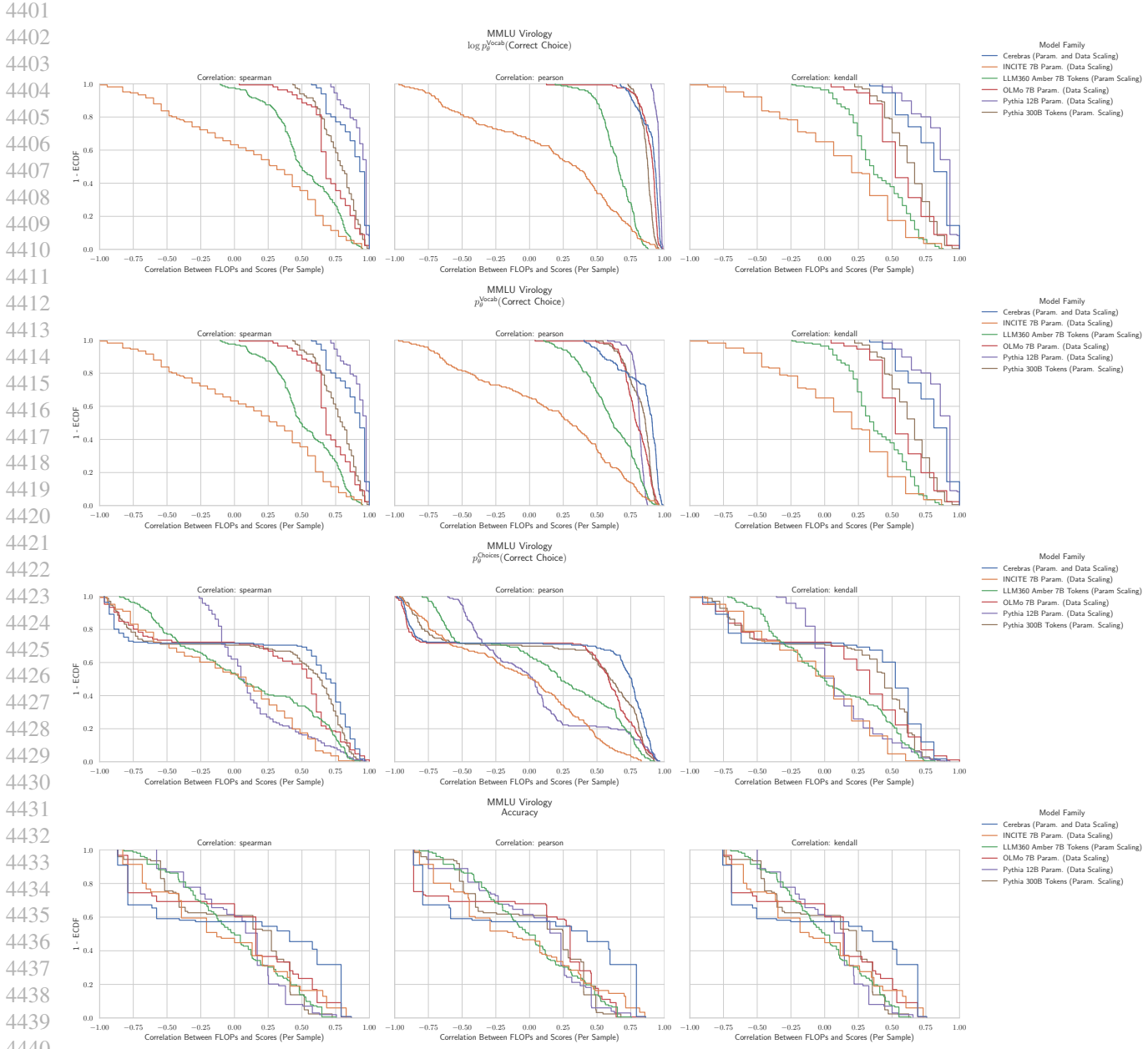
I.61. NLP Benchmark: MMLU US Foreign Policy (Hendrycks et al., 2020)


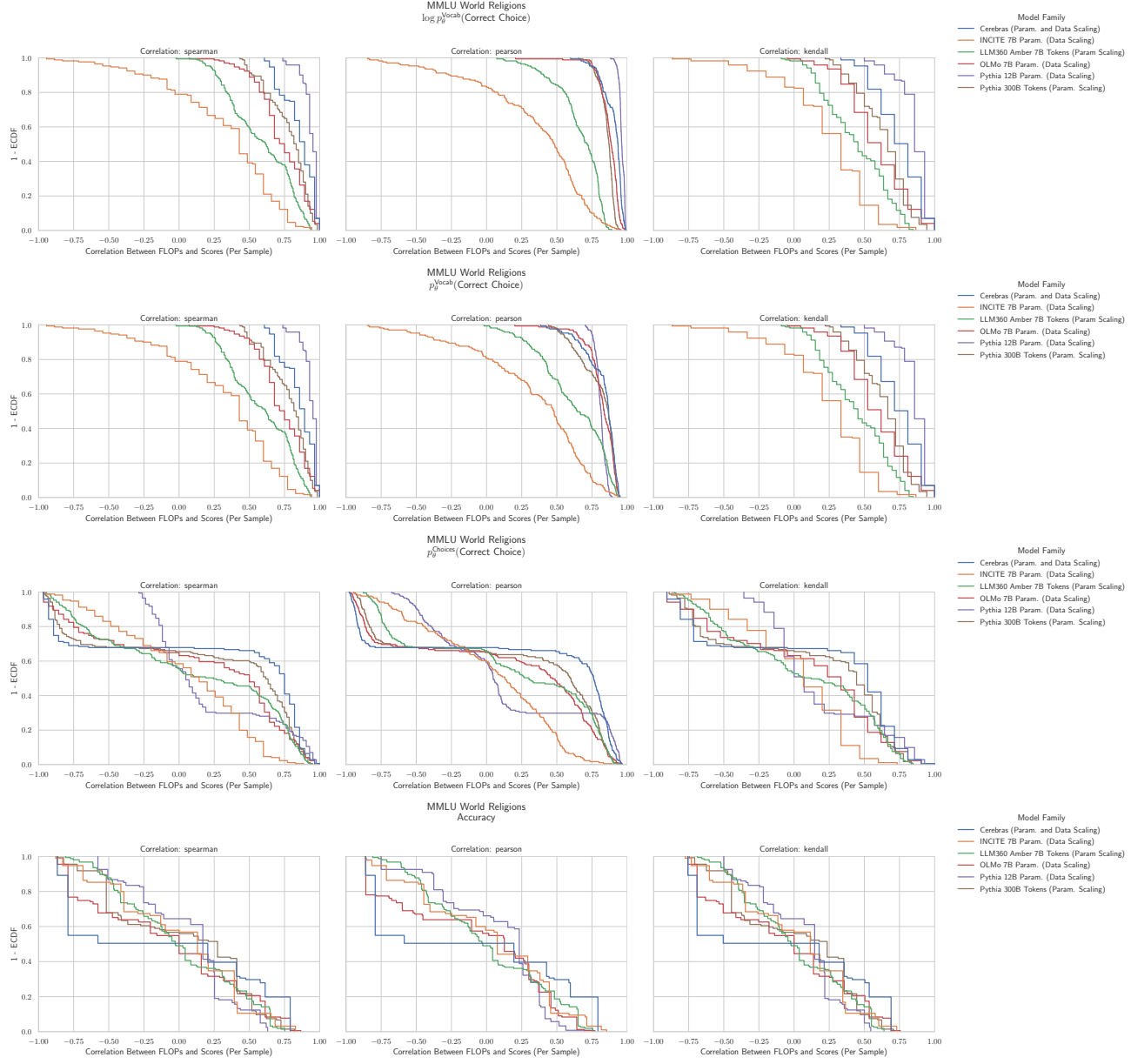
Figure 70. MMLU US Foreign Policy: Downstream performance is computed via a sequence of transformations that deteriorate correlations between scores and pretraining compute.

4400 **I.62. NLP Benchmark: MMLU Virology (Hendrycks et al., 2020)**



4440 **Figure 71. MMLU Virology: Downstream performance is computed via a sequence of transformations that deteriorate correlations between scores and pretraining compute.**

4455 I.63. NLP Benchmark: MMLU World Religions (Hendrycks et al., 2020)


 4497 **Figure 72. MMLU World Religions: Downstream performance is computed via a sequence of transformations that deteriorate**
 4498 **correlations between scores and pretraining compute.**

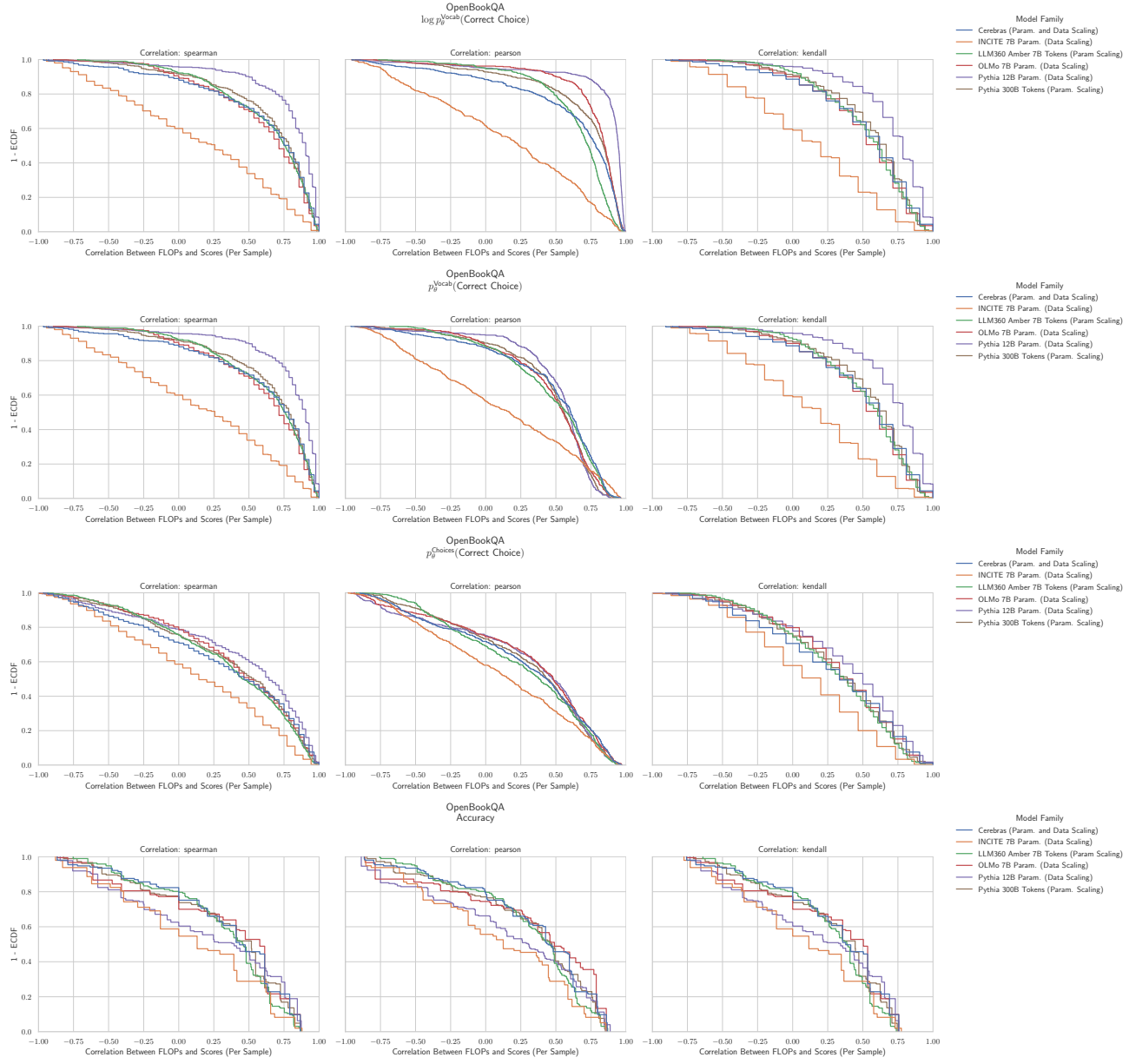
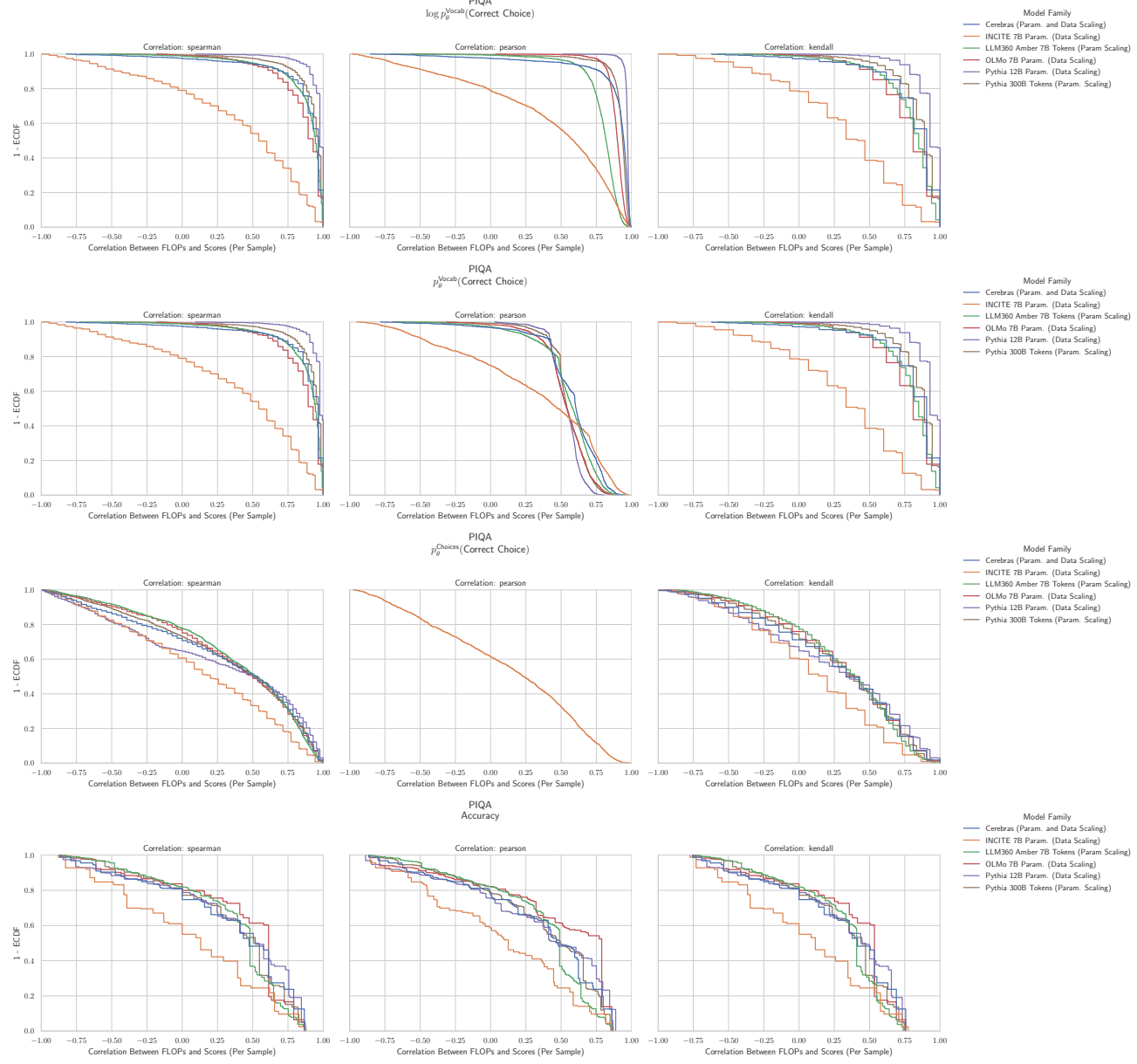
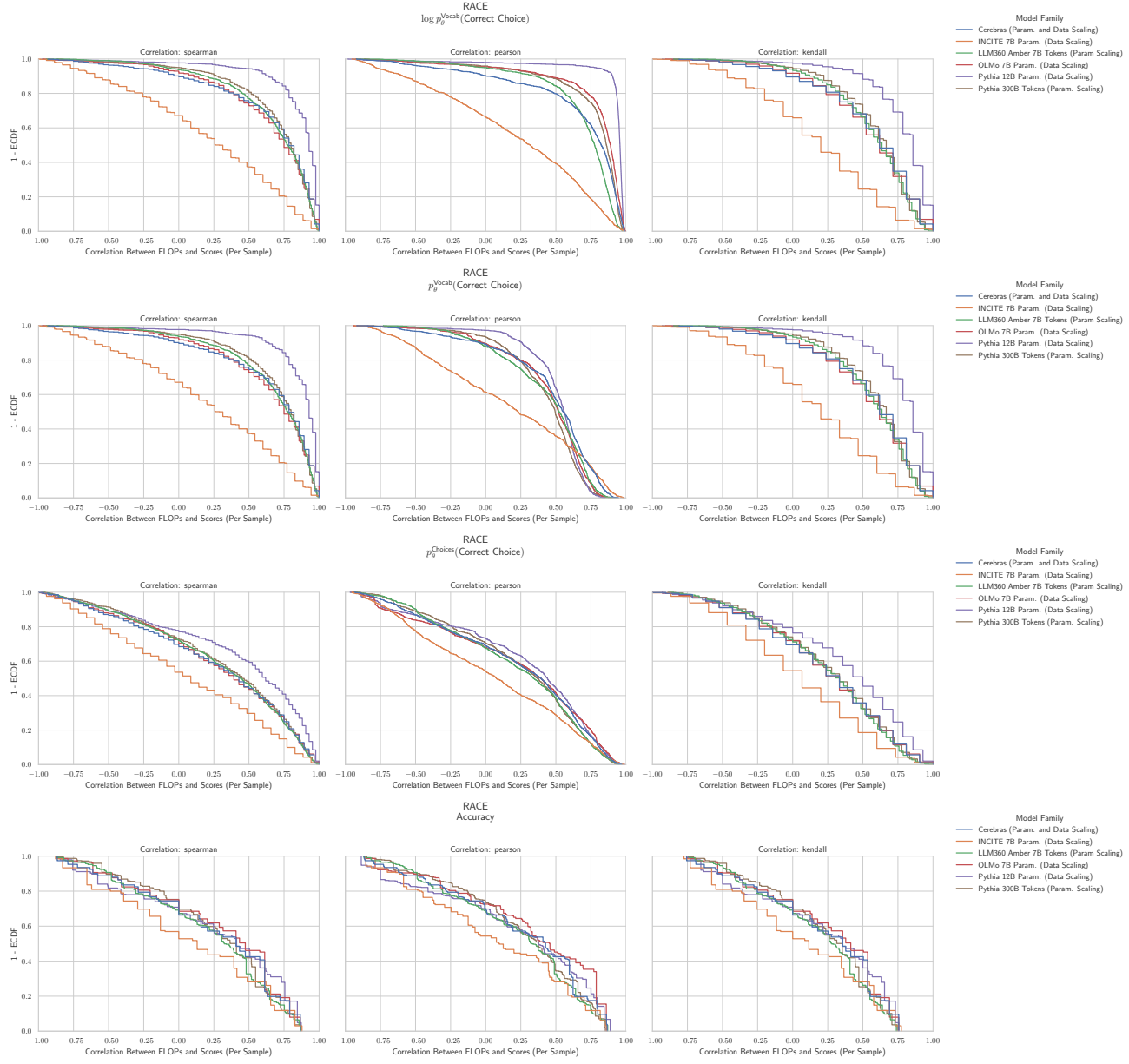
I.64. NLP Benchmark: OpenBookQA (Mihaylov et al., 2018)


Figure 73. OpenBookQA: Downstream performance is computed via a sequence of transformations that deteriorate correlations between scores and pretraining compute.

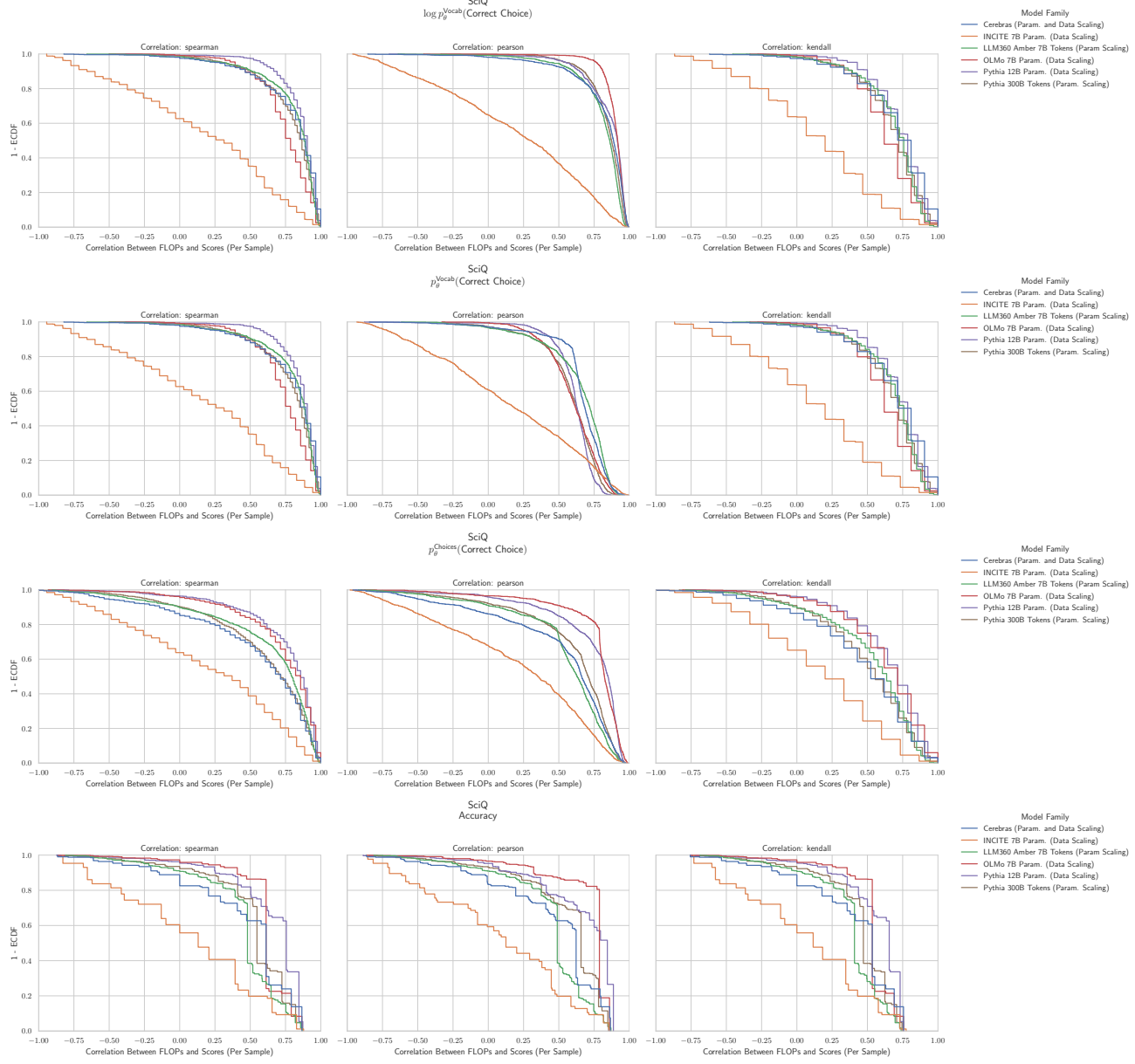
4565 I.65. NLP Benchmark: PIQA (Bisk et al., 2020)


 4607 **Figure 74. PIQA: Downstream performance is computed via a sequence of transformations that deteriorate correlations between**
 4608 **scores and pretraining compute.**

4620 I.66. NLP Benchmark: RACE (Lai et al., 2017)


 4662 **Figure 75. RACE: Downstream performance is computed via a sequence of transformations that deteriorate correlations between**
 4663 **scores and pretraining compute.**

4675 I.67. NLP Benchmark: SciQ (Welbl et al., 2017)


 4717 **Figure 76. SciQ: Downstream performance is computed via a sequence of transformations that deteriorate correlations between**
 4718 **scores and pretraining compute.**

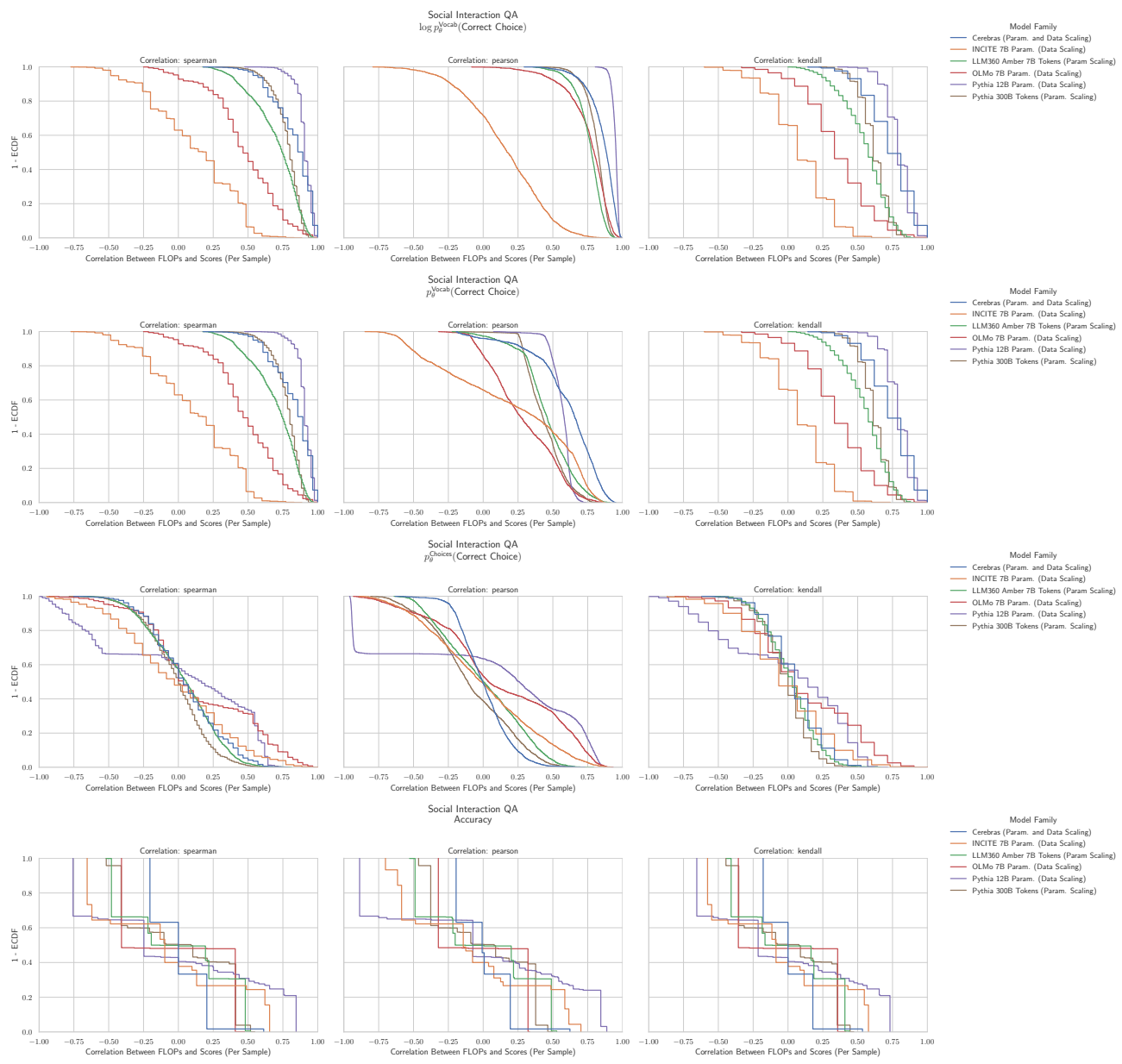
I.68. NLP Benchmark: Social IQA (Sap et al., 2019b)


Figure 77. Social IQA: Downstream performance is computed via a sequence of transformations that deteriorate correlations between scores and pretraining compute.

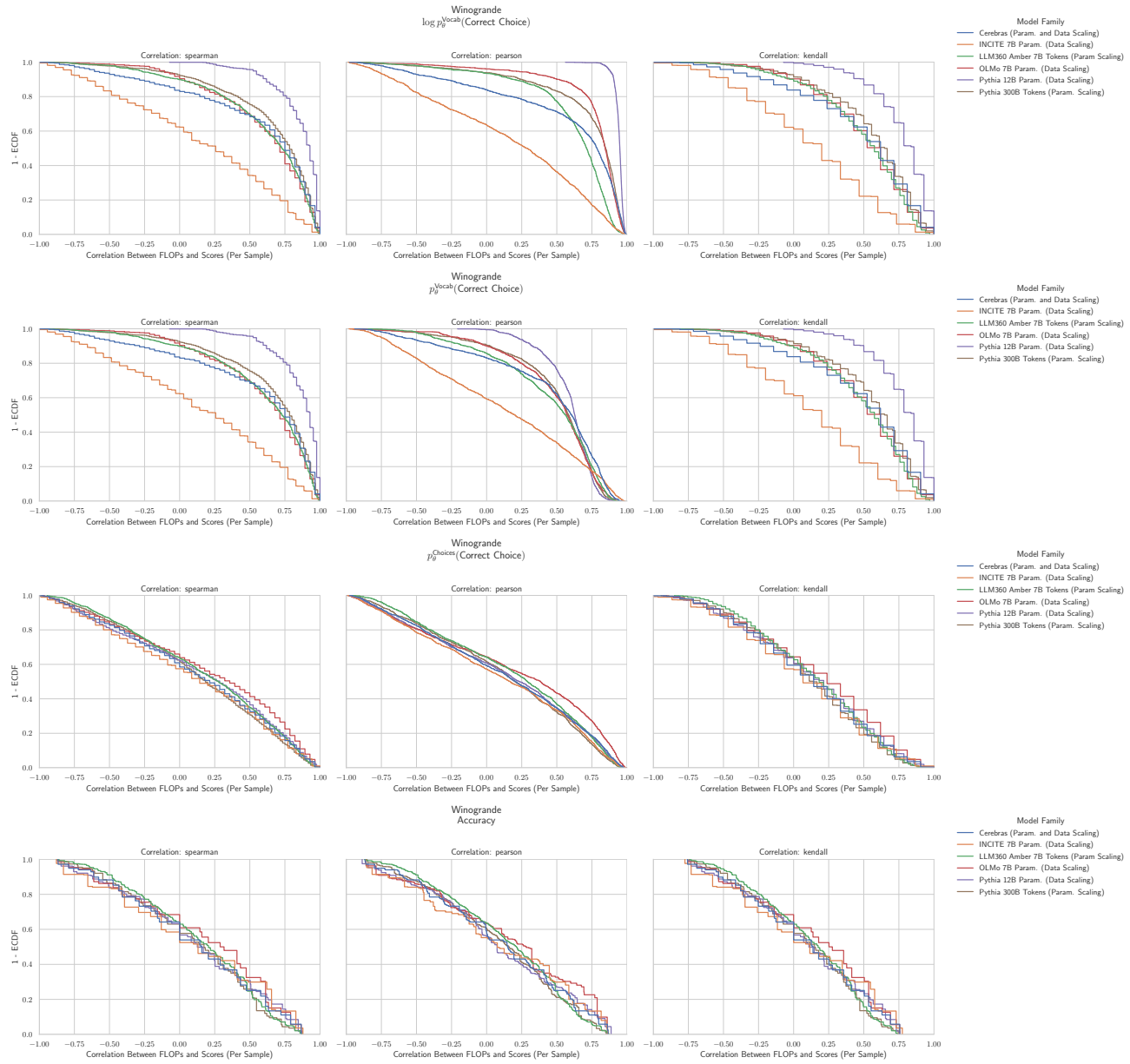
I.69. NLP Benchmark: Winogrande (Keisuke et al., 2019)


Figure 78. Social IQA: Downstream performance is computed via a sequence of transformations that deteriorate correlations between scores and pretraining compute.

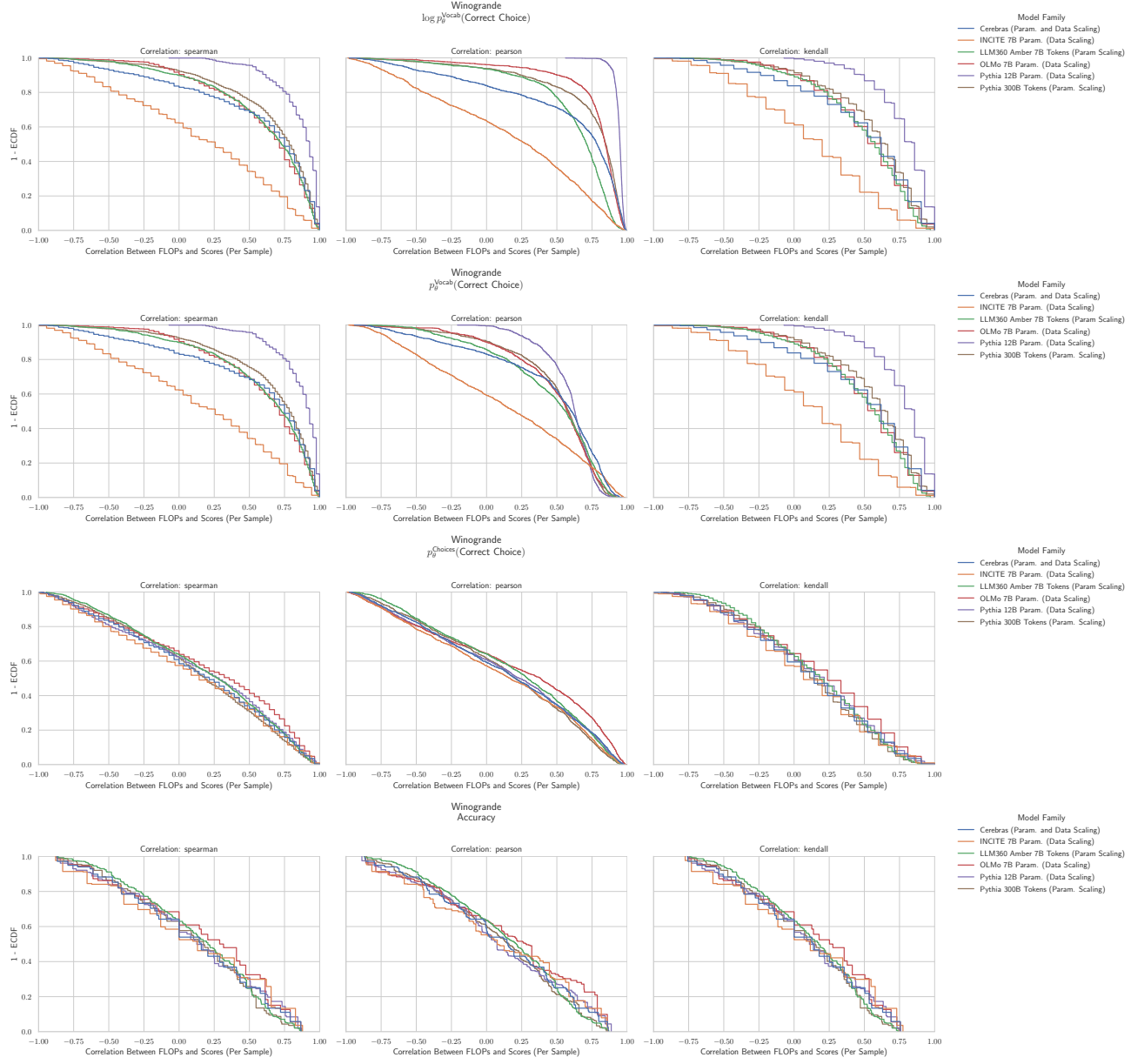
I.70. NLP Benchmark: XWinograd English (Muennighoff et al., 2023)


Figure 79. XWinograd English: Downstream performance is computed via a sequence of transformations that deteriorate correlations between scores and pretraining compute.